

# **For Reference**

---

**NOT TO BE TAKEN FROM THIS ROOM**

Ex LIBRIS  
UNIVERSITATIS  
ALBERTAEASIS







T H E   U N I V E R S I T Y   O F   A L B E R T A

RELEASE FORM

NAME OF AUTHOR.....Denise Gibbs.....

TITLE OF THESIS..Instability Domains of the Reversible..  
.....Oregonator.....

.....  
DEGREE FOR WHICH THESIS WAS PRESENTED.....M.Sc:.....

YEAR THIS DEGREE GRANTED.....1978.....

Permission is hereby granted to THE UNIVERSITY  
OF ALBERTA LIBRARY to reproduce single copies of this  
thesis and to lend or sell such copies for private,  
scholarly or scientific research purposes only.

The author reserves other publication rights,  
and neither the thesis nor extensive extracts from  
it may be printed or otherwise reproduced without  
the author's written permission.



THE UNIVERSITY OF ALBERTA

INSTABILITY DOMAINS OF THE REVERSIBLE OREGONATOR

by

DENISE GIBBS

(C)

A THESIS

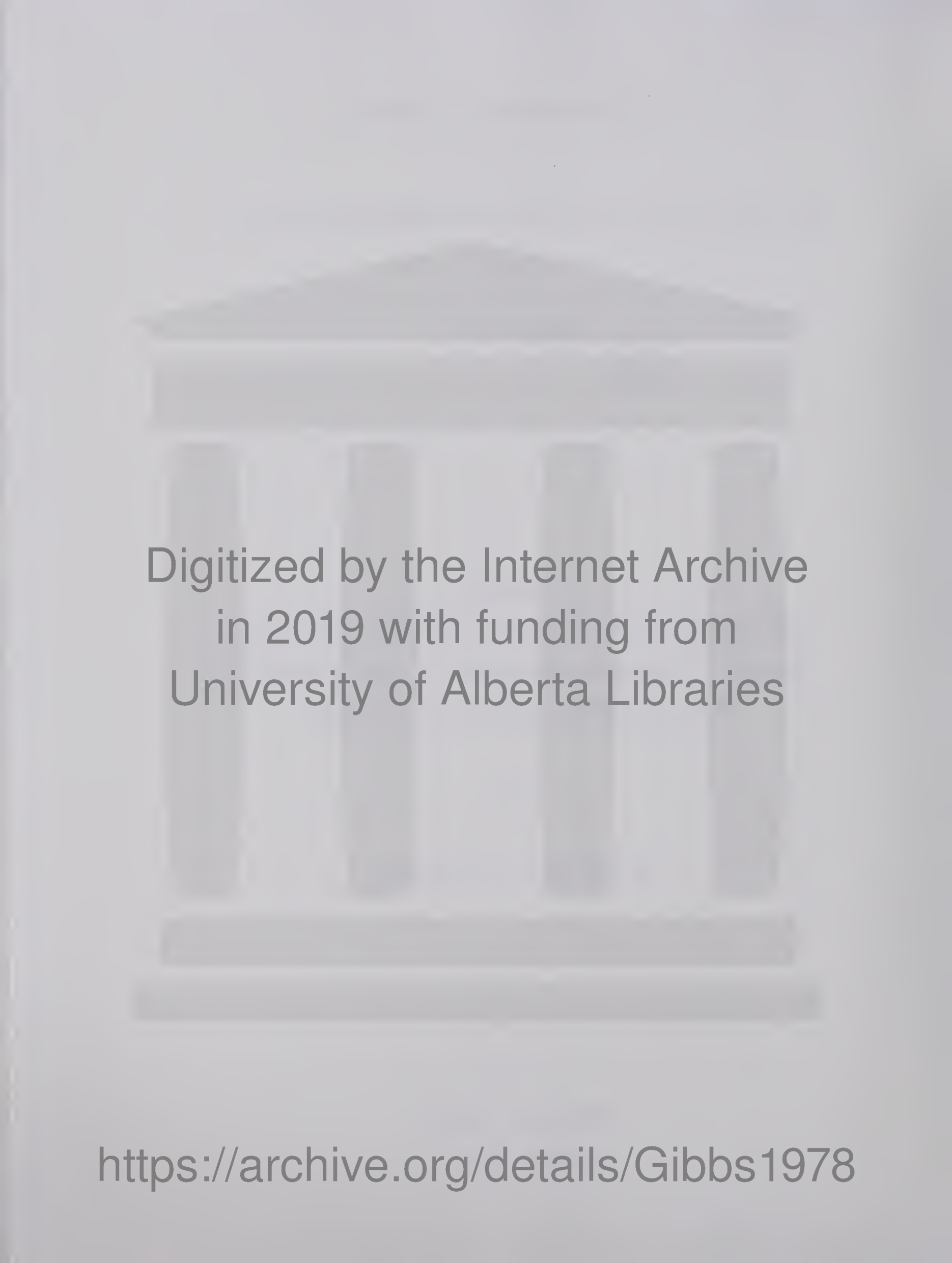
SUBMITTED TO THE FACULTY OF GRADUATE STUDIES AND  
RESEARCH IN PARTIAL FULFILMENT OF THE REQUIREMENTS  
FOR THE DEGREE OF MASTER OF SCIENCE

IN

DEPARTMENT OF CHEMISTRY

EDMONTON, ALBERTA

SPRING 1978



Digitized by the Internet Archive  
in 2019 with funding from  
University of Alberta Libraries

<https://archive.org/details/Gibbs1978>

78-2

THE UNIVERSITY OF ALBERTA  
FACULTY OF GRADUATE STUDIES AND RESEARCH

The undersigned certify that they have read,  
and recommend to the Faculty of Graduate Studies  
and Research, for acceptance, a thesis entitled  
INSTABILITY DOMAINS OF THE REVERSIBLE OREGONATOR  
submitted by Denise Gibbs in partial fulfilment  
of the requirements for the degree of Master of  
Science in Department of Chemistry.



## ABSTRACT

In the standard treatment of stability in chemical reaction systems by normal mode analysis, the stability of the non-equilibrium steady states is usually determined numerically. The recent development of a general analytic method for linear stability analysis has allowed the asymptotic boundary of the unstable steady states in parameter space to be determined, without assignment of the rate constants. A diagrammatic counterpart of this method is used to pinpoint the interactions which may cause instability, and also retains information on matrix qualitative stability.

The subject of the stability analysis in this thesis is the Oregonator model which was proposed to explain the significant mechanistic features of the Belousov-Zhabotinski reaction. The model is analyzed with the reverse reactions included. A comparison is made with the irreversible model to determine the effect of reversibility on the region of instability in the network. A variable stoichiometric coefficient is also contained in the model, and the effect of this parameter on the boundary of the unstable region is discussed in detail.



## ACKNOWLEDGMENTS

I would like to thank my supervisor Dr. B. L. Clarke for the advice and direction that I received in the completion of this project.

The members of my committee also deserve thanks for reading and commenting on my work. Especial thanks are due to Dr. W. R. Thorson for his advice while Dr. Clarke was on sabbatical leave.

I am indebted to Mrs. J. M. Jorgensen for secretarial assistance in the preparation of this thesis.



## TABLE OF CONTENTS

<u>CHAPTER</u>		<u>PAGE</u>
1	BACKGROUND	1
	1.1 INTRODUCTION	1
	1.2 KINETIC STABILITY	7
	1.3 THE BELOUSOV-ZHABOTINSKI REACTION	14
2	STABILITY THEORY FOR CHEMICAL NETWORKS	17
	2.1 INTRODUCTION	17
	2.2 CHEMICAL NETWORK PARAMETERS	25
	2.3 APPLICATION OF THE STABILITY CRITERION	47
	2.4 CONDITIONS FOR INSTABILITY	50
	2.5 DIAGRAMMATIC AIDS	65
3	THE STABILITY ANALYSIS	76
	3.1 INTRODUCTION	76
	3.2 IRREVERSIBLE MODEL RESULTS	78
	3.2.1 The cone of negative $\alpha_2$	81
	3.2.2 The cone of negative $\Delta_2$	87
	3.2.3 Summary	94
	3.3 REVERSIBLE MODEL RESULTS	102
	3.3.1 The cone of negative $\alpha_2$	111
	3.3.2 The cone of negative $\alpha_3$	132
	3.3.3 The cone of negative $\Delta_2$	137
	3.3.4 Summary	148
	3.4 RE-EVALUATION OF THE OMITTED EXTREME CURRENTS	152



<u>CHAPTER</u>		<u>PAGE</u>
3.5	COMPARISON OF THE REVERSIBLE AND IRREVERSIBLE RESULTS	160
3.6	GENERAL CONCLUSIONS	176



LIST OF TABLES

<u>TABLE</u>	<u>Description</u>	<u>PAGE</u>
3.1	The instability conditions for $\alpha_2$ in the irreversible model.	84
3.2	The instability conditions for the NMO $\Delta_2$ vertex in the irreversible model.	93
3.3	Summary of the destabilizing cycles in the irreversible model.	95
3.4	The negative vertices of $\Pi_{\alpha_2}$ for the reversible model.	112
3.5	A guide to the use of the tables of instability conditions for $\alpha_2$ of the reversible model.	119
3.6-3.10	The instability conditions for $\alpha_2$ in the reversible model.	120
3.11	The instability conditions for $\alpha_3$ in the reversible model.	135
3.12	$\Pi_{\Delta_2}$ negative vertices in the reversible model.	141
3.13	The instability conditions for the NMO $\Delta_2$ vertices in the reversible model.	145
3.14	Summary of the destabilizing cycles in the reversible model.	149
3.15	The instability conditions for the $\alpha_3$ in the reversible model for $f < 1$ .	158
3.16	Comparison of the irreversible model hyper-planes found in the four $\alpha_2$ destabilizing terms of the reversible model.	165



<u>TABLE</u>	<u>Description</u>	<u>PAGE</u>
3.17	Summary of the destabilizing extreme currents in the irreversible and reversible models.	175



LIST OF FIGURES

<u>FIGURES</u>	<u>Description</u>	<u>PAGE</u>
2.1	Plot of $\Delta_2(p)$ for the extreme current $j_A$ at $f = 1.1$ of the irreversible model.	52
3.1	(a) The extreme currents for the irreversible model. (b) The interaction diagrams for the irreversible model.	79
3.2	The exponent polytope $\Pi_{\Delta_2}$ for the irreversible model.	86
3.3	The diagrams contributing to the NMO vertex in $\Pi_{\Delta_2}$ .	89
3.4	The exponent polytope $\Pi_{\Delta_2}$ for the irreversible model.	92
3.5	Plot of the irreversible model hyperplanes at $f = 1.1$ .	96
3.6	The extreme currents of the reversible model.	103
3.7	Relationship between the extreme currents of the reversible model in the current polytope.	107
3.8	The interaction diagrams used in the reversible model analysis.	109
3.9	The appearance of new adjacent negative vertices for the pure destabilizing term (a) $j_A^2 xy$ and (b) $j_B^2 xy$ .	115
3.10	The diagrams contributing to the $\Pi_{\Delta_3}$ negative vertices in the reversible model.	133



<u>FIGURE</u>	<u>Description</u>	<u>PAGE</u>
3.11	The appearance of new negative vertices in $\Pi_{\Delta_2}$ with $f$ .	138
3.12	The diagrams contributing to the $\Pi_{\Delta_2}$ NMO negative vertices in the reversible model.	144
3.13	The interaction diagrams of the extreme currents $A^-$ , $B^-$ , $C^-$ and $D$ in the reversible model.	153
3.14	The diagrams contributing to the mixed destabilizing terms in $\alpha_3$ for $f < 1$ in the reversible model.	155
3.15	The extension of the NEEC's A and B in the reversible model.	163
3.16	Plot of the coefficients in Table 3.16 versus $f$ .	167



## CHAPTER ONE

### Background

#### 1.1. Introduction

In the past decade, the behavior of chemical reactions beyond the equilibrium steady state has been investigated with increasing enthusiasm.<sup>1</sup> This interest arose primarily due to the discovery of biological clocks and oscillating biochemical systems. Such systems include oscillatory metabolic reactions related to oxidative phosphorylation and glycolysis. Several review articles on the subject of oscillating reactions are available.<sup>2-4</sup>

Other areas of interest involving oscillating phenomena are hydrodynamics,<sup>5,6</sup> economics,<sup>7</sup> and ecology.<sup>8</sup> Ecologists, who studied the cyclic fluctuations in animal populations, promoted the use of qualitative criteria for stability of matrices.<sup>9,10</sup> Such a criterion was provided by Quirk and Rupert<sup>9</sup> as a result of studies done on economic systems. The matrix, which determines the stability of an ecological system, describes the predator-prey interactions between populations and is called the *community* or *interaction matrix*. The interaction matrix used by ecologists is analogous to the matrix formed in the linear stability of chemical systems.

In the matrices associated with chemical systems, every off-diagonal element of the matrix of the linearized



stability problem contains a parameter which also appears in a diagonal element, as a result of the reaction stoichiometry.<sup>11</sup> This restricts the possible matrix element variation and means that matrices occurring in chemical networks can violate the criterion for matrix qualitative stability, and yet have no regions of instability. An extension of the work of Quirk and Rupert to the chemical stability problem has been done by Clarke,<sup>11</sup> utilizing the quantitative method of analysis used in this thesis. Such qualitative results<sup>11</sup> from studies of chemical systems should apply to interaction matrices in ecology and economics also, since the parameters of these systems have similar interrelationships.

Other qualitative criteria for stability in chemical systems exist for the special case in which the reactions of the network obey mass action kinetics. One such criterion, due to Shear,<sup>12</sup> guarantees the uniqueness and global stability of equilibrium steady states in closed systems, as long as mass action kinetics hold. Since equilibrium and the states close to equilibrium cannot oscillate, they are not the ones of interest in this analysis. Another criterion is provided by Horn's zero deficiency theorem,<sup>13</sup> which gives a sufficient condition for qualitative stability of any reaction system obeying mass action kinetics. Since there is no



restriction to the states close to thermodynamic equilibrium, this criterion is more powerful than Shear's result. In particular, Horn's theorem greatly restricts the number of mass action systems that can possibly be unstable. However, it cannot guarantee instability will result in any particular system which violates the conditions of the theorem. In the model to be analyzed here some steps - like many experimentally determined rate expressions - do not obey mass-action kinetics, and therefore Horn's theorem does not apply. The necessity for considering non-mass action systems in the non-equilibrium region, has motivated other approaches to the stability of oscillating chemical systems, which shall now be mentioned briefly.

In general, the method of stability analysis used to study oscillating reactions can be classified as either thermodynamic or kinetic in approach.<sup>3</sup> The stability analysis of chemical systems has been approached by Prigogine *et al.* from a thermodynamic viewpoint by a local formulation which centers around the second law of thermodynamics.<sup>14,15</sup> In nonlinear processes, however, a thermodynamic potential function is available close to equilibrium only, where the system must be stable. Far from equilibrium, where oscillations may occur, a sufficient condition for stability can be expressed in terms of the second variation of entropy production,



even though no potential exists. This so called "Glandsdorff-Prigogine criterion" is not used in practice to test stability because chemical systems are defined kinetically, while the Glandsdorff-Prigogine criterion can only be used if the independent variables are the fluxes and affinities of irreversible thermodynamics. The introduction of thermodynamics into the stability problem increases the complexity of the problem and for this reason chemical reactions have not been readily analyzed by these methods.

Another thermodynamic attempt to formulate chemical reaction dynamics, called network thermodynamics, has been based on electrical network theory.<sup>16</sup> In this approach chemical reactions are represented by electric circuits in which the forces and flows obey Kirchhoff's Laws. The aim was to allow classical network theory to be applied to chemical systems through a linear graph theory. The important underlying idea is that it is the way in which the reactions are linked (i.e., the way the circuit is hooked up) that determines the stability of the network. Stability analysis within this framework leads to the Glandsdorff-Prigogine criterion. As before, the main drawback is that the independent variables are the chemical potentials instead of the dynamic concentrations. For this reason, network thermodynamics has the same drawbacks as the older thermodynamic approach



of Prigogine.

In the kinetic approach to chemical stability problems, the dynamic equations of motion are written in terms of the chemical concentrations and the reaction velocities explicitly. The usual procedure in a kinetic investigation is to apply a so called linear stability or normal mode analysis.<sup>3</sup> This is the only method which allows instability conditions to be determined directly in terms of the system parameters. However, the standard approach has difficulties in dealing with large chemical systems. As a result, a new approach to the linear stability analysis of chemical systems was developed by Clarke,<sup>17</sup> to enable the study of realistic chemical systems. Such improvements in the theory were necessary before quantitative analyses, such as the one presented in this thesis, were possible. The essential background for this theory is given in chapter 2, while the standard treatment of stability by normal mode analysis is briefly introduced in section 1.2.

The basic idea used in the approach of this analysis is that chemical networks have certain topological properties related to the dynamics of the system. The topology of the network is important because it plays an essential role in the algebraic relationships between the rate constants and concentrations, which determine the boundary of unstable states in parameter space.



This boundary is useful for testing experimental reaction mechanisms and rate constants. Also, the validity of models which represent complicated chemical reactions can be assessed by examination of the network topology. An important conjecture in this regard is that networks with similar topology, stoichiometry and kinetics have similar stability properties.<sup>18</sup> This has been substantiated in several cases and should simplify the analysis of complex networks.

In this paper a five step model of the Belousov-Zhabotinski reaction, which exhibits oscillations, is analyzed with the reverse reactions included. The boundary of the unstable steady states is found analytically. The analytic method used here has a diagrammatic counterpart<sup>19</sup> which can be used to visually recognize the unstable terms in the interaction matrix. The interaction matrix is the matrix of coefficients of the linear system of equations consisting of the perturbed kinetic equations linearized about steady state. The principal aim of the analysis is to establish relationships between the unstable non-equilibrium steady states and the responsible destabilizing terms in the interaction matrix. A variable stoichiometric coefficient is retained in the matrix, and the change in the boundary of the unstable states with this parameter is also found. The effect of the reverse reactions on the boundary of the unstable region is similarly of special interest.



## 1.2. Kinetic Stability

The dynamics of a chemically reacting system is governed by the kinetic equations. These equations are in general a set of coupled nonlinear partial differential equations, which can be written as

$$\frac{\partial c_i}{\partial t} = F_i(\underline{c}) + D_i \nabla^2 c_i, \quad i = 1, \dots, n \quad (1.1)$$

where  $\underline{c}(r, t)$  is the concentration vector whose components  $c_i$  are the time and space dependent concentrations of each species.  $F_i(\underline{c})$  represents the reaction kinetics for each reaction creating or destroying species  $c_i$ . The rate of change of the concentration of each species depends on the concentrations of the other species in the system and the rate constants  $K_j$ . The diffusion of species  $c_i$  is given by the second term in equation (1.1), where  $D_i$  is the diffusion coefficient given by Fick's law. Temperature variations and external forces of the type encountered in hydrodynamics are excluded. The system of equations (1.1) is autonomous, and as such the rate constants are not considered functions of time.

The stability of the solutions of the system (1.1) is determined from the stability theory of nonlinear differential equations. A particular solution of the equations (1.1) can be written as the set of functions  $u_i(t)$ ,  $i = 1, \dots, n$ . This solution is asymptotically stable in the sense of Liapounov,<sup>20</sup> if all other solutions,



$v_i(t)$ , coming near it approach it asymptotically. In more rigorous terms, the solution  $u_i(t)$  is stable if, given  $\epsilon > 0$  and  $t_o$ , there is  $\eta = \eta(\epsilon, t_o)$  such that any solution  $v_i(t)$  for which  $|u_i(t_o) - v_i(t_o)| < \eta$  satisfies  $|u_i(t) - v_i(t)| < \epsilon$  for  $t \geq t_o$ . If  $u_i(t)$  is stable, and in addition  $|u_i(t) - v_i(t)| \rightarrow 0$  as  $t \rightarrow \infty$ , then  $u_i(t)$  is *asymptotically stable*.<sup>20</sup>

Other definitions of stability which apply to autonomous systems concern the parametric trajectories or orbits of (1.1), which are the curves represented by the solutions of (1.1) in concentration space. *Closed orbits* are the curves represented by periodic solutions of (1.1), and correspond to physical oscillations. If  $u_i(t)$  is a nonconstant periodic solution of (1.1) then  $u_i(t + \omega) = u_i(t)$  for all  $t$ , where  $\omega$  is some minimum positive constant, the period. Let  $C$  be an orbit of (1.1). Then  $C$  is *orbitally stable* if, given  $\epsilon > 0$ , there is  $\eta > 0$  such that, if  $R$  is a representative point of another trajectory within a distance  $\epsilon$  of  $C$  at time  $\tau$ , then  $R$  remains within a distance  $\eta$  of  $C$  for  $t > \tau$ . If no such  $\eta$  exists,  $C$  is orbitally unstable. If  $C$  is orbitally stable and in addition, the distance between  $R$  and  $C$  tends to 0 as  $t \rightarrow \infty$ , then  $C$  is *asymptotically orbitally stable*.<sup>20</sup>

An orbit which is asymptotically orbitally stable is a *stable limit cycle*. A limit cycle is an isolated



closed trajectory, and is necessary for sustained oscillations which are independent of initial conditions. A limit cycle is a periodic motion in a nonlinear, nonconservative system which attracts the trajectories nearby, in the same way that a singular point such as a stationary state or equilibrium state attracts its nearby trajectories if stable. Another important property of some limit cycle type oscillations is that they can be self-exciting or self-starting. If a system, which is initially at rest, can evolve spontaneously to a stable limit cycle due to the infinitesimal fluctuations in the system alone, then the system is said to exhibit "soft excitation", while the other possibility, a "hard excitation", requires an initial impulse, greater than some threshold value. In two dimensions, soft-excitation occurs when an unstable stationary state (focus) is enclosed by a stable limit cycle. Unfortunately, in higher than two dimensions, the relationship between limit cycles and the nature of stationary states has not been found.

Since the solutions of equations (1.1) cannot be easily found in general, a starting point for the investigation of limit cycle type oscillation in chemical reactions is the stability of steady (stationary) states. The steady states of equations (1.1) are defined by

$$\frac{\partial c_i}{\partial t} = 0, \quad i = 1, \dots, n \quad (1.2)$$



and the spatially homogeneous steady state solutions are the set of concentrations, represented by the components of the vector  $\tilde{c}_0 = (c_{10}, c_{20}, \dots, c_{n0})$ , which satisfy the algebraic equations

$$F_i(\tilde{c}) = 0, \quad i = 1, \dots, n. \quad (1.3)$$

From the preceding definitions, the steady state  $\tilde{c}_0$  will be asymptotically stable if all trajectories starting sufficiently close to it tend to it asymptotically as  $t \rightarrow \infty$ .

If the system (1.1) is closed to the flow of matter, then the concentrations of the species evolve until the rate of change of reagents into products and *vice versa* is equal. The final steady state reached represents a state of chemical equilibrium. Thermodynamic<sup>21</sup> and kinetic<sup>12</sup> arguments both show that these steady states are always stable. This means that an arbitrary fluctuation in a closed system cannot cause the system to evolve away from the equilibrium steady state or the steady states that are close to thermodynamic equilibrium.

In an open system, a flow of matter through the system can occur. This means that one can distinguish two different types of species: the *external species*  $A_i$  which flow into and out of the system, and the *internal species*  $X_i$  which are contained in the system and are often called the chemical intermediates. The external



species can be kept at a constant concentration by adding reagents and removing products continuously, whereas the internal species have unrestricted concentrations, which evolve according to the kinetic equations (1.1). Since the external species can be fixed at some constant concentration, they may be incorporated into the rate constants, so that they do not appear explicitly in (1.1). The new set of *apparent* rate constants  $\tilde{k}$  for the system consists of the true rate constants  $K$  multiplied by the constant concentration of the appropriate external species. The steady state solutions of (1.1) are now found by solving (1.3) for the steady state concentrations of the internal species,  $c_{io}$ , for some particular set of apparent rate constants. For every choice of the apparent rate constants a different solution  $\tilde{c}_o$  can be found. At one particular ratio of the apparent rate constants, the equilibrium steady state occurs, and corresponds to no flow through the system. All other solutions  $\tilde{c}_o$  will correspond to non-equilibrium steady states where a net flow through the system is necessary for maintaining steady state.

In this way the thermodynamic equilibrium steady state solution is extended into the non-equilibrium region of parameter space. When the system is constrained far enough from equilibrium, unstable steady states may occur. This instability arises because the kinetic



equations are not linear and occurs at some finite distance from equilibrium, beyond the so-called thermodynamic branch of solutions.<sup>22</sup> These unstable steady states are of interest because most models of oscillating chemical reactions are associated with unstable steady states in open systems, although an unstable steady state is not mathematically necessary for oscillatory phenomena.

The stability of the non-equilibrium steady states can be studied by perturbing the system (1.1) about the steady state. Perturbed solutions of the form

$$\underline{c}(\underline{r},t) = \underline{c}_0 + \underline{\zeta}(\underline{r},t) \quad (1.4)$$

represent the deviation of the system away from the spatially homogeneous steady state concentration vector  $\underline{c}_0$ . The initial perturbation  $\underline{\zeta}(\underline{r},0)$  is assumed to be small in comparison with  $\underline{c}_0$ . If the system is stable, it is to be expected that the perturbed solutions  $\underline{c}(\underline{r},t)$  remain near the steady state solutions  $\underline{c}_0$  as time evolves. This is tantamount to saying that the fluctuations  $\underline{\zeta}(\underline{r},t)$  die out, (i.e.,  $\underline{\zeta}(\underline{r},t) \rightarrow 0$  as  $t \rightarrow \infty$ ).

The perturbed solutions (1.4) are substituted into equation (1.1) and a Taylor expansion of the resulting equation is made, which retains the terms to first order in the perturbation. This yields the variational equations



$$\frac{d\zeta_i}{dt} = \sum_{j=1}^n \left( \frac{\partial F_i}{\partial c_j} \right) \circ \zeta_j + D_i \nabla^2 \zeta_i, \\ i = 1, \dots, n \quad (1.5)$$

which are valid in a neighborhood of the steady state if the eigenvalues of the resulting matrix of the coefficients do not have zero real parts.

In the case that an eigenvalue with a zero real part occurs, the nonlinear terms of (1.1) must be included before stability can be determined. These solutions correspond to particular values of the constrained parameters  $\{K_i, A_i\}$  in a transformed parameter space  $\{\underline{h}, \underline{j}\}$ . The new parameters  $\{\underline{h}, \underline{j}\}$  are defined later in section 2.2. In any case, the nonlinear terms decide only whether the boundary is included in the unstable region or not, and the linearized equations are always valid up to the boundary. It is this boundary which will be determined in this analysis, for the model which is introduced in the next section.



### 1.3. The Belousov-Zhabotinski Reaction

In chemistry, one of the historically important oscillating reactions is the Belousov-Zhabotinski reaction, the cerium catalyzed oxidation of malonic acid by bromate in aqueous sulphuric acid. This reaction has steady state solutions to the kinetic equations, beyond an instability of the thermodynamic branch of solutions. These steady states if unstable, can give rise to the oscillation of the concentration of certain reagents in time. Indeed, this is the case as observed experimentally.<sup>23</sup> In addition, this reaction exhibits spacial structures in the form of travelling concentration bands, when the temporal oscillations are coupled with diffusion.<sup>1,11</sup>

The great interest in the Zhabotinski reaction caused the formation of a simple model, the Oregonator,<sup>24</sup> to explain the important features of the mechanism. This model consists of the following five steps:



where  $A = B = [\text{BrO}_3^-]$ ,  $P = [\text{HOBr}]$ ,  $X = [\text{HBrO}_2]$ ,  $Y = [\text{Br}^-]$ ,  $Z = [\text{Ce(IV)}]$  and  $Q = B + P$ .



In the original paper<sup>24</sup>  $z = [2\text{Ce(IV)}]$ , and the coefficients of 2 in front of  $z$  in steps (3) and (5) are left out. Several chemical reactions sum to form step (5), and the stoichiometric coefficient  $f$  represents experimental factors which are not yet determined. The actual value is thought to be close to 1, but Jwo and Noyes<sup>25</sup> found experimentally that  $f$  varied continuously in the range 0-2.

The Oregonator model (1.6) has been subjected to analysis by numerical integration techniques.<sup>24,26</sup> However, the analysis was complicated by the stiffness of the Oregonator kinetic equations. A good discussion of the difficulties encountered in numerical integration of stiff differential equations is given by Gelinas.<sup>27</sup> The model was later extended to include the reverse reactions.<sup>28</sup> Due to the oscillatory nature of the system, existence of a limit cycle was proposed and later proved analytically.<sup>29</sup>

The reversible model of (1.6) possesses a unique homogeneous stationary state which becomes unstable beyond a bifurcation point. The appearance of a second (periodic) solution to the kinetic equations then gives rise to stable homogeneous oscillations. These oscillations exhibit limit cycle behavior, and excitable dynamics. Turner<sup>30</sup> has demonstrated the existence of a hysteresis cycle between the stable stationary and oscillatory



states. An analysis of a more complicated model of the Zhabotinski reaction has been done by Clarke<sup>31,32</sup> with the reverse reactions omitted.

In the present analysis, the Oregonator model (1.6) with the reverse reactions is analyzed, with the variable stoichiometric coefficient  $f$  included. Even with such a simple model, the boundary between the stable and unstable steady states in the network is greatly complicated by the presence of the reverse reactions. Although these results are interesting in themselves, generalizations which increase the understanding of chemical network stability are also sought in this analysis.



Stability Theory for Chemical Networks2.1. Introduction

In this chapter, an analytic method developed by Clarke for determining the boundary of the unstable steady states in parameter space is explained. This theory is then applied to the model (1.6) and the results are given in Chapter 3. The effect of diffusion is neglected and only the homogeneous perturbation from steady state is considered. In this case the variational equations (1.5) are given in matrix notation as

$$\frac{d\zeta}{dt} = \underline{M} \zeta \quad (2.1)$$

where

$$M_{ij} = \left( \frac{\partial F_i}{\partial c_j} \right)_0$$

and  $\zeta = \underline{c} - \underline{c}_0$  represents a small fluctuation away from the steady state solution  $\underline{c}_0$ .  $\underline{M}$  is called the interaction matrix, and characterizes the linearized stability problem about steady state. The solutions of the matrix equation (2.1) in the case where  $\underline{M}$  is a constant  $n \times n$  matrix are found from the matrix<sup>33</sup>

$$\underline{\Phi}(t) = e^{\underline{M}(t-t_0)} \quad (2.2)$$



which is a principal matrix of solutions of (2.1). To understand the evolution of any initial  $\underline{\xi}$ , it is sufficient to calculate the matrix (2.2).

If  $\underline{\underline{P}}$  is a constant nonsingular matrix, the change of coordinates

$$\underline{\xi} = \underline{\underline{P}} \underline{x} \quad (2.3)$$

yields the equivalent system of differential equations

$$\dot{\underline{\xi}} = \underline{\underline{P}}^{-1} \underline{\underline{M}} \underline{\underline{P}} \underline{x} \quad (2.4)$$

which can be written as

$$\dot{\underline{\xi}} = \underline{\underline{A}} \underline{x} \quad (2.5)$$

where  $\underline{\underline{A}}$  is similar to  $\underline{\underline{M}}$ . It follows that the matrices  $\underline{\underline{A}}$  and  $\underline{\underline{M}}$  have the same characteristic polynomial

$$\det(\underline{\underline{I}}\underline{\omega} - \underline{\underline{M}}) = \det(\underline{\underline{I}}\underline{\omega} - \underline{\underline{A}}) \quad (2.6)$$

and so the eigenvalues are also the same. It is now sufficient to discuss the solutions of the system (2.5), whose fundamental matrix is

$$\underline{\underline{\Psi}} = e^{\underline{\underline{A}}t}$$

where one can consider that  $\underline{\underline{P}}$  is such that  $\underline{\underline{A}}$  is in Jordan canonical form.

When in Jordan canonical form,  $\underline{\underline{A}}$  is a block diagonal matrix where each block corresponds to one eigenvalue  $\omega_j$ ,



and each block has the structure<sup>34</sup>

$$\underline{A}_j = \begin{pmatrix} \underline{B}_{j1} & & & & \\ & \underline{B}_{j2} & & & \\ & & \ddots & & \\ & & & \ddots & \\ & & & & \underline{B}_{jr_i} \end{pmatrix} \quad (2.7)$$

where  $\underline{B}_{j1}, \underline{B}_{j2}, \dots, \underline{B}_{jr_i}$  are *basic Jordan blocks* belonging to the eigenvalue  $\omega_j$ . A basic Jordan block corresponding to  $\omega_j$  is a matrix with the structure

$$\underline{B}_{ji} = \begin{pmatrix} \omega_j & 1 & 0 & \dots & \dots & 0 \\ 0 & \omega_j & 1 & \dots & \dots & 0 \\ \vdots & & & & & \vdots \\ \vdots & & & & & \vdots \\ 0 & \dots & \dots & & & 1 \\ 0 & \dots & \dots & & & \omega_j \end{pmatrix} \quad (2.8)$$

Defined in this way, the dimension of the matrix  $\underline{A}_j$  corresponds to the *multiplicity*,  $\mu$ , of the eigenvalue  $\omega_j$ . The number of basic Jordan blocks  $r_i$  associated with an eigenvalue  $\omega_j$  is equal to the *nullity* of the eigenvalue  $\omega_j$ . The nullity,  $\nu$ , is defined as the number of linearly independent eigenvectors which correspond to an eigenvalue of multiplicity  $\mu$ .

The matrix  $e^{\underline{A}_j t}$  can be visualized by considering the structure of each block  $e^{\underline{B}_{ji} t}$  which can be written as



$$e^{\underline{A}jt} = \begin{pmatrix} 1 & t & t^2/2! & t^3/3! & \dots & \frac{t^{v-1}}{(v-1)!} \\ 0 & 1 & t & t^2/2! & \dots & \frac{t^{v-2}}{(v-2)!} \\ \vdots & & & & & \vdots \\ \vdots & & & & & \vdots \\ 0 & \dots & & & & 1 \end{pmatrix} \quad (2.9)$$

The solutions of (2.5) are linear combinations of the columns of  $e^{\underline{A}jt}$  and the solutions of (2.1) are obtained from (2.3).

If the eigenvalues are distinct then  $\underline{A}$  reduces to a diagonal matrix (each  $\underline{A}_j$  has one element,  $\omega_j$ ) and  $e^{\underline{A}t}$  has the form

$$e^{\underline{A}t} = \begin{pmatrix} e^{\omega_1 t} & 0 & 0 & \dots & 0 \\ 0 & e^{\omega_2 t} & 0 & \dots & 0 \\ \vdots & & & & \\ 0 & \dots & & & e^{\omega_n t} \end{pmatrix} \quad (2.10)$$

The solutions of (2.1) can now be written as

$$\xi(t) = \sum_{k=1}^n c_k \phi_k \quad (2.11)$$

where

$$\phi_k = p_k e^{\omega_k t}$$



$c_k$  is an arbitrary constant and  $\tilde{p}_k$  is a column vector of  $\underline{\underline{P}}$ .  $\tilde{p}_k$  is the eigenvector corresponding to the eigenvalue  $\omega_k$ , and satisfies

$$\underline{\underline{M}} \tilde{p}_k = \omega_k \tilde{p}_k \quad (2.12)$$

If the eigenvalues are not distinct, then each of the matrices  $\underline{\underline{B}}_{ji}$  which are of dimension  $s$ , say, contribute  $s$  linearly independent solutions of the form<sup>35</sup>

$$\tilde{\phi}_{j+m-1} = e^{\omega_j t} \sum_{k=1}^m \frac{t^{k-1}}{(k-1)!} \tilde{p}_{j+m-k}, \quad m = 1, \dots, s \quad (2.13)$$

to equation (2.11), which no longer has  $n$  linearly independent eigenvectors. Each of the solutions in (2.13) corresponds to a linearly independent solution of the degenerate eigenvalue  $\omega_j$ , given in terms of the generalized eigenvectors,<sup>36</sup>  $\tilde{p}_{j+m-k}$ , of the system. Each generalized eigenvector  $\tilde{p}_{j+m-k}$  satisfies the relation

$$(\underline{\underline{M}} - \omega_j)^m \tilde{p}_{j+m-k} = 0. \quad (2.14)$$

In particular, if  $m = 1$ , then equation (2.12) is obtained, and  $\tilde{p}_j$  is an eigenvector corresponding to  $\omega_j$ .

When the stability of these solutions is examined, it turns out that only the sign of the eigenvalue is of importance, since the factor  $e^{\omega_j t}$  dominates the series in  $t$ . However, if  $\omega_j$  is not distinct and has a zero



real part, then the series in  $t$  in equation (2.13) is important. The problem now reduces to an examination of the eigenvalues of  $\underline{\underline{M}}$ , determined by the equation

$$\det(\underline{\underline{I}}\omega - \underline{\underline{M}}) = 0. \quad (2.15)$$

This determinant has the associated characteristic polynomial,

$$p(\omega) = \det(\underline{\underline{I}}\omega - \underline{\underline{M}}) = \sum_{i=0}^n \alpha_i \omega^{n-i}, \quad (2.16)$$

and consequently the search for the eigenvalues of  $\underline{\underline{M}}$  is equivalent to finding the roots of the real polynomial (2.16).

In conclusion, the eigenvalues  $\omega$  determine the stability of the general steady state  $\underline{\underline{c}}_0$ . If all the eigenvalues have negative real parts, the solution is asymptotically stable. If one of the eigenvalues has a positive real part, the solution is unstable. If no eigenvalue has a positive real part, but some eigenvalue has a zero real part, nothing can be said since the nonlinear terms in (1.1) affect the stability.<sup>20</sup>

The eigenvalues  $\omega$  are a function of the rate constants and the concentrations of the reactants and possibly the products. Solution of the stability problem with the rate constants as the parameters is sometimes possible, but in general the algebra is considerably simplified if a new set of independent



parameters is chosen. These parameters are designated  $\underline{h}$  and  $\underline{j}$  and are introduced in section 2.2. The  $\underline{h}$ ,  $\underline{j}$  parameters were specifically chosen so that the interaction matrix  $\underline{\underline{M}}$  could be written as a bilinear form in  $\underline{h}$  and  $\underline{j}$ .

The next step in the analysis is to find a criterion which can guarantee the sign of the real parts of the eigenvalues of  $\underline{\underline{M}}$ . Such a criterion is provided by the Routh-Hurwitz conditions,<sup>37</sup> which are the subject of section 2.3. The Routh-Hurwitz criterion is based upon the signs of the Hurwitz determinants  $\Delta_\ell$ ,  $\ell = 1, \dots, m$ , whose elements are the coefficients  $\alpha_i$  in the characteristic polynomial of  $\underline{\underline{M}}$  given by equation (2.16); the  $i, j$  element in the  $\ell^{\text{th}}$  determinant is

$$(\Delta_\ell)_{ij} = \alpha_{2j-i}, \quad i < \ell, \quad j < \ell; \quad \text{if } 2j-i < 0 \text{ then}$$

$$\alpha_{2j-i} = 0, \quad (2.17)$$

and the criterion states that the real parts of the roots of  $p(\omega)$  are negative provided the Hurwitz determinants are all positive definite. Since the eigenvalues  $\omega$  change continuously with the parameters, the boundary between the stable and unstable states occurs when the largest real part of the eigenvalues of  $\underline{\underline{M}}$  is zero. Therefore, the boundary of the unstable states occurs when one of the Hurwitz inequalities

$$\Delta_\ell > 0 \quad \ell = 1, \dots, m \quad (2.18)$$

is first violated. (i.e.,  $\Delta_\ell = 0$  for some  $\ell$ .)



At this stage, the stability analysis has been reduced to the problem of finding the zeroes of the Hurwitz determinants, which are homogeneous polynomials in the elements of  $\underline{\underline{M}}$ . The approximate zeroes of the Hurwitz determinants are found by applying a method for finding the asymptotes of real power polynomial surfaces, which has been recently developed by Clarke.<sup>38</sup> The method is a generalization of Newton's Polygon which was first used in 1676 to find the roots of two variable polynomials by geometric considerations.<sup>39</sup> The application of this theory to the chemical stability problem yields an equation for the asymptotic boundary of the unstable states in parameter space and is discussed in section 2.4. In addition to the analytic theory of section 2.4, a diagrammatic approach is used to summarize the connection between the terms in  $\underline{\underline{M}}$  and the boundary of instability. These aspects of the theory are introduced in section 2.5.

The method used here can be applied to interaction matrices outside the field of chemical kinetics. In particular, an application was made to the Rayleigh-Benard instability of a binary mixture.<sup>6</sup> The complications introduced in the more general case will not be considered in this thesis, however.



## 2.2. Chemical Network Parameters

The chemical stability problem is usually set up with the rate constants as the independent parameters. However, in this case the interaction matrix usually has elements which are irrational polynomials in the rate parameters. This complication can be avoided by a judicious choice of a new set of independent parameters.

Given the rate constant  $k$  for each reaction, the steady state concentrations and the rate of each reaction are determined, and can be used as an alternate set of independent parameters  $(\underline{c}_0, \underline{v}^0)$  which corresponds to  $(\underline{k}, \underline{\epsilon})$  where  $\epsilon$  labels the possibly multiple steady states. Any steady state velocity vector  $\underline{v}^0$  may be represented as a sum of contributions from various independent overall reaction processes conserving the given steady state. These processes form a reference set of velocity vectors called the *extreme currents*. The coefficients in this sum are called the *currents*,  $j_k$ , and form a new set of independent parameters for the system, which must be positive to represent a physical reaction process.

The new set of parameters can also be denoted by  $(\underline{h}, \underline{j})$  where  $\underline{h}$  has components which are the reciprocal of the steady state concentrations and  $\underline{j}$  has components



which are the currents of the system. As will be shown below, this choice of independent parameters reduces the interaction matrix to a bilinear form in  $(\tilde{h}, \tilde{j})$  and then the expansion of the characteristic polynomial of  $\underline{\underline{M}}$  is homogeneous in the parameters of the system:

$$\underline{\underline{M}} = \sum_{k=1}^n j_k \underline{\underline{M}}^{(k)}$$

where

$$m_{ij}^{(k)} = s_{ij}^{(k)} h_j, \quad (2.19)$$

and the summation is over the  $n$  currents,  $j_k$ , of the system.

The matrix  $\underline{\underline{S}}^{(k)}$  has elements which are some pure numbers. The important point to note is that the stability of any state  $(\tilde{k}, \epsilon)$  is identical to the stability of any of the associated states  $(\tilde{h}, \tilde{j})$ . Therefore, finding the region of instability in  $(\tilde{h}, \tilde{j})$  space will determine the region of  $\tilde{k}$ -space which is unstable. The rest of this section is devoted to deriving the current parameters specifically and illustrating the theory with relevant examples.

The equations of motion (1.1) for any chemical system can be written in matrix notation as

$$\frac{dc}{dt} = \underline{\underline{V}} \tilde{v}, \quad (2.20)$$



where  $\underline{v}$  is a constant matrix reflecting stoichiometric effects in the kinetic equations, and  $\underline{v} = (v_1, v_2, \dots, v_r)$  where  $v_k$  is the velocity of the  $k^{\text{th}}$  reaction.

If there are  $n$  independent internal species, (i.e., the dependent species have been eliminated) then  $\underline{v}$  is a  $n \times r$  constant matrix. The steady state condition becomes

$$\underline{v} \cdot \underline{v} = 0, \quad (2.21)$$

and the velocity vectors which satisfy this equation will be denoted by  $\underline{v}^0$ . Any general steady state of the network is represented by a vector  $\underline{v}^0$ .

Since the  $n$  species are independent, the rows of  $\underline{v}$  span a  $n$ -dimensional subspace  $S$  which is orthogonal to the  $r-n$  dimensional complementary subspace  $S_{\perp}$ , in which  $\underline{v}^0$  lies.<sup>31</sup> All this means, is that the solutions  $\underline{v}^0$  must be orthogonal to the subspace in which  $\underline{v}$  lies. As a result, the steady states  $\underline{v}^0$  can be expressed in terms of any basis set which spans  $S_{\perp}$ :

$$\underline{v}^0 = \sum_{k=1} \mathbf{j}_k \underline{v}_k, \quad (2.22)$$

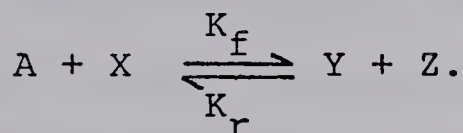
where the  $\mathbf{j}_k$  are some arbitrary constants. The minimal basis set for  $S_{\perp}$  will contain  $r-n$  basis vectors.

However, there is a directional requirement on the velocity of a reaction,

$$v_i \geq 0, \quad i = 1, \dots, r, \quad (2.23)$$



which is necessary if the reaction is to occur in the direction as written. A component of  $\underline{v}$  which is negative has no physical meaning: it is not equivalent to the reverse of a reaction. Take for example the reaction



The velocity of the forward reaction is  $K_f AX$  while the velocity of the reverse reaction is  $K_r YZ$ . These rates are only equal at equilibrium. At a non-equilibrium steady state (open system) the rates are not equal, and it is this lack of symmetry in the flow of matter that complicates the dynamics of chemical systems. In a reversible network, each reaction and its reverse must be treated as two separate reactions, each with its own non-negative velocity  $v_i$ .

The conditions (2.23) on the velocity components place a restriction on the choice of the basis set of vectors  $\underline{i}$ , because  $\underline{v}^0$  must now be expressed as a positive linear combination of  $\underline{i}$ :

$$\underline{v}^0 = \sum_k j_k \underline{i}_k, \quad j_k \geq 0. \quad (2.24)$$

Each of the conditions (2.23) determines a halfspace which passes through the origin. The solutions of (2.21) will have to lie in a subspace of the convex polyhedral



cone defined by the intersection of the halfspaces (2.23). With this restriction, the correct set of basis vectors (2.24) necessary to span the solution space of  $\tilde{v}^0$  are found, although this basis is not necessarily the minimal one.

When the steady state velocity vector is expressed as in (2.24), the  $j_k$  are a positive, unrestricted set of parameters which satisfy the steady state condition (2.21) subject to (2.23). The  $j_k$  in (2.24) are therefore the required *current* parameters. The associated set of basis vectors  $\{\tilde{i}_k\}$  of  $S_\perp$  are called the *extreme currents* and are a reference set of currents for the network.<sup>29</sup>

The complete set of extreme currents defines a set of halflines which extend from the origin in the direction given by each of the vectors  $\tilde{i}_k$ . This set of halflines determines a set of halfspaces whose intersection is a convex cone, denoted by  $C_C$ . The set of halflines which form the edges of this cone are said to span the cone and together they define the cone's frame.<sup>40</sup> The points which lie on the surface or interior of  $C_C$  are the physically acceptable solutions of (2.21),  $\tilde{v}^0 \in C_C$ , and satisfy (2.24).  $C_C$  is called the system's *steady state current cone*,<sup>29</sup> and lies in the  $r-n$  dimensional subspace  $S_\perp$ .



The intersection of the current cone  $C_C$  with the unit hyperplane,

$$\tilde{v}^0 \cdot (1, 1, \dots, 1) = 1, \quad (2.25)$$

yields a convex polytope, called the *current polytope*  $\Pi_C$ . All steady states on a line through the origin in  $C_C$  are mapped into a single point in  $\Pi_C$ , and the extreme points of the current polytope are the extreme currents. Any general steady state velocity vector  $\tilde{v}^0$  of the network is given by

$$\tilde{v}^0 = \lambda \sum_k j'_k \tilde{z}'_k, \quad (2.26)$$

where

$$\sum_k j'_k = 1, \quad j'_k \geq 0,$$

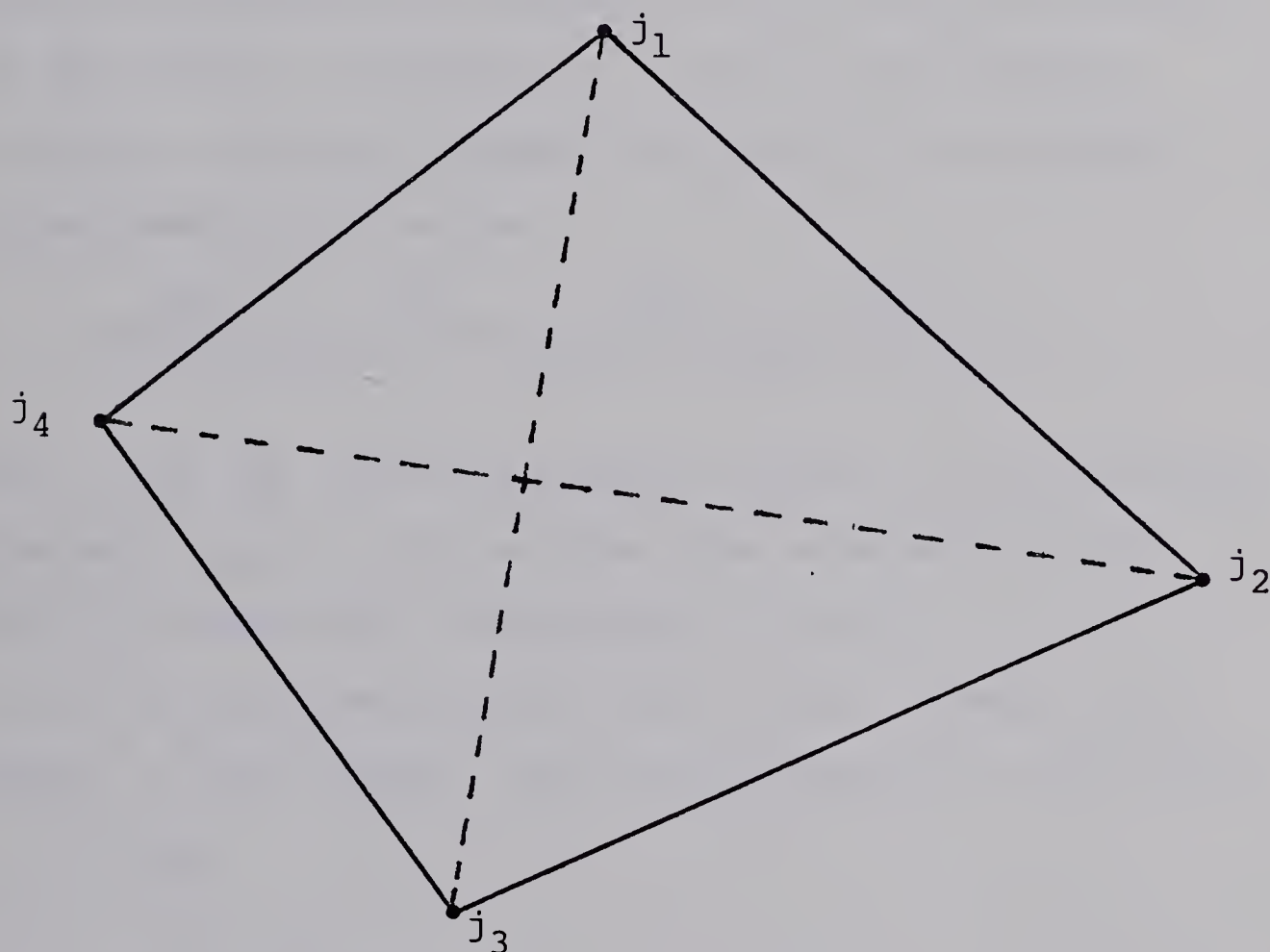
$$\tilde{z}'_k = \frac{i_k}{|i_k|},$$

and  $\lambda$  is a scaling factor.

The current polytope is a cross-section of the current cone and lies in a subspace of one less dimension ( $r-n-1$ ). The important thing to note is that all steady states in  $C_C$  on a line through the origin have the same stability by virtue of (2.19), and so need not be distinguished. The significance of the current polytope is that it can be used to decompose the full



stability problem into a sum of smaller ones, by a procedure called *simplicial decomposition*.<sup>41</sup> This method is typically used for reducing the dimension of the stability problem when the complete set of extreme currents is larger than the minimal basis set, as often occurs in practice. For example, take the current polytope consisting of four points in the plane as follows:

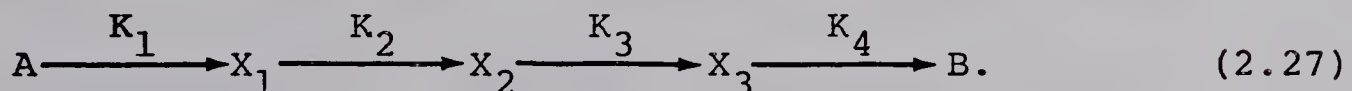


where each of the points  $j_1$  to  $j_4$  corresponds to an extreme current of the network. Either of the diagonal lines joining  $j_1j_3$  or  $j_2j_4$  can be used to form two simplices (triangles) consisting of three points. The stability problem can now be solved for any point in



the plane by using the current parameters determined by the simplex in which it lies. This reduces the number of current parameters needed in the interaction matrix by one.

In order to illustrate the concept of an extreme current, two simple examples will be discussed next. Then an extreme current of the Oregonator model (1.6) will be derived as an example of those which are found in the results of Chapter 3. As the first example, consider a reaction network consisting of a stepwise transformation of matter:



The  $x_i$  are the internal species and the A, B are external species.  $K_1, \dots, K_4$  are the rate constants of the reaction steps with corresponding velocity  $v_1, \dots, v_4$ . It can be seen immediately that only one steady state exists in this system, and the requirement on the rates  $v_i$  is that

$$v_1 = v_2 = v_3 = v_4 .$$

The matrix of the net stoichiometric coefficients for (2.27) is

$$\underline{v} = \begin{pmatrix} 1 & -1 & 0 & 0 \\ 0 & 1 & -1 & 0 \\ 0 & 0 & 1 & -1 \end{pmatrix}$$



and the equations of motion are

$$\frac{d\tilde{x}}{dt} = \underline{\underline{v}}\tilde{v},$$

where  $v$  can be written explicitly in terms of its components as  $v_1 = K_1 A$ ,  $v_2 = K_2 x_1$ ,  $v_3 = K_3 x_2$ ,  $v_4 = K_4 x_3$  and  $x_i$  is the concentration of the  $i^{\text{th}}$  species. The steady state solutions are the velocity vectors  $\tilde{v}^0$  which satisfy

$$\underline{\underline{v}} \cdot \tilde{v}^0 = 0, \quad v_i^0 \geq 0. \quad (2.28)$$

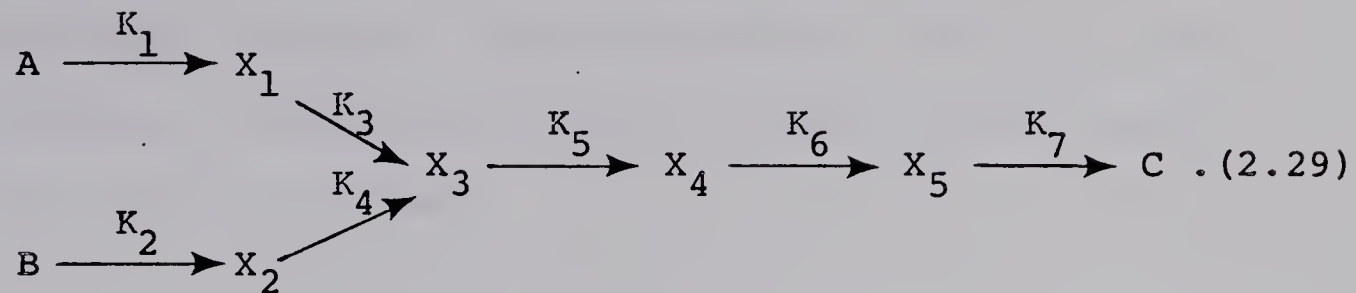
The rows of  $\underline{\underline{v}}$  span a three dimensional subspace of the four dimensions of  $\tilde{v}$ . Therefore, solutions of (2.28) are the vectors  $\tilde{v}^0$  which lie in the one dimensional subspace orthogonal to  $\underline{\underline{v}}$ . The current cone  $C_C$  for this system is a single vector which extends in the direction  $\tilde{i}_1 = (1, 1, 1, 1)$  from the origin, where  $\tilde{i}_1$  is the extreme current for the network (2.27). The intersection of  $C_C$  with the unit hyperplane given by  $\tilde{v}^0 \cdot (1, 1, 1, 1) = 1$ , yields the current polytope  $\Pi_C$  for the system, which in this case is a single point, representing the extreme current  $\tilde{i}_1$ . This is the simplest convex set consisting of one extreme point only. The general steady state solution is a constant multiple of  $\tilde{i}_1$ ,

$$\tilde{v}^0 = j_1 \tilde{i}_1, \quad j_1 \geq 0,$$



where  $j_1$  is an arbitrary constant.

As a second example, consider the reaction sequence



Once again the internal species are denoted by  $x_i$ , while the external species are A, B, C. In this case two alternate extreme reaction sequences are seen which can satisfy the steady state requirement:

$$v_1 = v_3 = v_5 = v_6 = v_7$$

$$v_2 = v_4 = v_5 = v_6 = v_7 .$$

Here the subscript on  $v_i$  corresponds to the  $K_i$  marked in (2.29). These sequences correspond to two extreme currents:

$$\underline{\underline{i}}_1 = (1, 0, 1, 0, 1, 1, 1)$$

$$\underline{\underline{i}}_2 = (0, 1, 0, 1, 1, 1, 1)$$

which are obtained by solving (2.28) with the net stoichiometric matrix

$$\underline{\underline{v}} = \begin{pmatrix} 1 & 0 & -1 & 0 & 0 & 0 & 0 \\ 0 & 1 & 0 & -1 & 0 & 0 & 0 \\ 0 & 0 & 1 & 1 & -1 & 0 & 0 \\ 0 & 0 & 0 & 0 & 1 & -1 & 0 \\ 0 & 0 & 0 & 0 & 0 & 1 & -1 \end{pmatrix}$$



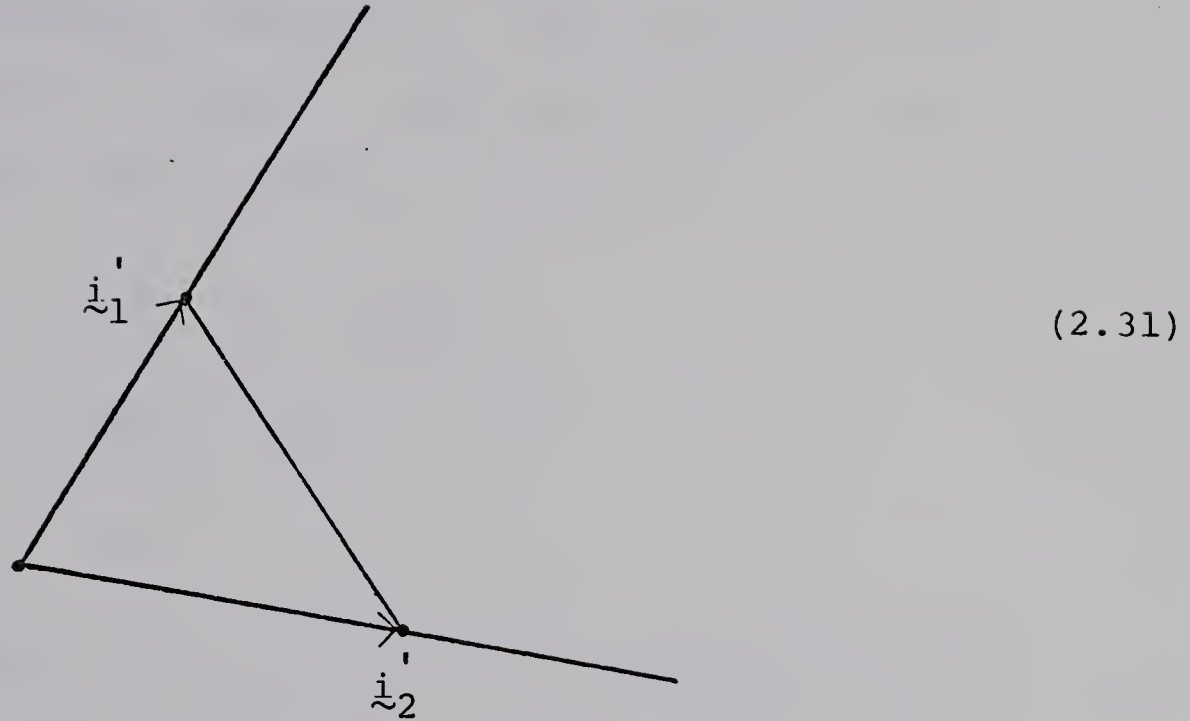
and where  $\mathbf{y} = (v_1, v_2, v_3, v_4, v_5, v_6, v_7)$ .

In this example, the null space of (2.28) is a 2-dimensional subspace, and the extreme currents  $\mathbf{i}_1$  and  $\mathbf{i}_2$  determine two halflines which span the current cone  $\mathcal{C}_C$  which lies in a plane:



Once again, the intersection of the current cone with the unit hyperplane yields the current polytope  $\Pi_C$  for the system, which in this case is a line segment:





whose endpoints are the extreme currents  $\dot{i}_1'$  and  $\dot{i}_2'$ .

Any general steady state solution for the system (2.29) lies on this line segment according to

$$\dot{z}^o = \lambda (j_1' \dot{i}_1' + j_2' \dot{i}_2'), \quad j_1', j_2' \geq 0,$$

where  $\lambda \geq 0$ , is some scaling factor and  $j_1' + j_2' = 1$ .

In other words (2.25) has the effect of projecting the points which lie in the plane (2.30) into the line in (2.31). This is valid because the steady states lying on a line through the origin in  $C_C$  have the same stability.

The final example will be drawn from the Oregonator model (1.6). The extreme current derived here occurs in both the reversible and irreversible models, and is



one of the important sources of instability in the analysis presented in Chapter 3. For this reason, the treatment will be detailed. From the Oregonator reactions in (1.6), the equations of motion are

$$\begin{aligned}\dot{X} &= k_1 Y - k_2 XY + k_3 X - 2k_4 X^2 \\ \dot{Y} &= -k_1 Y - k_2 XY + fk_5 Z \\ \dot{Z} &= 2k_3 X - 2k_5 Z\end{aligned}\quad (2.32)$$

where the external reactants A and B are included in the rate constants  $k_i$ , so that the network can be considered an open system depending on the three dynamic concentrations X, Y and Z. The k's are written explicitly as

$$k_1 = K_1 A, \quad k_2 = K_2, \quad k_3 = K_3 B, \quad k_4 = K_4 \quad \text{and} \quad k_5 = K_5.$$

In the usual matrix notation, these equations become

$$\frac{d\tilde{c}}{dt} = \underline{\underline{v}} \cdot \tilde{v},$$

where  $\tilde{c} = (X, Y, Z)$  is the concentration vector,  $\underline{\underline{v}}$  is the net stoichiometric matrix,

$$\underline{\underline{v}} = \begin{pmatrix} 1 & -1 & 1 & -2 & 0 \\ -1 & -1 & 0 & 0 & f \\ 0 & 0 & 2 & 0 & -2 \end{pmatrix},$$

and  $\tilde{v}$  is the velocity vector whose components are



$$v_1 = k_1 Y, v_2 = k_2 XY, v_3 = k_3 X, v_4 = k_4 X^2, v_5 = k_5 Z. \quad (2.33)$$

Every steady state satisfies

$$\underline{v} \cdot \underline{v}^0 = 0, \quad v_i^0 \geq 0. \quad (2.28)$$

The rows of  $\underline{v}$  span a three dimensional subspace  $S$  which is orthogonal to the complementary 2-dimensional subspace  $S_\perp$  in which  $\underline{v}^0$  lies. It follows from the preceding discussion that the current cone  $C_C$  is 2-dimensional and that the current polytope  $\Pi_C$  is one dimensional. The net result is that only two extreme currents can exist in this case and they are the extreme points of the line segment  $\Pi_C$ .

Two features of this model are different from the usual case. First the stoichiometric parameter  $f$  in reaction (5) is included in  $\underline{v}$ , and secondly the reactions (1.6) are not linearly independent. In this example, only the case  $f > 1$  is considered, and further details are left until Chapter 3. The singular nature of  $\underline{v}$  is overcome by utilizing the condition for normalization of the velocity in an extreme current,

$$\sum_i v_i^0 = 1, \quad (2.34)$$

in addition to (2.28). The condition (2.34) provides an extra equation



$$(1, 1, 1, 1, 1) \cdot \underline{\underline{v}}^O = 1$$

and can be combined with (2.28) to yield

$$\underline{\underline{v}}' \cdot \underline{\underline{v}}^O = \underline{\underline{b}}' \quad (2.35)$$

where

$$\underline{\underline{v}}' = \begin{pmatrix} 1 & -1 & 1 & -2 & 0 \\ -1 & -1 & 0 & 0 & f \\ 0 & 0 & 2 & 0 & -2 \\ 1 & 1 & 1 & 1 & 1 \end{pmatrix}.$$

and the transpose of  $\underline{\underline{b}}'$  is the vector  $(0, 0, 0, 1)$ .

One may show that the extreme solutions of (2.35) are found by deleting all possible combinations of columns (reactions) of  $\underline{\underline{v}}'$  until no steady state remains. When the particular columns 1, 2, 3, and 5 are chosen, equation (2.35) becomes

$$\begin{pmatrix} 1 & -1 & 1 & 0 \\ -1 & -1 & 0 & f \\ 0 & 0 & 2 & -2 \\ 1 & 1 & 1 & 1 \end{pmatrix} \begin{pmatrix} v_1^O \\ v_2^O \\ v_3^O \\ v_5^O \end{pmatrix} = \begin{pmatrix} 0 \\ 0 \\ 0 \\ 1 \end{pmatrix}.$$

Solving these relations for  $\underline{\underline{v}}^O$  yields the extreme current

$$\underline{\underline{i}}_A = \underline{\underline{v}}^O = \left( \frac{f-1}{2}, \frac{f+1}{2}, 1, 0, 1 \right), \quad f \geq 1, \quad (2.36)$$



and the scaling factor  $1/f+2$ , where  $\tilde{i}_A' = 1/f+2 \tilde{i}_A$  from (2.26).

The extreme current  $\tilde{i}_A$  represents a steady state of the system in which

$$v_1^o = \frac{f-1}{2} = k_1 Y_o$$

$$v_2^o = \frac{(f+1)}{2} = k_2 X_o Y_o$$

$$v_3^o = 1 = k_3 X_o$$

$$v_5^o = 1 = k_5 Z_o$$

for the current  $j_A = 1$  M/sec. The mapping between the rate constants and the steady state concentrations  $X_o$ ,  $Y_o$ ,  $Z_o$  for  $\tilde{i}_A$  can be written from the equations above as:

$$k_1 = \frac{(f-1)}{2Y_o}, \quad k_2 = \frac{(f+1)}{2X_o Y_o}, \quad k_3 = \frac{1}{X_o}, \quad k_5 = \frac{1}{Z_o}.$$

Substituting these relations into equations (2.32) now yields the following set of dynamic equations:

$$\begin{aligned} \dot{X} &= \left(\frac{f-1}{2Y_o}\right) Y - \left(\frac{f+1}{2X_o Y_o}\right) XY + \left(\frac{1}{X_o}\right) X \\ \dot{Y} &= - \left(\frac{f-1}{2Y_o}\right) Y - \left(\frac{f+1}{2X_o Y_o}\right) XY + \left(\frac{f}{Z_o}\right) Z \\ \dot{Z} &= \left(\frac{2}{X_o}\right) X - \left(\frac{2}{Z_o}\right) Z. \end{aligned}$$

At this stage it can be seen that the extreme current  $\tilde{i}_A$  represents the full nonlinear kinetic equations for the reactions (1), (2), (3) and (5) of the Oregonator model (1.6).



The interaction matrix  $\underline{\underline{M}}_A$  can be written for this extreme current as follows. Consider an arbitrary perturbation  $\underline{\zeta} = (\Delta X, \Delta Y, \Delta Z) = (X - X_0, Y - Y_0, Z - Z_0)$  about the steady state  $(X_0, Y_0, Z_0)$  and neglect the nonlinear terms, then the equations

$$\begin{aligned}\dot{\Delta X} &= \left(\frac{f-1}{2}\right) \Delta Y / Y_0 - \left(\frac{f+1}{2}\right) \Delta Y / Y_0 - \left(\frac{f+1}{2}\right) \Delta X / X_0 + \Delta X / X_0 \\ \dot{\Delta Y} &= - \left(\frac{f-1}{2}\right) \Delta Y / Y_0 - \left(\frac{f+1}{2}\right) \Delta Y / Y_0 - \left(\frac{f+1}{2}\right) \Delta X / X_0 + f \Delta Z / Z_0 \\ \dot{\Delta Z} &= 2 \Delta X / X_0 - 2 \Delta Z / Z_0\end{aligned}$$

are obtained. If new variables are defined by  $h_x = 1/X_0$ ,  $h_y = 1/Y_0$ ,  $h_z = 1/Z_0$ , then these equations are equivalent to equation (2.1) where  $\underline{\underline{M}}_A$  is given by (2.19) for  $j_k = j_A$ .  $\underline{\underline{M}}_A$  is written explicitly as follows:

$$\underline{\underline{M}}_A = \begin{pmatrix} -\left(\frac{f-1}{2}\right) h_x & -h_y & 0 \\ -\left(\frac{f+1}{2}\right) h_x & -fh_y & fh_z \\ 2h_x & 0 & -2h_z \end{pmatrix}, \quad f \geq 1. \quad (2.37)$$

Each extreme current  $\underline{i}_k$  of the system has an associated matrix  $\underline{\underline{M}}_k$  which appears in the interaction matrix  $\underline{\underline{M}}$  as a weighted sum,  $j_k \underline{\underline{M}}_k$ , as stated in equation (2.19).

For the irreversible model (1.6) two more extreme currents were similarly found:

$$\begin{aligned}\underline{i}_B &= (0, f, 1, \frac{1-f}{2}, 1), \quad f \leq 1 \\ \underline{i}_C &= (f, 0, 1, \frac{1+f}{2}, 1), \quad \text{all } f.\end{aligned} \quad (2.38)$$



In each region of  $f$ , the elements of the interaction matrix  $\underline{\underline{M}}$  are a sum of the elements occurring in each matrix  $\underline{\underline{M}}_k$  corresponding to an extreme current  $\underline{\underline{i}}_k$ , as follows:

$$\underline{\underline{M}} = \begin{cases} j_A \underline{\underline{M}}_A + j_C \underline{\underline{M}}_C, & f \geq 1 \\ j_B \underline{\underline{M}}_B + j_C \underline{\underline{M}}_C, & f \leq 1. \end{cases}$$

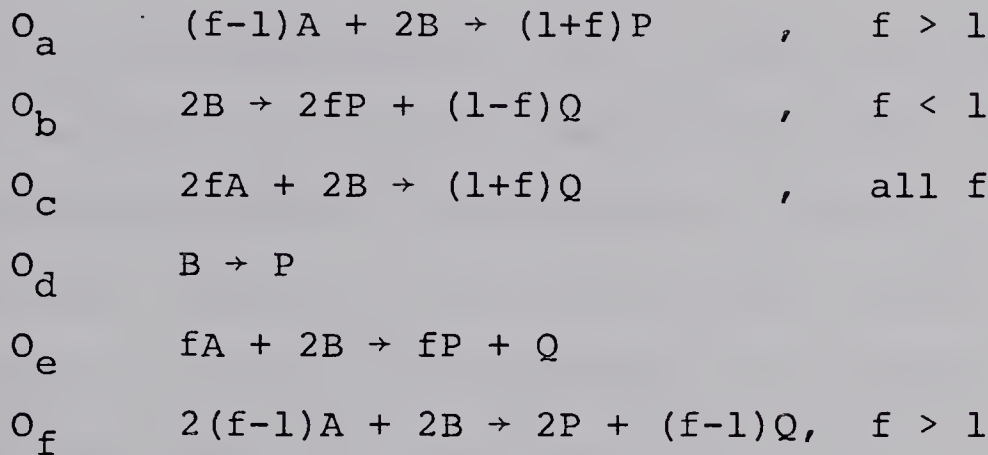
Note that  $\underline{i}_A = \underline{i}_B$  at  $f = 1$  as required by continuity of the solution of  $f = 1$ .

The above procedure for obtaining the interaction matrix from the net stoichiometric matrix is completely analytic. In the case of complex reaction networks, a computer program exists which calculates all the extreme currents, by the procedure given above.<sup>42</sup> The representation of the general steady state of the network as a positive linear combination of the extreme currents, guarantees that the correct overall stoichiometry is obtained for the net chemical change of the external species. To illustrate this important result, the irreversible Oregonator model will be used as an example of the difficulties which may arise in finding the correct overall reaction in a network.

The original claim that the Oregonator generates the unique stoichiometry  $fA + 2B \rightarrow 2P + Q$  for the net reaction, has been corrected by Noyes.<sup>43</sup> In his



discussion, the correct overall reaction is given as a positive linear combination of any two of the following steps, except  $O_c$  or  $O_f$



in the system's oscillatory region.

The steps  $O_d$  to  $O_f$  represent some of the possible overall reactions which can occur when the network (1.6) is at steady state. It can be shown, using the extreme currents for this network that only the steps  $O_a$  to  $O_c$  are necessary, and any general steady state of the network is a positive linear combination of either  $O_a$  and  $O_c$  or  $O_b$  and  $O_c$ . Since any general steady state in the network is a positive linear combination of the extreme currents, the general overall reaction can be written as a positive linear combination of the extreme overall reactions. The extreme overall reactions are obtained directly from the extreme currents which represent a particular linear combination of the reactions in the network. For example,  $2\tilde{i}_A = (f-1, f+1, 2, 0, 2)$  from equation (2.36) represents a possible steady state of



the network consisting of a sum of reactions (1), (2), (3) and (5) as follows:

$$(f-1)(R1) + (f+1)(R2) + 2(R3) + 2(R5)$$

where  $\dot{i}_A$  is multiplied by two to remove fractions. When the reactions in (1.6) are substituted into this sum, the extreme overall reaction given in step  $O_a$  above is obtained. Similarly, when the extreme currents  $\dot{i}_B$  and  $\dot{i}_C$  given in (2.38) are considered, the extreme overall reactions found, can be identified with the stoichiometries  $O_b$  and  $O_c$  above, respectively. Since any general steady state of the network is a positive linear combination of  $\dot{i}_A$  and  $\dot{i}_C$  for  $f > 1$ , step  $O_f$  above can be expressed in terms of  $\dot{i}_A$  and  $\dot{i}_C$  as follows

$$\left(\frac{2}{1+f}\right) \dot{i}_A + \left(\frac{f-1}{1+f}\right) \dot{i}_C , \quad f > 1. \quad (2.39)$$

The step  $O_e$  which is valid in both regions of  $f$  represents the following linear combination of the extreme currents:

$$\left(\frac{f}{1+f}\right) \dot{i}_A + \left(\frac{1}{1+f}\right) \dot{i}_C , \quad f > 1$$

$$\dot{i}_B + \dot{i}_C , \quad f < 1$$

$$\dot{i}_B + \dot{i}_C = \dot{i}_A + \dot{i}_C , \quad f = 1$$

Finally, the step  $O_d$  represents the extreme overall reaction for the extreme currents  $\dot{i}_A$  or  $\dot{i}_B$  at  $f = 1$ .

(Recall  $\dot{i}_A = \dot{i}_B$  at  $f = 1$ .)

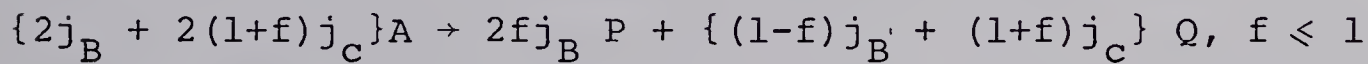
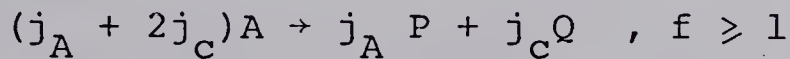


In summary, the extreme overall reactions are  $O_a$ ,  $O_b$  and  $O_c$ . Any general steady state of the network (1.6) has an overall reaction which is some positive linear combination of the extreme overall reactions; in particular for each region of  $f$ :

$$j'_A O_A + j'_C O_C , j'_A + j'_C = 1, \quad f \geq 1$$

$$j'_B O_B + j'_C O_C , j'_B + j'_C = 1, \quad f \leq 1$$

where  $j_k$  is the current corresponding to the extreme current  $i_k$ . Since  $A = B = [BrO_3^-]$ ,  $B$  can be eliminated from the overall reactions represented by these relations as follows:



The ratio of the currents for the network (1.6) can be determined from these equations if it is known whether  $f$  is greater or less than one, for example:

$j_A:j_C$  is in the ratio  $P:Q \quad f \geq 1$ .

Any particular steady state of the network is represented by a certain ratio of currents, and has a corresponding overall reaction which is a sum of extreme overall reactions. The extreme currents have determined the overall reaction stoichiometry without any assumptions



being necessary.

Using the relative rates of the reactions, Noyes<sup>43</sup> concluded  $O_c$  and  $O_f$  were not permissible overall reactions in the systems oscillatory region. From the analysis of the Oregonator model (1.6) in Chapter 3, it will be shown that  $\tilde{i}_c$  is a stable extreme current and so  $O_c$  would represent the extreme overall reaction of a stable steady state for any value of the rate constants. Step  $O_f$ , on the other hand, contains the extreme current  $\tilde{i}_A$  which is the source of instability for  $f \geq 1$ . The stability of the steady states represented by the extreme overall reaction  $O_f$  will therefore depend on the instability conditions defining the boundary of the unstable region, which will give the necessary condition on the ratio  $j_A/j_c$  for which the linear combination  $j_A \tilde{i}_A + j_c \tilde{i}_c$  is an unstable steady state for any particular set of rate constants.



### 2.3. Application of the Stability Criterion

Once the interaction matrix  $\underline{\underline{M}}$  has been derived, the characteristic polynomial (2.16) is known. The network is stable if all perturbations from the steady state decay, or alternately, the eigenvalues of  $\underline{\underline{M}}$  have negative real parts. This can only occur if all the Routh-Hurwitz conditions are satisfied. The theorem of Routh-Hurwitz will now be given, as well as the explicit form of the Hurwitz determinants,  $\Delta_\ell$ , defined in equation (2.17).

The criterion of Routh-Hurwitz states<sup>37</sup> that all the roots of the real polynomial  $p(\omega) = \alpha_0 \omega^n + \alpha_1 \omega^{n-1} + \dots + \alpha_n$  ( $\alpha_0 \neq 0$ ) have negative real parts if and only if the inequalities

$$\alpha_0 \Delta_1 > 0, \Delta_2 > 0, \alpha_0 \Delta_3 > 0, \dots, \begin{cases} \alpha_0 \Delta_n > 0, & n \text{ odd} \\ \Delta_n > 0, & n \text{ even} \end{cases}$$

all hold. The  $\Delta$ 's can be written explicitly if  $\alpha_0 > 0$  as follows:

$$|\alpha_1| > 0, \begin{vmatrix} \alpha_1 & \alpha_3 \\ \alpha_0 & \alpha_2 \end{vmatrix} > 0, \begin{vmatrix} \alpha_1 & \alpha_3 & \alpha_5 \\ \alpha_0 & \alpha_2 & \alpha_4 \\ \vdots & \alpha_1 & \alpha_3 \end{vmatrix} > 0, \dots,$$

$$\begin{vmatrix} \alpha_1 & \alpha_3 & \alpha_5 & \cdot & \cdot & \cdot & \cdot & \alpha_0 \\ \alpha_0 & \alpha_2 & \alpha_4 & \cdot & \cdot & \cdot & \cdot & \alpha_1 \\ \vdots & \vdots & \vdots & \cdot & \cdot & \cdot & \cdot & \vdots \\ \alpha_0 & \alpha_0 & \alpha_0 & & & & & \alpha_n \end{vmatrix} > 0 \quad .$$



In the case  $\alpha_0 > 0$ , an alternate set of necessary and sufficient conditions, the Liénard-Chipart stability criterion, is available. This theorem states<sup>37</sup> that for all the roots of the real polynomial  $p(\omega) = \alpha_0 \omega^n + \alpha_1 \omega^{n-1} + \dots + \alpha_n (\alpha_0 > 0)$  to have negative real parts, the necessary and sufficient conditions can take any of the following forms:

- i)  $\alpha_n > 0, \alpha_{n-2} > 0, \dots; \Delta_1 > 0, \Delta_3 > 0, \dots$
- ii)  $\alpha_n > 0, \alpha_{n-2} > 0, \dots; \Delta_2 > 0, \Delta_4 > 0, \dots$
- iii)  $\alpha_n > 0, \alpha_{n-1} > 0, \alpha_{n-3} > 0, \dots; \Delta_1 > 0, \Delta_3 > 0, \dots$
- iv)  $\alpha_n > 0, \alpha_{n-1} > 0, \alpha_{n-3} > 0, \dots; \Delta_2 > 0, \Delta_4 > 0, \dots$

(2.40)

The advantage in using one of these sets of conditions is that the analysis of a higher order Hurwitz determinant is avoided. (In this analysis,  $\Delta_3$ .)

When the Liénard-Chipart conditions are applied to the characteristic polynomial (2.16) for  $\underline{M}$ , a set of stability inequalities,  $f_p(\underline{p}) > 0, p = 1, \dots, k$ , are obtained from (2.40) which are polynomials in the parameters of the system,  $\underline{p} = (\underline{h}, \underline{j})$ . Network instability occurs in regions of parameter space where at least one of the inequalities  $f_p(\underline{p}) > 0$  is violated. Therefore, the region of parameter space where any of the polynomials  $f_p(\underline{p})$  is negative is part of the system's unstable region, and the various portions of its boundary are given by  $f_p(\underline{p}) = 0$  for some  $p$ . A method for finding the approximate solutions to



the equations  $f_{\rho}(\tilde{p}) = 0$  has been developed by Clarke<sup>38</sup> and is the subject of the next section. Since the method applies to every stability inequality, the subscript  $\rho$  will be dropped from  $f_{\rho}(\tilde{p})$  in the future.



## 2.4. Conditions for Instability

The unstable region of the network, denoted by  $f(\underline{p}) < 0$  in the previous section, is bounded in parameter space by the surface defined by  $f(\underline{p}) = 0$ . The necessary approximation to this surface is obtained as a set of asymptotes in the theory which follows. First, however, an example from the Oregonator model (1.6) will be used to show the motivation behind the development of such a theory.

We shall consider the polynomial obtained for  $\Delta_2$  from the interaction matrix  $\underline{\underline{M}}_A$  given in (2.37). For convenience, consider the case  $f = 1.1$ , then the characteristic equation for  $\underline{\underline{M}}_A$  becomes

$$\det(\underline{\underline{I}}\omega - \underline{\underline{M}}_A) = \begin{pmatrix} \omega + 5.0 \times 10^{-2}x & y & 0 \\ 1.05x & \omega + 1.1y - 1.1z & \\ -2x & 0 & \omega + 2z \end{pmatrix} \quad (2.41)$$

where new variables  $x = j_A h_x$ ,  $y = j_A h_y$ ,  $z = j_A h_z$  have been defined. Expanding this determinant yields the characteristic polynomial

$$\begin{aligned} p(\omega) &= \omega^3 + \omega^2 \{5.0 \times 10^{-2}x + 1.1y + 2z\} + \\ &\quad \omega \{2.2yz + 0.1xz - 0.995xy\} + \omega^0 (0.21xyz) \\ &= \omega^3 + \omega^2 \alpha_1 + \omega \alpha_2 + \omega^0 \alpha_3. \end{aligned}$$

The second Hurwitz determinant,  $\Delta_2$ , is the polynomial



formed by the product  $\alpha_1 \alpha_2 - \alpha_3$  since  $\alpha_0 = 1$ , and yields

$$f_1(\tilde{p}) = \Delta_2(\tilde{p}) = 4.4yz^2 + 0.2xz^2 + 2.42 y^2z - 1.81 xy^2 - 1.98xyz + 5.0 \times 10^{-3}x^2z - 4.98 \times 10^{-2}x^2y. \quad (2.42)$$

In order to illustrate the solutions to  $\Delta_2(\tilde{p}) = 0$ , the projection on the  $(\log x, \log z)$  plane is taken, by setting  $y = 1$  in (2.42):

$$f_2(\tilde{p}) = 4.4z^2 + 0.2xz^2 + 2.42z - 1.09x - 1.98 xz + 5 \times 10^{-3}x^2z - 4.98 \times 10^{-2}x^2 \quad (2.43)$$

When the zeroes of this polynomial are plotted in the  $\log_{10}$  parameter space  $\tilde{\pi} = (\log x, \log z)$ , the curve in figure 2.1 results. The asymptotes to this curve for large  $\tilde{\pi}$  are also shown in figure 2.1.

If a vector\*  $\tilde{y} = (y_1, y_2)$  is defined corresponding to each term of  $f_2(\tilde{p})$ , where  $y_1$  is the power to which  $x$  is raised in  $f_2(\tilde{p})$ , while  $y_2$  is the power to which  $z$  is raised, then the points labelled  $\tilde{y}_1$  to  $\tilde{y}_7$  in figure 2.1 are obtained. For example, the third term in (2.43) is  $2.42 x^0 z^1$  which has the associated vector  $\tilde{y}_3 = (0, 1)$ . These seven points define a polygon of minimum area, which is outlined in figure 2.1.

The interesting feature of this polygon is that each asymptote to the curve in figure (2.1) is perpendicular

---

\*Do not confuse the vector  $\tilde{y}$  with the current parameter  $y = 1/Y_0$  previously set equal to one.



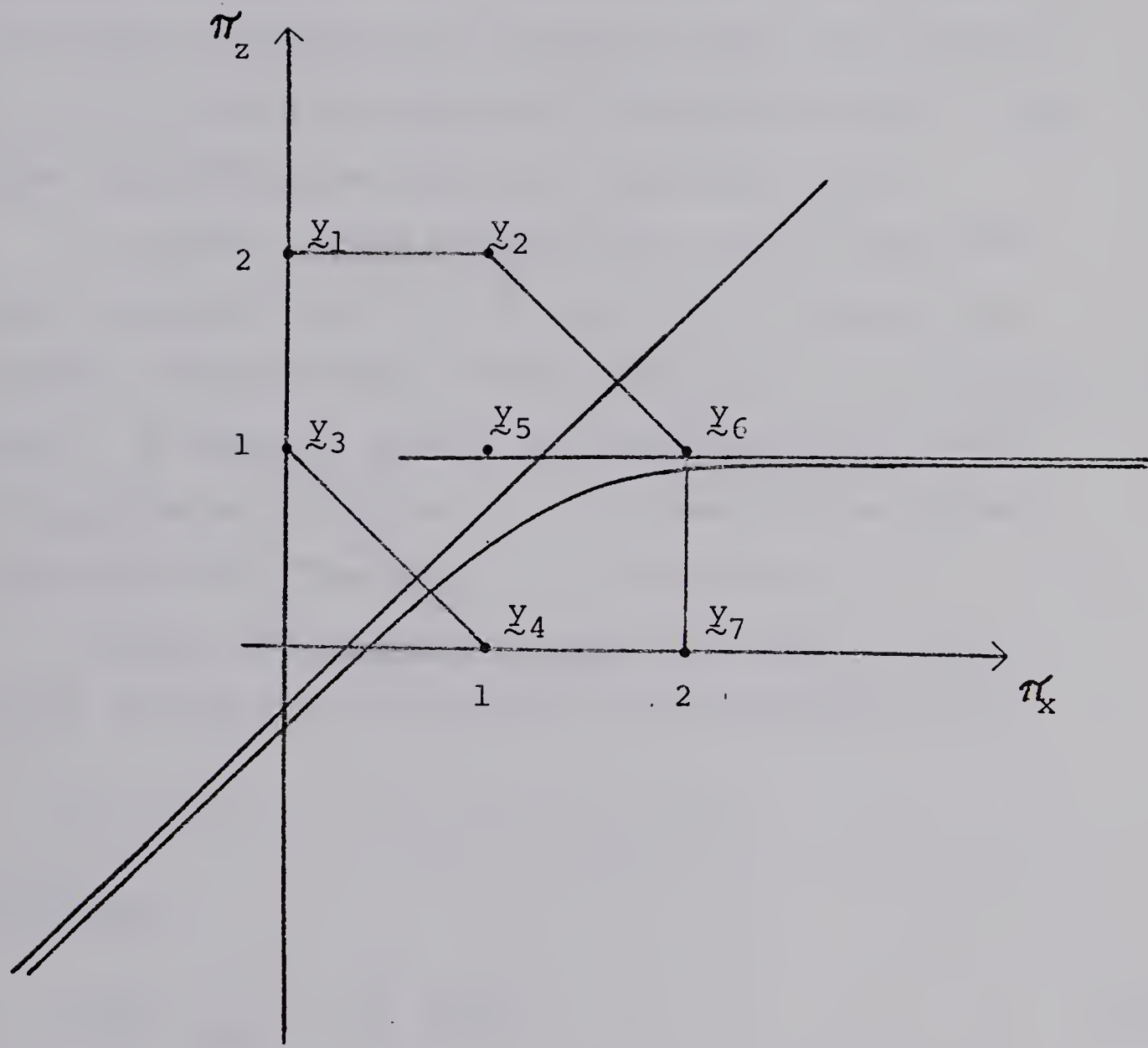


Figure 2.1

Plot of  $\Delta_2(p)$  for the extreme current  $i_A$ , at  $f = 1.1$  of the irreversible model, projected on the  $\pi = (\log x, \log z)$  plane.



to one of the polygon's edges. The second point to note is that each of these edges contains two points of the polygon which correspond to terms of  $f_2(\underline{p})$  with coefficients of opposite sign. For example, from figure 2.1 the points associated with negative terms in  $f_2(\underline{p})$  are  $\underline{y}_4, \underline{y}_5, \underline{y}_7$ , and the asymptotes are perpendicular to the edges containing the points  $\underline{y}_3, \underline{y}_4$  and  $\underline{y}_6, \underline{y}_7$ .

In general, these observations hold for any real power polynomial and are the basis of the method for finding the approximate surface of  $f(\underline{p}) = 0$  in parameter space. In order to find an equation which will yield the asymptotes in figure 2.1, the ideas of the preceding example will now be put on a firm basis.

Consider any stability inequality  $f(\underline{p}) > 0$  which can be written as a polynomial in the parameter set,

$$\{p_i \mid 0 < p_i < \infty, i = 1, \dots, n\},$$

as follows

$$f(\underline{p}) = \sum_{j=1}^m c_j \prod_{k=1}^n p_k^{y_{kj}} \quad (2.44)$$

where the polynomial contains  $m$  terms with real coefficients  $c_j$ , and  $\underline{p} \in \mathbb{R}^n$  is a  $n$ -tuple of real numbers. The  $i^{\text{th}}$  term in (2.44) is

$$c_i p_1^{y_{1i}} p_2^{y_{2i}} p_3^{y_{3i}}, \dots, p_n^{y_{ni}}$$

and has the *exponent vector*



$$\underline{y}_i = (y_{1i}, y_{2i}, \dots, y_{ni}), \underline{y}_i \in \mathbb{R}^n. \quad (2.45)$$

By choosing any base  $a$ ,  $a \in \mathbb{R}$ ,  $a > 1$ , for the logarithmic function, the term  $p_k^{y_k}$  may be written as

$$a^{(y_k \log_a p_k)}.$$

The definitions

$$Y = \{\underline{y}_i \mid i = 1, \dots, n\}$$

$$\underline{\pi} = (\log_a p_1, \log_a p_2, \dots, \log_a p_n) \quad (2.46)$$

applied to the  $i^{\text{th}}$  term of (2.44) now gives

$$c_i a^{\underline{\pi} \cdot \underline{y}_i},$$

where  $\underline{\pi}$  and  $\underline{y}_i$  can be interpreted as points in the Euclidean space  $E^n$ , with the usual definitions holding for the inner product and norm. The polynomial (2.44) written in terms of the transformed parameters  $\underline{\pi}$  becomes

$$g(\underline{\pi}) = \sum_{\underline{y} \in Y} c(\underline{y}) a^{\underline{\pi} \cdot \underline{y}} \quad (2.47)$$

where  $c(\underline{y})$  is the sum of the coefficients of all the terms in  $f(\underline{p})$  with the exponent vector  $\underline{y}$ :

$$c(\underline{y}) = \sum_{i \mid \underline{y}_i = \underline{y}} c_i(\underline{y}_i). \quad (2.48)$$

The set of exponent vectors  $\{\underline{y} \mid c(\underline{y}) \neq 0\}$  for any  $g(\underline{\pi})$  is a finite point set  $Y$  in  $E^n$ . This set of points



determines a convex polytope called the *exponent polytope*  $\Pi$ , which is defined as the convex hull of  $Y$ . The convex hull of a finite point set  $Y$  is the smallest convex set containing  $Y$ , defined by the set of all convex linear combinations of  $\underline{y}_1, \dots, \underline{y}_m$ , which is the set of line segments<sup>40</sup>

$$\{\underline{\pi} | \underline{\pi} = \sum_{i=1}^m \lambda_i \underline{y}_i, \lambda_i \geq 0, \sum_{i=1}^m \lambda_i = 1\} . \quad (2.49)$$

Returning to the previous example, it can be seen that the seven points in the polygon of figure 2.1 correspond to the exponent vectors of  $f_2(\underline{p})$  given in (2.43). In this case

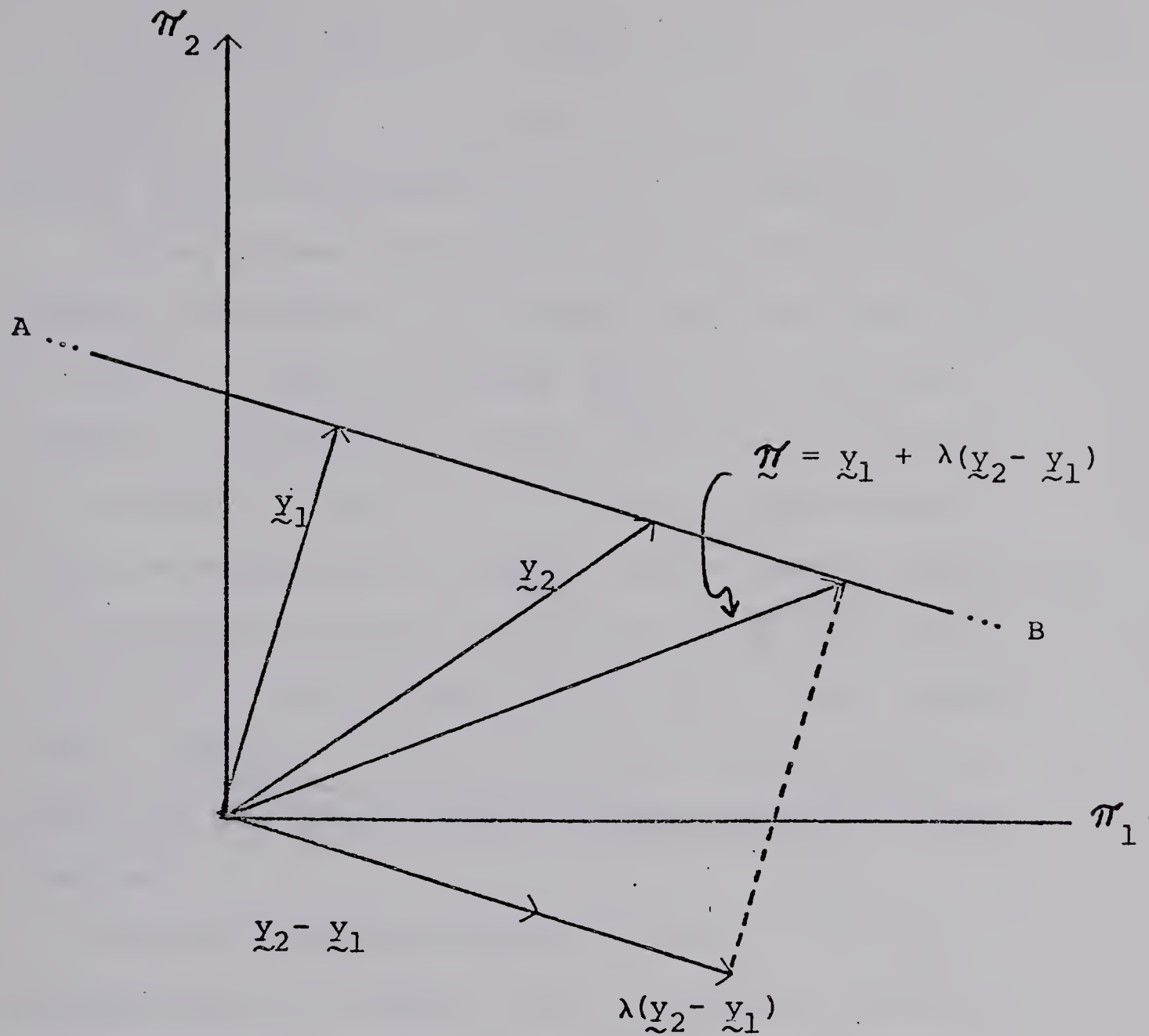
$$Y_2 = \{(0,2), (1,2), (0,1), (1,0), (1,1), (2,1), (2,0)\}$$

and the convex hull of this finite point set is the polygon which is plotted in figure 2.1. The convex hull of  $Y_2$  consists of all the points on the boundary of the polygon plus its interior. The line segment joining any two points of  $Y_2$  can be written as

$$\{\underline{\pi} | \underline{\pi} = \lambda \underline{y}_2 + (1-\lambda) \underline{y}_1, 0 \leq \lambda \leq 1\} \quad (2.50)$$

from the 2-dimensional case of (2.49). The line segment (2.50) is visualized below on the line AB with the vector  $\underline{\pi}$  restricted to the line segment joining  $\underline{y}_1$  and  $\underline{y}_2$ .<sup>44</sup>





When  $\lambda$  is unrestricted (all real  $\lambda$ ), the set of points  $\tilde{y}$  in (2.50) is the line  $AB$  passing through  $\tilde{y}_1$  and  $\tilde{y}_2$ . In  $E^2$ , the equation for a line can be written as

$$b = c_1 \pi_1 + c_2 \pi_2 \quad (2.51)$$

where  $b$ ,  $c_1$  and  $c_2$  are given constants. Generalizing to  $E^3$  defines a plane;  $b = c_1 \pi_1 + c_2 \pi_2 + c_3 \pi_3$ , and finally in  $E^n$  the set of points  $\tilde{y}$  satisfying



$$b = c_1 \pi_1 + c_2 \pi_2 + \dots + c_n \pi_n = \underline{c} \cdot \underline{\pi} \quad (2.52)$$

are said to define a *hyperplane* for given values of  $b$  and  $\underline{c}$ . Note the hyperplane (2.52) is orthogonal to  $\underline{\pi}$ .

In any convex polytope  $\Pi$ , there will be certain points  $\underline{\pi}$  which do not lie between any other two points of the set. From the diagram above this means that  $\underline{\pi}$  cannot be expressed as a linear combination of any  $\underline{y}_1$ ,  $\underline{y}_2$  in the set  $Y$  with  $0 < \lambda < 1$ . Or in other words,  $\underline{\pi}$  cannot be expressed as a proper convex linear combination of any other two points in the set  $\Pi$ . In this case  $\underline{\pi}$  is called an *extreme point* of the set. In the example shown in figure 2.1, all the points labelled  $\underline{y}_1$  to  $\underline{y}_7$ , except  $\underline{y}_5$ , are extreme points of the exponent polytope (hexagon).

From the discussion above, it follows that an extreme point is a special type of boundary point of a convex polytope. In particular, the extreme points determine the surface structure of  $\Pi$ , since the convex hull of the set of extreme points in  $Y$  is  $\Pi$ . In general  $\Pi$  is a solid embedded in a  $n$ -dimensional parameter space,  $\underline{\pi} = (\log_a p_1, \log_a p_2, \dots, \log_a p_n)$ . The surface structure of this solid can be described as sets of 0, 1, 2, ...,  $n-1$  dimensional *faces*, which correspond to extreme points, lines (edges), planes and hyperplanes.

The significance of the facial structure of  $\Pi$  is that it can be used to form a series of approximations



to the surface where  $g(\underline{\pi}) = 0$ . In other words, the polynomials formed from the terms corresponding to the points in  $Y$  which lie on the faces of  $\Pi$ , denoted by  $g_F(\underline{\pi})$ , are a limiting form for  $g(\underline{\pi})$ . To show this result, the generalization of (2.50) to the case of a halfline which starts at a *base point*  $\underline{\pi}_0$  and extends to infinity in the direction  $\hat{\pi}$  is needed. Such a halfline is called a *ray*, and is defined as the set of points

$$\Lambda(\underline{\pi}_0, \hat{\pi}) = \{\underline{\pi}(\lambda) \mid \underline{\pi}(\lambda) = \underline{\pi}_0 + \lambda \hat{\pi}, \lambda > 0, \underline{\pi}(\lambda) \in E^n\} \quad (2.53)$$

where the substitutions  $\underline{y}_1 = \underline{\pi}_0$ ,  $\underline{y}_2 - \underline{y}_1 = \hat{\pi}$  have been made in (2.50). Consider any point  $\underline{\pi}(\lambda)$  on a ray which is perpendicular to the hyperplane passing through a face  $F$ , say, of  $\Pi$ . Assume also that  $\underline{\pi}(\lambda)$  is chosen so that  $g_F(\underline{\pi}_0) \neq 0$ , then the following theorem holds:

Theorem 1 (Clarke)<sup>38</sup>

$$\lim_{\lambda \rightarrow \infty} g_F(\underline{\pi}(\lambda))/g(\underline{\pi}(\lambda)) = 1$$

If the dimension of the face used is  $k$ , then  $g_F(\underline{\pi})$  is called a  $k$ -face approximation. In the chemical stability problem, the approximation usually used is called the edge approximation, because the points  $y$  on the 1-dimensional faces of  $\Pi$  are used to define  $g_F(\underline{\pi})$ .

Theorem 1 allows  $g(\underline{\pi})$  to be replaced by the polynomials  $g_F(\underline{\pi})$  in the limit  $\lambda \rightarrow \infty$ , and means that the surface



$g(\underline{\pi}) = 0$  has an approximation given by  $g_F(\underline{\pi}) = 0$ . In the case of an edge approximation, where no interior points occur on the edge, (2.47) yields

$$g_F(\underline{\pi}) = c_1 a^{\underline{\pi} \cdot \underline{y}_1} + c_2 a^{\underline{\pi} \cdot \underline{y}_2} \quad (2.54)$$

where  $\underline{y}_1, \underline{y}_2$  are the extreme points of the edge and  $c_1, c_2$  are the corresponding coefficients. If the zeros of the polynomial  $g(\underline{\pi}) = 0$  are to be approximated by  $g_F(\underline{\pi}) = 0$ , then  $c_1$  and  $c_2$  in (2.54) must be of opposite sign, since the exponents are always  $\geq 0$ . Roughly, what one is doing is finding the zeros of the polynomial  $g(\underline{\pi}) = 0$  by examining the approximate polynomials  $g_F(\underline{\pi}) = 0$  formed from the points of  $Y$  which lie on an edge of  $\Pi$ , where the function  $g(\underline{\pi}) = 0$  changes sign.

It follows that using higher dimensional faces of  $\Pi$  for  $g_F(\underline{\pi})$  would include a greater number of terms from  $g(\underline{\pi})$  in the approximation, hence improving the asymptotic surface obtained for  $g(\underline{\pi}) = 0$ . However, the edge approximation is good for large  $||\underline{\pi}||$ , when  $\underline{\pi}$  is not almost orthogonal to a higher dimensional face of  $\Pi$  (such as a plane). In chemical systems where the concentrations of intermediates may vary over large orders of magnitude, the condition  $||\underline{\pi}||$  large is usually met and so the error incurred for small  $||\underline{\pi}||$  should be a physically insignificant region of the available parameter space.



The equation for the asymptotes of the surface  $g(\underline{\pi}) = 0$ , can now be found with the aid of two more theorems which clarify the form of the ray,  $\Lambda(\underline{\pi}_0, \hat{\pi})$ , which is necessary if  $\Lambda(\underline{\pi}_0, \hat{\pi})$  is to be an asymptote of  $g(\underline{\pi}) = 0$ .

Theorem 2 (Clarke)<sup>38</sup>

Consider the direction vector  $\hat{\pi}$ , and the highest dimensional face  $F$  of  $\Pi$  lying farthest in the direction  $\hat{\pi}$ . Choose any base point  $\underline{\pi}_0$ , then the ray  $\Lambda(\underline{\pi}_0, \hat{\pi})$  which extends from  $\underline{\pi}_0$  in the direction  $\hat{\pi}$  is perpendicular to  $F$ . If  $\underline{\pi}_0$  is such that  $g_F(\underline{\pi}_0) \neq 0$ , then the ray  $\Lambda(\underline{\pi}_0, \hat{\pi})$  is not an asymptote of the surface  $g(\underline{\pi}) = 0$ .

This theorem is actually saying that asymptotic rays of the surface  $g(\underline{\pi}) = 0$  must be orthogonal to a  $k$ -face for  $k > 0$ . The following theorem gives a sufficient but not necessary condition for  $\Lambda(\underline{\pi}_0, \Pi)$  to be an asymptote, and can be used to find a base point  $\underline{\pi}_0$  for an asymptote of  $g(\underline{\pi}) = 0$ .



Theorem 3 (Clarke)<sup>38</sup>

Consider the direction vector  $\hat{\pi}$ , and the highest dimensional face  $F$  of  $\Pi$  lying farthest in the direction  $\hat{\pi}$ . Given the ray  $\Lambda(\tilde{\pi}_0, \hat{\pi})$  which is perpendicular to  $F$ , and any  $\tilde{\pi}_0$  satisfying  $g_F(\tilde{\pi}_0) = 0$  such that  $g_F(\tilde{\pi})$  changes sign at  $\tilde{\pi}_0$ ; then the ray  $\Lambda(\tilde{\pi}_0, \hat{\pi})$  is an asymptote of the surface  $g(\tilde{\pi}) = 0$  as  $\lambda \rightarrow \infty$ .

This theorem allows an asymptotic ray to the surface  $g(\tilde{\pi}) = 0$  to be chosen so that the base point  $\tilde{\pi}_0$  lies on the edge  $F$ , say, and satisfies  $g_F(\tilde{\pi}_0) = 0$ . Hence from (2.54)

$$g_F(\tilde{\pi}_0) = c^+ a^{\tilde{\pi}_0} \cdot \tilde{y}_1 + c^- a^{\tilde{\pi}_0} \cdot \tilde{y}_2 = 0 \quad (2.55)$$

where  $\tilde{y}_1, \tilde{y}_2$  are the extreme points of the edge  $F$ , and  $c^+, c^-$  are the positive and negative coefficients, respectively. Because  $c^+ > 0$  and  $c^- < 0$ ,  $g_F(\tilde{\pi}_0)$  changes sign at  $\tilde{\pi}_0$  as required by theorem 3 and it follows from  $g_F(\tilde{\pi}_0) = 0$  that

$$a^{\tilde{\pi}_0} \cdot (\tilde{y}_2 - \tilde{y}_1) = |c^+ / c^-|$$

or taking the  $\log_a$  of each side

$$\tilde{\pi}_0 \cdot (\tilde{y}_2 - \tilde{y}_1) = \log_a |c^+ / c^-| \quad (2.56)$$



The component of  $\underline{\pi}_0$  perpendicular to the edge vector  $(\underline{y}_2 - \underline{y}_1)$  does not affect this equation. If any ray  $\Lambda(\underline{\pi}_0, \hat{\pi})$  passing through  $\underline{\pi}_0$  is chosen so that  $\hat{\pi}$  is perpendicular to  $(\underline{y}_2 - \underline{y}_1)$  also, then any point  $\underline{\pi} = \underline{\pi}_0 + \lambda \hat{\pi}$ ,  $\lambda \geq 0$ , on this ray will also satisfy (2.56). Therefore the equation

$$\underline{\pi} \cdot (\underline{y}_2 - \underline{y}_1) = \log_a |c^+/c^-| \quad (2.57)$$

holds.

This is the equation for a hyperplane (compare with (2.52)) which is perpendicular to the edge of  $\Pi$  joining the extreme points  $\underline{y}_1$  and  $\underline{y}_2$ . The hyperplane (2.57) determines an asymptote to the surface in  $\Pi$  where  $g(\underline{\pi}) = 0$ , and has an associated halfspace defined by

$$\underline{\pi} \cdot (\underline{y}_2 - \underline{y}_1) > \log_a |c^+/c^-| \quad (2.58)$$

which gives the region where  $g(\underline{\pi})$  is negative. Each extreme point of  $\Pi$  is called a *positive* or *negative vertex* according to whether the corresponding coefficient is positive or negative. Two adjacent extreme points are connected by an edge of  $\Pi$ . The intersection of the halfspaces (2.58) defined by each edge of a negative vertex determines a polyhedral cone  $C^k$ , which gives the asymptotic region of instability due to the vertex. In any exponent polytope  $\Pi$ , the approximate unstable region will be a union of the cones  $C^k$  defined



by each negative vertex. The total approximate region of instability in a chemical network will be a union of each set of cones  $C^k$  occurring for each stability inequality  $f(\underline{\pi}) > 0$ .

Returning to the example of figure 2.1, the equations for the asymptotes can be determined from (2.57), for the two edges joining  $\underline{y}_3, \underline{y}_4$  and  $\underline{y}_6, \underline{y}_7$  in  $\Pi$ . This yields

$$\underline{\pi} \cdot (\underline{y}_4 - \underline{y}_3) = \underline{\pi} \cdot (1, -1) = \log 0.35$$

$$\underline{\pi} \cdot (\underline{y}_7 - \underline{y}_6) = \underline{\pi} \cdot (0, -1) = \log 0.1$$

where  $\underline{\pi} = (\log x, \log z)$ , and the conditions for instability (2.58) become

$$\log x > \log z + 0.35$$

$$\log z < 1$$

where in the original parameter space  $x = 1/X_o$ ,  $z = 1/Z_o$  in terms of the steady state concentrations  $X_o, Z_o$ .

It should be noted that if a point occurs on the edge joining adjacent positive and negative vertices, then the point would have to be included in (2.55). Let the point on the edge, denoted by the exponent vector  $\underline{y}_3$ , correspond to a positive coefficient  $c_3$ , then  $g_F(\underline{\pi}_o) = 0$  means that

$$|c^-| a \underline{\pi}_o \cdot \underline{y}_2 = c^+ a \underline{\pi}_o \cdot \underline{y}_1 + c_3 a \underline{\pi}_o \cdot \underline{y}_3$$

from (2.55). If  $\underline{y}_3$  is a midpoint of the  $\underline{y}_2 - \underline{y}_1$  edge,



then

$$|c^-|a \cdot \pi_0 \cdot (\underline{y}_2 - \underline{y}_1) = c^+ + c_3 a \cdot \pi_0 \cdot (\underline{y}_3 - \underline{y}_1) .$$

Let  $a \cdot \pi_0 \cdot (\underline{y}_3 - \underline{y}_1) = \zeta$ , then since  $\underline{y}_2 - \underline{y}_1 = 2(\underline{y}_3 - \underline{y}_1)$  it follows that:

$$c^- \zeta^2 + c_3 \zeta + c^+ = 0,$$

and the equation for the asymptotic hyperplane to the edge  $\underline{y}_2 - \underline{y}_1$  becomes, in parallel to (2.57),

$$\pi \cdot (\underline{y}_2 - \underline{y}_1) = 2 \log_a \zeta$$

where  $\zeta$  is the positive root of the quadratic equation above:

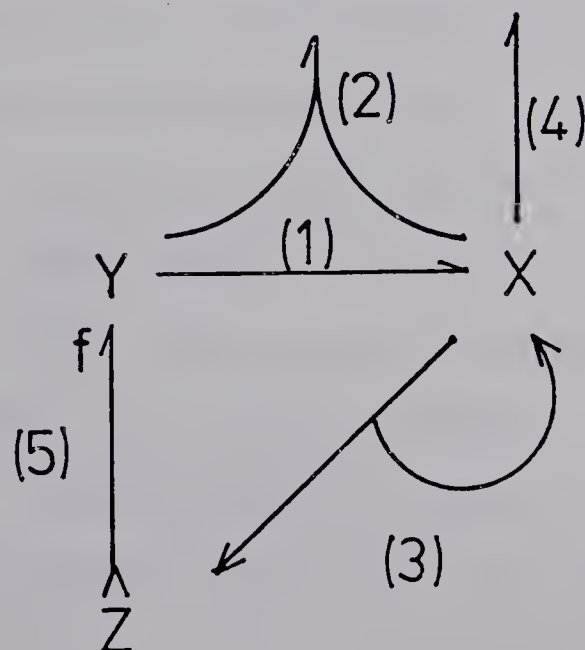
$$\zeta = \{-c_3^{\pm} \sqrt{c_3^2 + 4c^-c^+}\} 1/2c^- .$$



## 2.5. Diagrammatic Aids

The method developed in the last section allows the boundary of the unstable states to be determined analytically. This computation can be further simplified if the destabilizing terms can be recognized by inspection of the interaction matrix  $\underline{M}$ . In order to accomplish this,  $\underline{M}$  is given in terms of a collection of diagrams. It is the purpose of this section to show that these diagrams are equivalent to the terms of  $\underline{M}$  and that certain of the cycle diagrams are associated with instability.

The starting point for the diagrammatic approach is the *reaction diagram*.<sup>19</sup> The reaction diagram contains each chemical reaction in the network together with the stoichiometry and kinetics, and corresponds to the full nonlinear kinetic equations. For example, the Oregonator model (1.6) has the following reaction diagram:





Each arrow represents a reaction, and is labelled (1) to (5) in a parallel fashion to the reaction steps in (1.6). Reactions which produce or consume more than one species are denoted by a split arrow. The internal species are labelled X, Y and Z. The external species A, B, P and Q do not appear in the reaction diagram as they can be included in the rate constants. An arrow which points away from a species represents a reaction which consumes that species, while incoming arrows represent reactions which produce the species. The number of feathers and barbs is also important. A standard convention for arrows when facing from the tail to the tip is that the number of feathers on the left hand side of the shaft is denoted by  $f_L$ . The value of  $f_L$  gives the kinetic order of the reaction, while the total number of feathers on a shaft gives the stoichiometry. The number of barbs corresponds to the stoichiometry of the product, and there is no left-right distinction. As an example, consider reaction (3) in the above reaction diagram, which corresponds to the reaction,  $X \rightarrow 2Z + 2X$ .

From the reaction diagram above two rough cycles can be seen. These consist of  $R(1) + R(3) + R(5)$  and  $R(2) + R(3) + R(5)$ . Thus one may suspect that two extreme currents exist corresponding to these combinations of reactions. In the actual solution,  $R(4)$  will also be needed to conserve the balance of mass, since the



production of each species in an extreme current is zero at steady state.

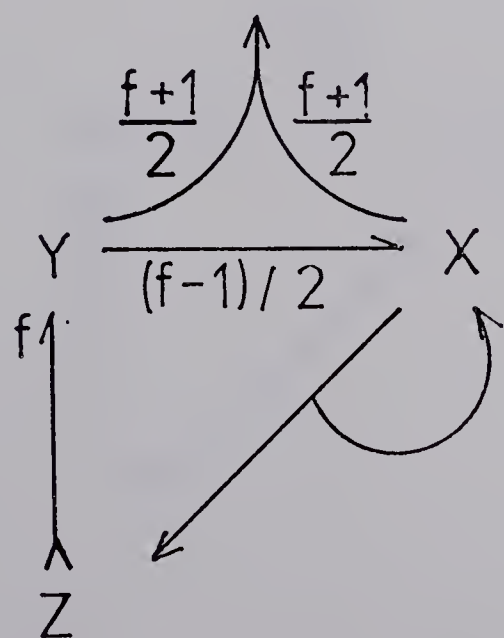
As a specific example, take the extreme current  $\tilde{i}_A$  given in (2.36) for  $f \geq 1$ , as

$$\tilde{i}_A = \left( \frac{f-1}{2}, \frac{f+1}{2}, 1, 0, 1 \right) .$$

This vector expresses the steady state solution in terms of the components of  $\tilde{v}^0$  which satisfy

$$(2/f-1)v_1^0 = (2/1+f)v_2^0 = v_3^0 = v_5^0 . \quad (2.59)$$

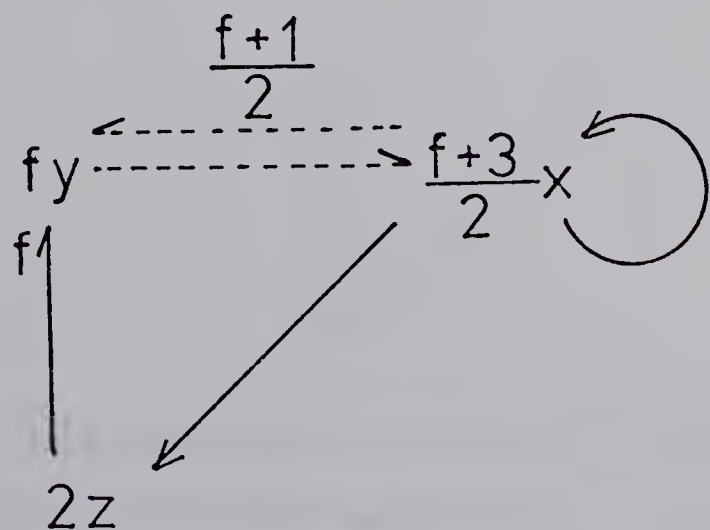
If the velocity of steady state in reaction (5) is set equal to  $j_A$ ,  $v_5^0 = j_A$ , then (2.59) says that  $v_1^0 = (f-1)/2 j_A$ . Therefore, the velocity in each reaction at steady state can be written as a scaled multiple of the current  $j_A$ . This can be written diagrammatically as follows





where the appropriate reactions from the reaction diagram have been chosen. This diagram is called an *extreme current diagram*. It is interpreted in the same way as the reaction diagram given previously. When a label such as  $(f-1)/2$  appears beside an arrow, the entire reaction is multiplied by that factor. Hence reaction (1) is  $(f-1)/2 Y \rightarrow (f-1)/2 X$ .

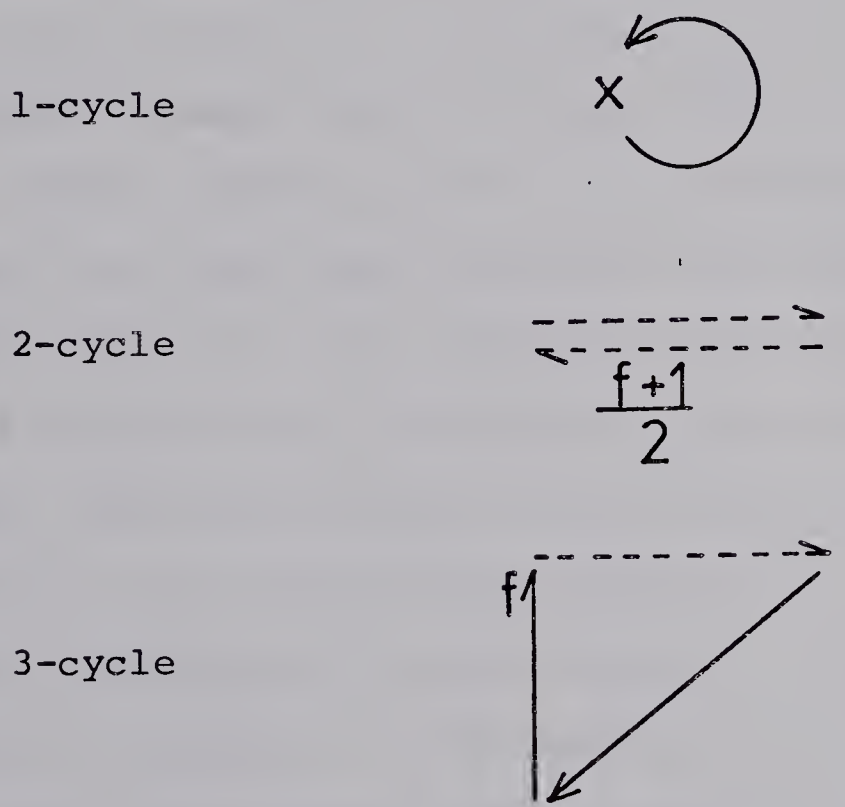
The next step is to reduce the extreme current diagram to the *interaction diagram*, which corresponds to the linearized perturbed equations. However, the interaction diagram for the extreme current  $\tilde{i}_A$  will simply be given and its term by term equivalence to the interaction matrix  $\underline{\underline{M}}_A$ , given in (2.37), shown. The interaction diagram for the extreme current  $\tilde{i}_A$ ,  $f \geq 1$ , given above is





The arrows in this diagram link the different states of a reaction. A solid arrow links a reactant to a product, and corresponds to a positive matrix element. A dashed arrow, on the other hand, links different reactants, and corresponds to a negative matrix element. Solid arrows are called *activators* and dashed arrows are called *inhibitors*.

The arrows form cycles which are called *k*-cycles, where *k* is the number of arrows in the cycle. For example, the interaction diagram above contains three cycles:



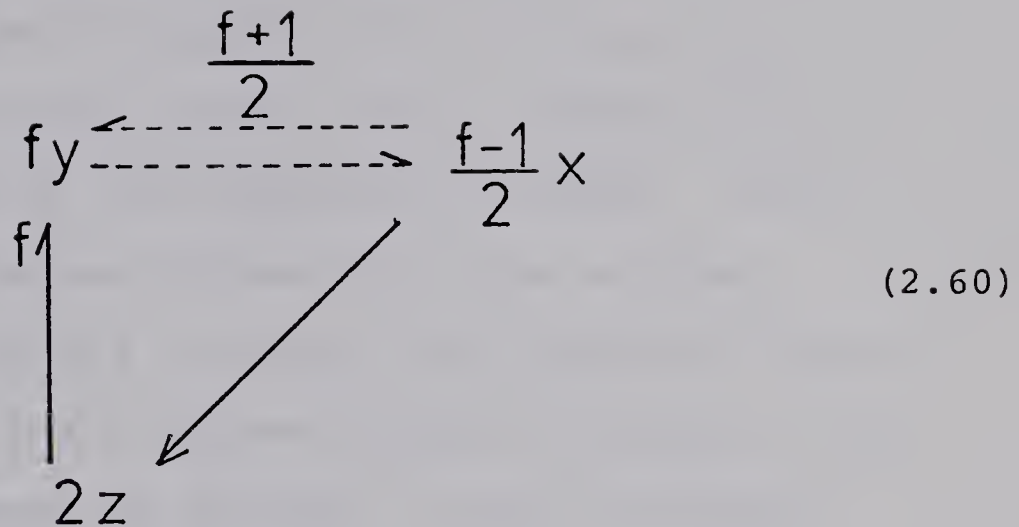
The factors  $f$ ,  $(f+1)/2$  multiply the value of the arrow. Each reactant has an associated parameter  $x = j_A h_x$ ,  $y = j_A h_y$ , or  $z = j_A h_z$ , where  $h_x$ ,  $h_y$ ,  $h_z$  are the reciprocal steady state concentrations and  $j_A$  is the current. The



value of an arrow is given by the reactant at the arrow's tail, multiplied by the number of barbs and also any factor which multiplies the arrow. For example, the cycles above have the values  $2x$ ,  $(f+1)/2 xy$  and  $-2fxyz$ , respectively. The sign of each term is determined by the product of the signs of each arrow in the cycle, where dashed arrows are negative and solid arrows are positive.

The arrows point towards or away from a second type of diagrammatic element called a *stabilizer*. The stabilizers are denoted in the interaction diagram above as  $(f+1)/2 x$ ,  $fy$  and  $2z$ , and are represented diagrammatically by a dot. The stabilizers contain the contribution to the diagonal matrix elements coming from reactions that consume a species, and are negative terms in  $\underline{M}$ . Besides the stabilizers, the only other diagrams which contribute to  $m_{ii}$  are the 1-cycles. The stabilizer and 1-cycles which occur at a species can be combined to form a modified coefficient, while the diagram which survives cancellation is kept in the interaction diagram (i.e., a stabilizer if the coefficient is positive, or a 1-cycle if the coefficient is negative). For example, in the interaction diagram above, the species  $x$  has a net coefficient  $(f-1)/2$  for the stabilizer, because  $f \geq 1$ . This is valid because the matrix elements with the same parameters cannot be distinguished when the determinant is expanded. The interaction diagram for the extreme current  $i_M$  becomes





and the diagonal elements of  $\underline{\underline{M}}_A$  are:  $-(\frac{f-1}{2})x$ ,  $-fy$ ,  $-2z$ .

The 2 and 3-cycles in this interaction diagram correspond to the product of matrix elements  $M_{12} M_{21}$  and  $M_{12} M_{23} M_{31}$  from  $\underline{\underline{M}}_A$ , respectively. This can be deduced by considering the arrow

$j \longrightarrow i.$

The matrix element is then  $M_{ij}$ , where  $M_{1j} = ax$ ,  $M_{2j} = by$  and  $M_{3j} = cz$  and  $a$ ,  $b$ ,  $c$  are some coefficients which are a function of the stoichiometric parameter  $f$  in some cases. Note that the components of  $\underline{\underline{\zeta}}$  are assumed to be defined in the order:  $\underline{\underline{\zeta}} = (x-x_o, y-y_o, z-z_o)$  as in section 2.2. In conclusion, the cycles which are found in the interaction diagrams of a network give directly



the responsible product of matrix elements in the interaction matrix.

From this discussion, it is clear that the interaction diagram above is identical to the matrix  $\underline{\underline{M}}_a$ . In general, the interaction matrix for any network can be expressed as a sum of the interaction diagrams. Since the interaction diagrams correspond to the extreme currents, it is possible to derive the interaction matrix by formally reducing the extreme current diagrams to the corresponding interaction diagrams. This is done by applying a set of rules given by Clarke:<sup>31</sup>

- 1) A solid arrow is drawn to  $i$  from  $j$  whenever  $j$  is a reactant and  $i$  is a product of the same reaction. The number of barbs on the new arrow equals the number of left feathers,  $f_L$ , times the number of barbs on the reaction arrow.
- 2) A dashed arrow is drawn to  $i$  from  $j$  whenever  $j$  and  $i$  are reactants in the same reaction. The number of barbs equals the product of  $f_L$  at  $j$  and the total number of feathers at  $i$ .
- 3) The value of the stabilizer of each reactant is the sum over all outgoing reactions of the product of the numbers of total feathers and  $f_L$ .

In the case of variable stoichiometric parameters, as in the present analysis, the arrows of the interaction



diagrams are labelled instead of using barbs, for convenience. Applying Clarke's rules to the extreme current diagrams is exactly the same as applying the procedure used in section 2.2 to find  $\underline{M}_A$  from the extreme current  $\underline{i}_A$ , and gives an alternate method of deriving the interaction matrix from the extreme currents.

Several theorems have been given by Clarke that distinguish the types of cycle diagrams which can destabilize chemical networks. The ones pertinent to this analysis are the following:

- 1) Cycles with even numbers of dashed arrows (inhibitors) make negative contributions to  $\alpha_i$ . (Theorem 4, Reference 19).

The  $k$ -cycles with even numbers of inhibitors are called *positive feedback  $k$ -cycles* or *PF  $k$ -cycles*. If a positive feedback  $k$ -cycle contains inhibitors then the abbreviation *PFI  $k$ -cycle* will be used. For example, in the interaction diagram for  $i_A$  given in (2.60), a PFI 2-cycle can be seen.

- 2) Cycles with an odd number of inhibitors are called *negative feedback  $k$ -cycles*, or *NF  $k$ -cycles*. The conditions under which a NF 3-cycle can destabilize a network is given in the following theorem:

A NF 3-cycle, which passes through a reactant whose stabilizer in the same extreme current is exactly cancelled



by autocatalysis (PF 1-cycle), destabilizes the network if no other cycles containing only parameters occurring in the 3-cycle pass through the autocatalytic species except one 2-cycle. (Theorem 3, Reference 11).

A 1-cycle which exactly cancels a stabilizer at a species, is called a *critical 1-cycle*. Although a critical 1-cycle does not violate the conditions for qualitative stability, in the presence of a negative feedback 3-cycle instability can result. In the interaction diagram for  $\tilde{i}_A$  given above, the negative feedback 3-cycle which is present does not pass through a critical 1-cycle for  $f \neq 1$ , and hence this cycle cannot destabilize in this case. However, when  $f = 1$ , a critical 1-cycle appears at  $x$ , and the conditions of the theorem above are satisfied. In the results of Chapter 3, it will be shown that a negative vertex appears in  $\Pi_{\Delta_2}$  corresponding to the negative feedback 3-cycle in  $\tilde{i}_A$ , at  $f = 1$ .

Up to this point the extreme current and interaction diagrams that have been considered correspond to a single extreme point in the current polytope  $\Pi_c$ . In principle, similar diagrams also exist for every other point in  $\Pi_c$ . However, since every non-extreme point in  $\Pi_c$  can be expressed as a non-negative linear combination of the extreme currents, only the extreme current diagrams are needed. Thus, for any given point in  $\Pi_c$ , determined by the current vector  $j$ , there is a sum of weighted interaction



diagrams which determine the interaction matrix  $\underline{\underline{M}}$ .

Since each element of  $\underline{\underline{M}}$  is given by a weighted sum of diagrammatic elements, one from each extreme current, the expansion of the determinant for  $\underline{\underline{M}}$  yields the characteristic polynomial as a homogeneous sum of diagrams. Each stability inequality (2.40) in the network can also be written as a homogeneous sum of diagrams. It follows that a set of diagrams corresponds to the set of points in each exponent polytope,  $\Pi$ . Therefore, the identification of the destabilizing terms in  $\tilde{f}(\underline{p})$ , corresponding to negative vertices of  $\Pi$ , can be made through the diagrams. The diagrams allow easy recognition of unstable states which have only an abstract topological relationship in the network. In order to determine the conditions for instability, the adjacent positive vertices must also be found. Unfortunately, rules have not been found that can identify all the cycles associated with the adjacent positive vertices, and computer programs<sup>45</sup> are used to calculate the adjacent vertices at present. However, the diagrams are still useful for eliminating certain extreme currents from the analysis, such as those which do not lie adjacent to the destabilizing extreme currents in the current polytope. The diagrams also retain information about the chemical interactions which cause instability, and so pinpoint the cause of chemical instabilities.



The Stability Analysis

3.1. Introduction

In this chapter the results of the stability analysis performed on the Oregonator model (1.6) are given. The irreversible model is considered in section 3.2 and the reversible model in section 3.3. These results are then compared in section 3.5. The results of the analysis give the change in the boundary of the unstable steady states when the reactions are allowed to reverse in the network. Several generalizations emerge and are given in section 3.6.

The coefficients of the terms in the stability polynomials are a function of the stoichiometric parameter  $f$ . The corresponding vertices in the exponent polytope will also have coefficients which are a function of  $f$ . The surface structure of the exponent polytope will change only for values of  $f$  at which a coefficient of a vertex vanishes. This causes a truncation of the polytope, and the region of instability may be altered. The changes in the boundary of the unstable states with  $f$  is discussed in detail in sections 3.2 and 3.3. It is interesting to note that adding reverse reactions does not alter the important singular values of  $f$  which are present in the



irreversible model. These occur at  $f = 0.5$  , 1 and  $1 + \sqrt{2}$ .

The complete set of extreme currents for the network defines terms in the stability polynomials  $f(\underline{p})$  which are called *pure* or *mixed terms*. The pure terms are derived from one extreme current only, while the mixed terms arise from the overlap of different extreme currents. If any of these terms is *dominant*, it can be used as a one term approximation to  $g(\underline{\pi}) = 0$  and is therefore a vertex of the corresponding exponent polytope. A dominant negative term is called a *destabilizing term*. The purpose of the analysis is to look for a connection between the destabilizing terms in  $f(\underline{p})$  and the resulting boundary of stability.



### 3.2. Irreversible Model Results

The theory developed in the previous chapter can be applied to the irreversible model (1.6) without difficulty due to the small number of parameters involved. The results of this analysis give the background for comparison with the results obtained when reversibility is included in the Oregonator. In fact, the results of the irreversible model are contained in the reversible model analysis, and represent the special case when the reverse rate constants are set equal to zero.

The interaction matrix is derived in the manner of section 2.2, with the stoichiometric parameter  $f$  included as an additional variable. The singular nature of the value  $f = 1$ , necessitates the division of the analysis into two parts:  $f \leq 1$  and  $f \geq 1$ . There are only two extreme currents in each region of  $f$ , as shown in figure 3.1a. In the region  $f \leq 1$  the extreme currents B and C exist, while for  $f \geq 1$  the extreme currents A and C exist. Note that at  $f = 1$  current A equals current B as required by the continuity of the solutions at  $f = 1$ . The extreme current A was derived explicitly in section 2.2, and its diagrammatic representation was given in section 2.5.

The interaction diagrams corresponding to each extreme current are given in figure 3.1b. Note that all the elements of the interaction diagram for the extreme current A have been multiplied by two to avoid fractions.



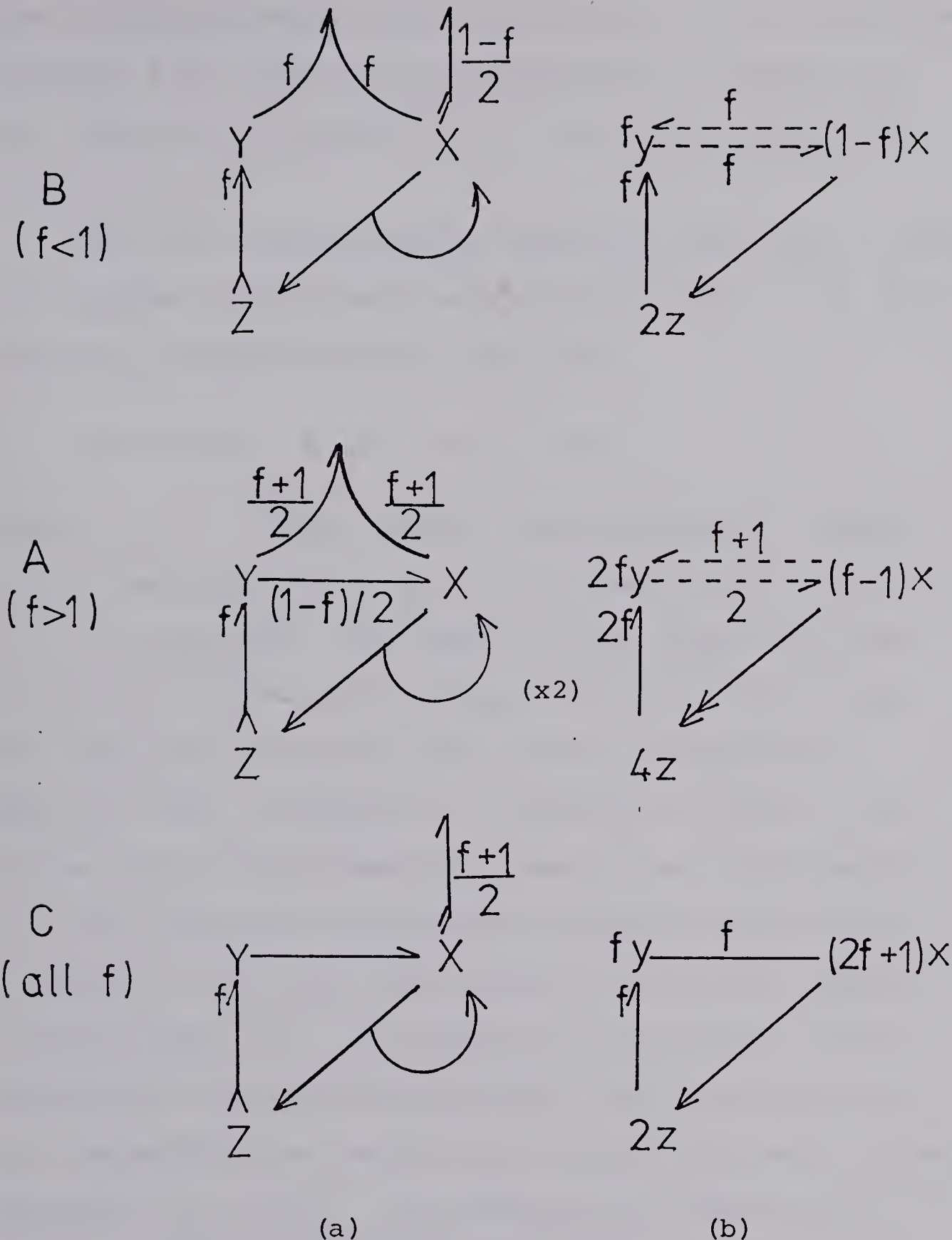


Figure 3.1

(a) The extreme currents for the irreversible model.  
 (b) The interaction diagrams for the irreversible model.



The interaction matrix  $\underline{M}$  in each region of  $f$  is determined directly from the sum of the diagrammatic elements of the interaction diagrams B and C for  $f \leq 1$ , and A and C for  $f \geq 1$ .

When the Lienard-Chipart stability conditions (2.40) are applied to the characteristic polynomial for  $\underline{M}$ , the stability inequalities take the form

$$\alpha_1 > 0, \alpha_3 > 0, \Delta_2 = \alpha_1 \alpha_2 - \alpha_0 \alpha_3 > 0$$

where  $\alpha_0 = 1$ . However as will be discussed in section 3.2.2, the analysis of  $\Delta_2$  is simplified if the inequality  $\alpha_2 > 0$  is included. The destabilizing terms were found to occur in two of these inequalities,  $\alpha_2$  and  $\Delta_2$ , only.

The responsible destabilizing cycles can be chosen directly from the interaction diagrams in figure 3.1b, on the basis of the theorems given at the end of section 2.5 which identify the possible destabilizing cycles in a network. Since only two extreme currents are present in each region of  $f$ , the exponent polytopes are readily plotted for the irreversible model, and the conditions for instability can be written directly from each exponent polytope,  $\Pi_{\alpha_2}$  and  $\Pi_{\Delta_2}$ . No destabilizing terms occur in  $\alpha_1$  or  $\alpha_3$  which are positive for all values of  $f$ . The destabilizing terms in  $\alpha_2$  and  $\Delta_2$  will now be discussed and a summary given in section 3.2.3.



### 3.2.1. The Cone of Negative $\alpha_2$

The stability inequality for  $\alpha_2$ ,  $\alpha_2 > 0$ , is a polynomial which is homogeneous of order 2 in the powers of each of the parameters  $\tilde{h}$  and  $\tilde{j}$ . The parameters will be denoted here as  $j_A$ ,  $j_C$ ,  $x$ ,  $y$ ,  $z$  in the region  $f > 1$ , and as  $j_B$ ,  $j_C$ ,  $x$ ,  $y$ ,  $z$  in the region  $f < 1$ , where  $x$ ,  $y$ , and  $z$  are the reciprocals of the steady state concentrations  $x_o$ ,  $y_o$ ,  $z_o$ , respectively. Each term in the polynomial  $\alpha_2$  is a sum of all the 2-cycles and 2-stabilizers which occur in the interaction diagrams with the same parameter values. The value of each diagrammatic element is read from the interaction diagram in figure 3.1b according to the discussion given in section 2.5.

The only destabilizing cycle in  $\alpha_2$  is the inhibitory positive feedback (PFI) 2-cycle between  $x$  and  $y$ , which occurs in the extreme currents A and B as shown in figure 3.1b. The destabilizing term in  $\alpha_2$  which corresponds to this 2-cycle is found in each region of  $f$  by summing the pure stabilizer and PFI 2-cycle diagrams



present in each of the extreme currents A and B. The coefficients of this destabilizing term in each region of  $f$  are as follows:



	<u><math>f &lt; 1</math></u>	<u><math>f = 1</math></u>	<u><math>f &gt; 1</math></u>
$j_B^2 xy$	$f(1-2f)$	-1	-
$j_A^2 xy$	-4	$2(f^2 - 2f - 1)$	

Note, current A was multiplied by 2, so that  $j_A^2 = 2^2 j_B^2$  at  $f = 1$ . These  $\alpha_2$  terms are negative in the region  $0.5 < f < 1 + \sqrt{2}$ . At  $f = 0.5$  and  $f = 1 + \sqrt{2}$  the coefficient of the destabilizing term vanishes. The remaining terms in  $\alpha_2$  are positive, and so  $\alpha_2 > 0$  for both these values of  $f$ . Similarly, when  $f < 0.5$  or  $f > 1 + \sqrt{2}$ , no negative terms occur in  $\alpha_2$ . Therefore, there is no unstable region in  $\Pi_{\alpha_2}$  for  $f \leq 0.5$  and  $f \geq 1 + \sqrt{2}$ .

The unstable region in  $\Pi_{\alpha_2}$  can be discussed separately in each of the regions  $0.5 < f \leq 1$  where current B exists and  $1 \leq f < 1 + \sqrt{2}$  where current A exists. In the region  $0.5 < f < 1$  the only destabilizing term is  $j_B^2 xy$  which corresponds to a vertex of the exponent polytope  $\Pi_{\alpha_2}$ . This vertex has three edges with adjacent positive vertices corresponding to the terms  $j_C^2 xy$ ,  $j_B^2 xz$  and  $j_B^2 yz$ . The three edges determine three inequalities which are the approximate necessary and sufficient conditions for the negative term to be larger than the sum of positive terms on each edge. Hence, the asymptotic boundary of the unstable region in  $\alpha_2$  is given by the hyperplane



$$\underline{\pi} \cdot (\underline{y}_2 - \underline{y}_1) = \log |c^+/c^-|$$

where  $\underline{\pi} = (\log j_A, \log j_B, \log j_C, \log x, \log y, \log z)$ , and the cone of negative  $\alpha_2$  is the intersection of the associated halfspaces

$$\underline{\pi} \cdot (\underline{y}_2 - \underline{y}_1) > \log |c^+/c^-|$$

as defined in section 2.4. In this notation for  $\underline{\pi}$ , the vertex corresponding to the term  $j_B^2 xy$  has the exponent vector  $\underline{y}_2 = (0, 2, 0, 1, 1, 0)$ .  $\underline{\pi}$  is defined in this way, although  $j_A = 0$  for all  $f < 1$ , to maintain consistency with the labelling of the reversible model currents of section 3.3. The cone of negative  $\alpha_2$  is defined for the region  $0.5 < f < 1$ , by the instability conditions given in Table 3.1a. Note that the first instability condition corresponds to an edge of  $\Pi_{\alpha_2}$  containing the midpoint  $(0, 1, 1, 1, 1, 0)$ , which has been included (for further details see the end of section 2.4).

In the region  $1 < f < 1 + \sqrt{2}$ , the only destabilizing term is  $j_A^2 xy$ , which has the exponent vector  $\underline{y}_2 = (2, 0, 0, 1, 1, 0)$ . The terms corresponding to the adjacent positive vertices are  $j_C^2 xy$ ,  $j_A^2 xz$  and  $j_A^2 yz$ . The conditions for instability in this region are given in Table 3.1b.

The terms in  $\alpha_2$  in the regions  $0.5 < f < 1$  and  $1 < f < 1 + \sqrt{2}$  differ only by the current component  $j_A$  or  $j_B$ . Substituting one of these currents for the other in



Table 3.1

The instability conditions for  $\alpha_2$  in the irreversible model, where  $\pi = (\log j_A, \log j_B, \log j_C, \log x, \log y, \log z)$  for  $f$  in the range (a)  $0.5 < f < 1$ , (b)  $1 < f < 1 + \sqrt{2}$ , (c)  $f = 1$ .

$0.5 < f < 1$       Vertex  $(0,2,0,1,1,0)$   $f(1-2f)$

Adjacent Vertex	Coefficient	Instability Condition
1. $(0,0,2,1,1,0)$	$f(1+2f)$	$(2f-1)(j_B/j_C)^2 > (1+2f) + 2(1+f)j_B/j_C$
2. $(0,2,0,1,0,1)$	$2(1-f)$	$f(2f-1)y > 2(1-f)z$
3. $(0,2,0,0,1,1)$	$2f$	$(2f-1)x > 2z$

(a)

$1 < f < 1 + \sqrt{2}$       Vertex  $(2,0,0,1,1,0)$   $2(f^2-2f-1)$

Adjacent Vertex	Coefficient	Instability Condition
1. $(0,0,2,1,1,0)$	$f(1+2f)$	$1/2 f^2-2f-1 (j_A/j_C)^2 > f(1+2f) + 2f(1+3f)j_A/j_C$
2. $(2,0,0,1,0,1)$	$4(f-1)$	$ f^2-2f-1 y > 2(f-1)z$
3. $(2,0,0,0,1,1)$	$8f$	$ f^2-2f-1 x > 4fz$

(b)

$f = 1$       Vertex  $(0,2,0,1,1,0)$  2

Adjacent Vertex	Coefficient	Instability Condition
1. $(0,0,2,1,1,0)$	3	$(j_B/j_C)^2 > 3 + 4j_B/j_C$
2. $(0,1,1,1,0,1)$	6	$j_By > 6j_Cz$
3. $(0,2,0,0,1,1)$	2	$x > 2z$

(c)



any term of  $\alpha_2$  only modifies the coefficient for these ranges of  $f$ . As a result, the instability conditions given in tables 3.1a and 3.1b are the same, except for the coefficients which shift the asymptotic hyperplane defining the cone of negative  $\alpha_2$ .

At  $f = 1$  the extreme currents  $A$  and  $B$  are equal. It follows that the instability conditions for each region of  $f$  are equal, apart from the factor of two which multiplies current  $A$ . However, a critical 1-cycle occurs at  $x$  in the currents  $A$  and  $B$  when  $f = 1$ , and as a result the term  $j_A^2xz$  ( $= j_B^2xz$ ) vanishes, since no 2-cycle passes through  $x$  and  $z$ . This truncates the exponent polytope, allowing a different exponent vector to become a vertex of  $\Pi_{\alpha_2}$ . The result is that a new positive vertex  $(0,1,1,1,0,1)$  occurs in  $\Pi_{\alpha_2}$  for  $f = 1$ , and a new edge is formed with the negative vertex  $(0,2,0,1,1,0)$ . The instability conditions for  $f = 1$  are given in table 3.1c.

The exponent polytope  $\Pi_{\alpha_2}$  can be visualized in  $(\log x, \log y, \log z)$  space by plotting the exponent vectors corresponding to constant current terms in the plane perpendicular to the vector  $\underline{\pi} = (1,1,1)$ . Such a plot has been made in figure 3.2 for various values of  $f$ . The maximal polytope is truncated at  $f = 0.5, 1$  and  $1 + \sqrt{2}$  as expected.



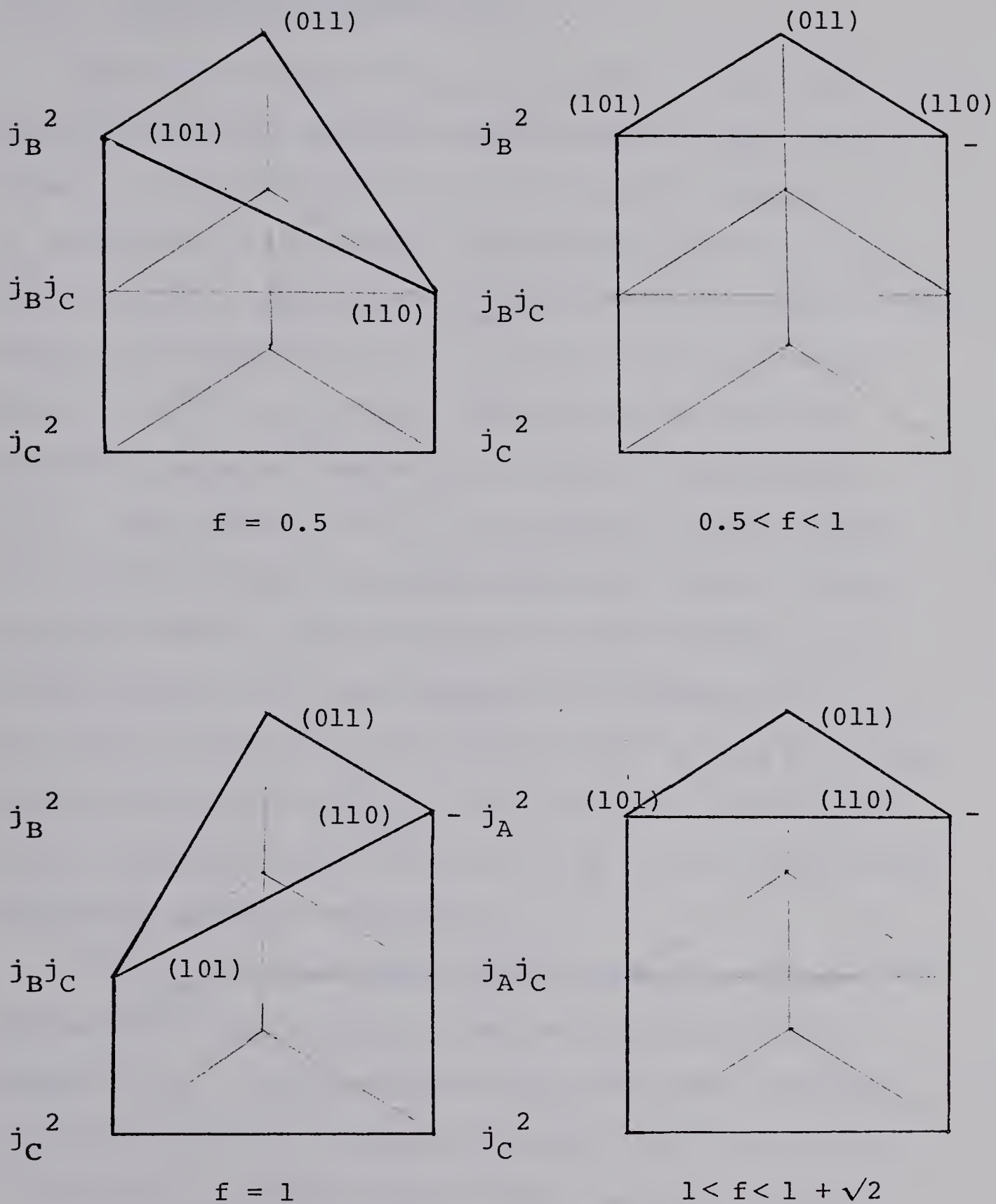


Figure 3.2

The exponent polytope  $\Pi_{\alpha_2}$  for the irreversible model at various values of  $f$ . The vector  $\pi = (1,1,1)$  is normal to the face of constant  $j$ .



### 3.2.2. The Cone of Negative $\Delta_2$

The cone of negative  $\Delta_2$  is a union of the cones arising from each negative vertex and its edges in  $\Pi_{\Delta_2}$ . Since  $\alpha_1 > 0$ , the product  $\alpha_1 \alpha_2$  is negative whenever  $\alpha_2$  is negative. Therefore, the diagonal product,  $\alpha_1 \alpha_2$ , of  $\Delta_2$  defines a polytope  $\Pi_{\text{diag}}$  whose set of negative cones arise from the division of  $C_{\alpha_2}$  by the positive dominant terms of  $\alpha_1$ .<sup>31</sup>  $\Pi_{\text{diag}}$  has a maximum volume when all possible parameter combinations occur in the product  $\alpha_1 \alpha_2$ . The vertices of  $\Pi_{\text{diag}}$  are called *maximum overlap (MOD)* vertices which are associated with *maximum overlap diagrams (MOD's)*, and correspond to the dominant terms in the product  $\alpha_1 \alpha_2$  (see theorem 10, reference 19). If all the vertices of  $\Pi_{\Delta_2}$  have MOD's then  $\Pi_{\Delta_2}$  has the same surface structure as  $\Pi_{\text{diag}}$ . In this case, the boundary of the unstable region of  $\Pi_2$  is given by the instability conditions defining the cone  $C_{\alpha_2}$ .

If  $\Pi_{\text{diag}}$  is truncated from the maximum polytope because MOD's are missing, then new vertices will be formed in  $\Pi_{\Delta_2}$ . These vertices may arise from terms in  $\Delta_2$  which do not have maximum overlap, such as  $-\alpha_3$  terms. A vertex of  $\Pi_{\Delta_2}$  which does not have maximum overlap is referred to as a *non maximum overlap (NMO)* vertex and the associated diagrams are called *non maximum overlap diagrams (NMOD's)*. When terms in  $\Delta_2$  which have NMOD's are vertices of  $\Pi_{\Delta_2}$  the cone of negative  $\Delta_2$  may destabilize



regions of parameter space not included in  $C_{\alpha_2}$ . It follows that the only vertices that need to be considered in  $\Pi_{\Delta_2}$  are the negative NMO vertices which occur when  $\Pi_{\Delta_2}$  is truncated from its maximum configuration.

The presence of a negative NMO vertex in  $\Pi_{\Delta_2}$  is guaranteed by theorem 2 in section 2.5, which identifies the necessary destabilizing cycle. According to this rule, a negative feedback (NF) 3-cycle which passes through a critical 1-cycle is a possible source of instability in  $\Delta_2$ . The theorem holds because the NF 3-cycle acquires a minus sign in the expansion of the determinant  $\Delta_2$ , and the critical 1-cycle eliminates parameter combinations in  $\alpha_1 \alpha_2$  that could possibly cancel the 3-cycle. By inspection of the interaction diagrams in figure 3.1b, a NF 3-cycle is found in currents A and B. However, a critical 1-cycle occurs only at  $f = 1$ , when the coefficient of the x-stabilizer vanishes in both currents A and B.

The destabilizing term in  $\Delta_2$  at  $f = 1$ , which corresponds to the negative NMO vertex found in  $\Pi_{\Delta_2}$ , is  $j_B^3 xyz$ . The diagrams which contribute to this term from the product  $\alpha_1 \alpha_2$  when  $f$  differs from one are shown in figure 3.3. The coefficient of this NMO term is:

$$\begin{array}{lll}
 j_B^3 xyz & 2f(2-3f) & f < 1 \\
 j_A^3 xyz & 16f(f-2) & f > 1 \\
 & -2 & f = 1
 \end{array}$$



$$\begin{aligned}
 \Delta_2 &= \alpha_1 \alpha_2 - \alpha_3 \\
 &= 3 \begin{array}{c} \bullet \\ \cdot \\ \bullet \end{array} - \begin{array}{c} \nearrow \\ \swarrow \end{array} - \left\{ \begin{array}{c} \bullet \\ \cdot \\ \bullet \end{array} - \begin{array}{c} \nearrow \\ \swarrow \end{array} - \begin{array}{c} \nearrow \\ \swarrow \end{array} \right\} \\
 &= 2 \begin{array}{c} \bullet \\ \cdot \\ \bullet \end{array} + \begin{array}{c} \nearrow \\ \swarrow \end{array} \\
 &= + \begin{array}{c} \nearrow \\ \swarrow \end{array}, \text{ at } f = 1.
 \end{aligned}$$

Figure 3.3

The diagrams contributing to the NMO vertex in  $\Pi_{\Delta_2}$ .



Note that  $j_A^3 = 2^3 j_B^3$  at  $f = 1$ . The coefficient of this term is negative throughout the region  $2/3 < f < 2$ . However, within this range of  $f$  the polytope  $\Pi_{\text{diag}}$  is truncated from its maximum configuration only at  $f = 1$ , allowing the NMO term to possibly destabilize additional regions of  $\Pi_{\Delta_2}$ .

The truncation of the polytope  $\Pi_{\Delta_2}$  at  $f = 1$  occurs because the critical 1-cycle at  $x$  in current  $B$  ( $=A$ ) causes the maximum overlap (MO) terms  $j_B^3 x^2 y$ ,  $j_B^3 x^2 z$  and  $j_B^3 x z^2$ , which correspond to vertices of  $\Pi_{\Delta_2}$ , to vanish. Each of these terms can be identified with the product  $\alpha_1 \alpha_2$ . Since  $\alpha_1 > 0$  for  $f \neq 1$  (the  $x$ -stabilizer does not vanish),  $\Pi_{\text{diag}}$  will be maximal when  $\Pi_{\alpha_2}$  is maximal. From the discussion in section 3.2.1,  $\Pi_{\alpha_2}$  is only truncated when  $f = 0.5, 1$  and  $1 + \sqrt{2}$ . The case  $f = 1$  has already been discussed, where the truncation in  $\Pi_{\Delta_2}$  is due to the  $\alpha_2$  term  $j_B^2 x z$  vanishing as a result of the critical 1-cycle at  $x$ . When  $f = 0.5$  and  $1 + \sqrt{2}$ , the coefficients of the  $\alpha_2$  terms  $j_B^2 x y$  and  $j_A^2 x y$  vanish respectively. This causes both of the corresponding MO terms  $j^3 x^2 y$  and  $j^3 x y^2$  to vanish in  $\Delta_2$ , truncating the polytope  $\Pi_{\text{diag}}$ . Since there is no critical 1-cycle passing through the NF 3-cycle for these values of  $f$ , no negative NMO vertex exists to cause possible additional destabilization in  $\Pi_{\Delta_2}$ . In fact the  $j_B^3 x y z$ ,  $j_A^3 x y z$  terms are positive and lie on an edge of  $\Pi_{\Delta_2}$  for  $f = 0.5$  and  $f = 1 + \sqrt{2}$ .



respectively. The exponent polytope  $\Pi_{\Delta_2}$  is sketched for several values of  $f$  in figure 3.4. Once again the vector  $(1,1,1)$  in  $(\log x, \log y, \log z)$  space is perpendicular to the face of constant  $j$ .

The instability conditions for the one NMO negative vertex at  $f = 1$  are given in Table 3.2 where  $\pi$  is the same as previously defined in section 3.2.1. The instability conditions define hyperplanes with the positive adjacent vertices which are identical to those defined by  $C_{\alpha_2}$  for  $f = 1$ . Therefore,  $C_{\alpha_2}$  has not been extended by the cone of negative  $\Delta_2$  due to the negative NMO vertex present at  $f = 1$  in this model.



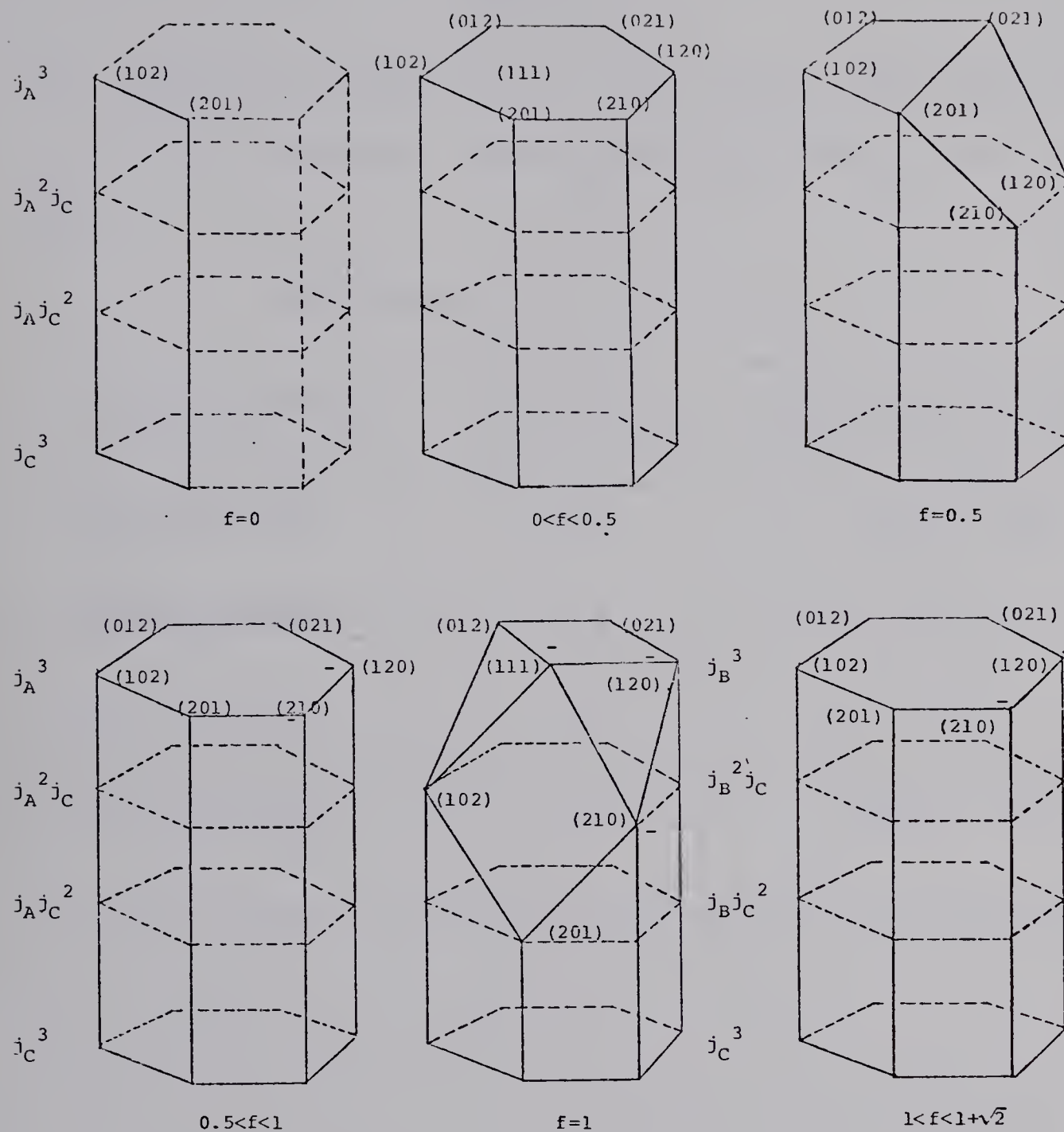


Figure 3.4

The exponent polytope  $\Pi_{\Delta_2}$  for the irreversible model, shown for various values of  $f$ .



Table 3.2

The instability conditions for the negative NMO vertex in  $\Delta_2$  at  $f = 1$ , where  $\mathfrak{L} = (\log j_A, \log j_B, \log j_C, \log x, \log y, \log z)$ .

NMO Vertex (0,3,0,1,1,1,-2)

Adjacent Vertex	Coefficient	Instability Conditions
1. (0,2,1,1,0,2)	12	$j_B y > 6j_C z$
2. (0,3,0,0,1,2)	4	$x > 2z$
3. (0,3,0,1,2,0)	-1	$2z > y$
4. (0,2,1,2,1,0)	-3	$2j_B z > 3j_C x$



### 3.2.3. Summary

In the irreversible model, one negative term occurred in a stability inequality according to the following table:

	$0 < f \leq 0.5$	$0.5 < f < 1$	$f = 1$	$1 < f < 1 + \sqrt{2}$	$f > 1 + \sqrt{2}$
--	------------------	---------------	---------	------------------------	--------------------

$\alpha_2$	+	-	-	-	+
$\alpha_3$	+	+	+	+	+
$\Delta_2$	+	+	-	+	+

The responsible destabilizing cycle and the extreme current in which the cycle originated, for each destabilizing term in the table above, is summarized in Table 3.3. One pure destabilizing term occurs in  $\alpha_2$  and destabilizes the network for  $0.5 < f < 1 + \sqrt{2}$ . At  $f = 1$ , one pure NMO destabilizing term occurs in  $\Delta_2$ , due to the negative feedback 3-cycle, but does not extend the boundary of the unstable states defined by  $C_{\alpha_2}$ .

The asymptotic boundary of the unstable steady states in the network is given by the three instability conditions which are listed in Table 3.1 for each region of  $f$ . For  $f \neq 1$ , two of the instability conditions define hyperplanes in the log of reciprocal concentration space independently of the currents. These hyperplanes have been plotted in Figure 3.5 for the case  $f = 1.1$ . If the value of  $f$  is changed, then the planes defining the asymptotic boundary are shifted parallel to the axis



Table 3.3

Summary of the cycles causing instability in the irreversible model.

---

Destabilizing cycles	The extreme currents involved	Unstable range of f
----------------------	-------------------------------	---------------------

$\alpha_2$	-----> -----<	pure A pure B	$1 \leq f < 1 + \sqrt{2}$ $0.5 < f \leq 1$
------------	------------------	------------------	---

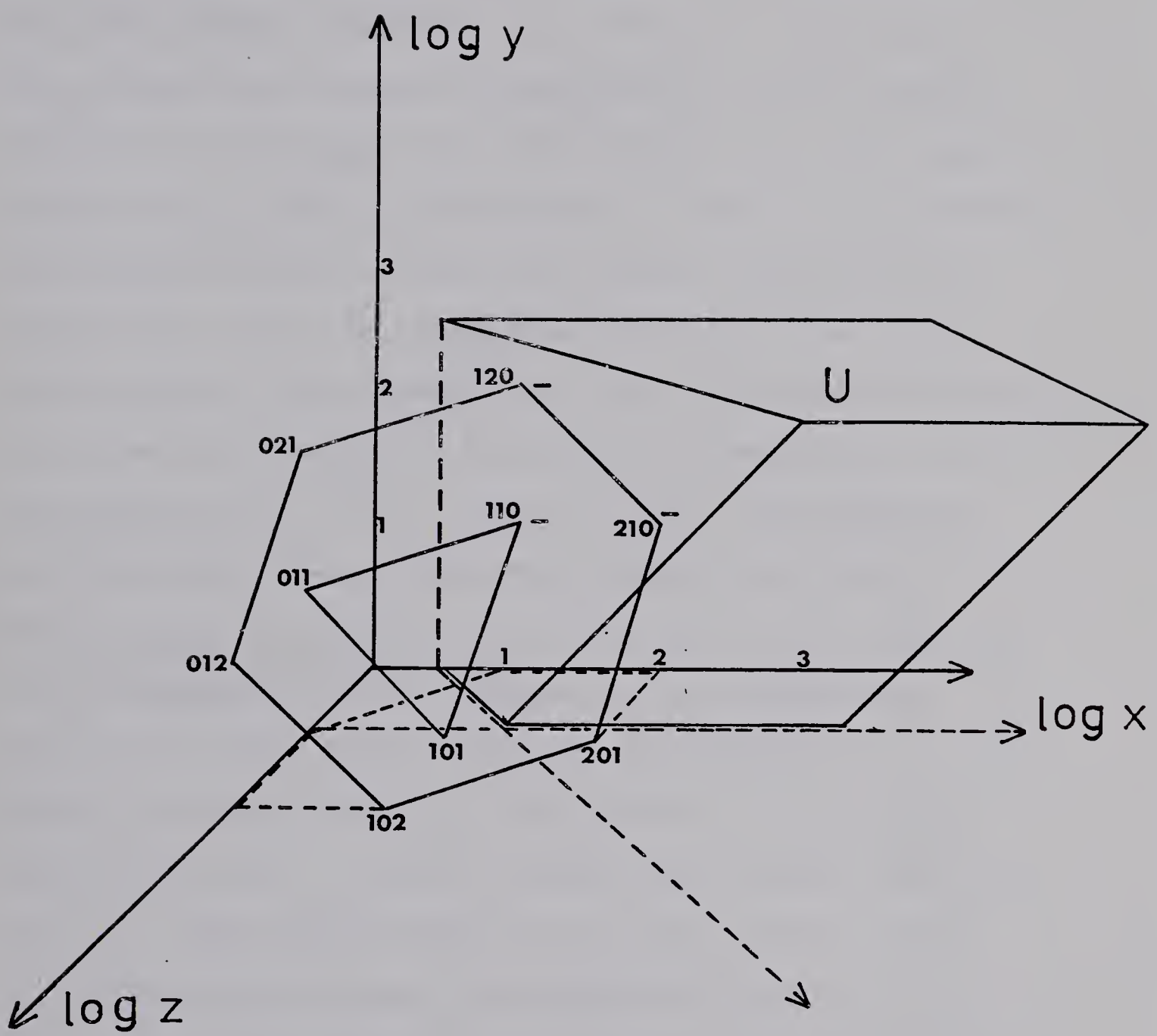
$\alpha_3$	none
------------	------

$\Delta_2$ (NMO)	----->  -----> *----->	pure A pure B	$f = 1$ $f = 1$
------------------	------------------------------	------------------	--------------------

---

\* A critical 1-cycle is necessary in addition.





Plot of the irreversible model hyperplanes at  $f=1.1$ . The unstable region is designated by U.



intercepted in the positive orthant. The result is that the "wedge" of unstable parameter space is also shifted. The relationship between these asymptotic hyperplanes and the exponent polytopes  $\Pi_{\alpha_2}$  and  $\Pi_{\Delta_2}$  is indicated by the triangle and hexagon respectively, outlined perpendicular to the vector  $(1,1,1)$  in Figure 3.5. The exponent polytopes  $\Pi_{\alpha_2}$  and  $\Pi_{\Delta_2}$  of Figures 3.2 and 3.4 are reduced to two dimensions by taking the current dependency of each vertex into the coefficient of that vertex, and then summing these coefficients over the exponent vectors with the same reciprocal concentration parameters (i.e., the points of  $\Pi_{\alpha_2}$  or  $\Pi_{\Delta_2}$  which lie on a line parallel to the vector  $(1,1,1)$  are represented by one point of the triangle or hexagon with a coefficient which depends on the currents and  $f$ ). Figure 3.5 is interesting because it shows how the hyperplanes defined by  $C_{\alpha_2}$  can become extended into  $C_{\Delta_2}$ . From Figure 3.5, it is not surprising that  $C_{\Delta_2}$  did not extend the boundary defined by  $C_{\alpha_2}$ . The dashed lines on the  $(\log x, \log z)$  plane give the position where the asymptotic planes of the unstable region in the  $f = 1.1$  case cut the  $(\log x, \log z)$  plane. The projection of the hexagon onto the  $(\log x, \log z)$  plane is also outlined in Figure 3.5, and can be compared to Figure 2.1 which corresponds to the case  $j_C = 0, j_A = 1$  and  $y = 1$ .



In section 2.2 the steady state represented by the overall reaction,

$$O_f: \frac{2}{1+f} j_A + \frac{f-1}{1+f} j_C, \quad f > 1,$$

was given. To test the stability of the steady state represented by this combination of the extreme currents, the ratio of  $j_A/j_C$  which must be violated for instability is needed. The criterion for an unstable ratio of these currents is determined by the instability condition

$$\frac{1}{2} |f^2 - 2f - 1| (j_A/j_C)^2 > f(1+2f) + f(1+3f) (j_A/j_C) \quad (3.1)$$

given in Table 3.1b for  $\alpha_2$  ( $f > 1$ ). The inequality (3.1) implies that  $j_A/j_C$  must be greater than the positive root of the quadratic equation obtained by substituting an equal sign for the inequality. For the case  $f = 1.1$  this equation yields  $j_A/j_C > 5.4$ , while the linear combination  $O_f$  above has  $j_A/j_C = 20$  for  $f = 1.1$ . Therefore,  $O_f$  is a possibly unstable steady state for  $f = 1.1$ . For any particular steady state concentration of the species, the remaining instability conditions in Table 3.1b must be tested, before instability can be determined. In the case  $f = 1.5$  the instability condition (3.1) gives  $j_A/j_C > 10.1$  while  $O_f$  yields  $j_A/j_C = 4$ . This means that  $O_f$  represents a stable steady state for  $f = 1.5$ . It follows that  $O_f$  is possibly unstable only for values of  $f$  close to one. In addition, instability condition (3.1)



implies that as  $f$  increases, the current necessary in the extreme current  $A(f > 1)$  for instability also increases.

The instability conditions give the requirements on the parameters for unstable steady states. As such they do not guarantee instability will occur, only that the parameters can be adjusted so that the steady state will become unstable. The actual rate constants may not allow a portion of the unstable region to be attained in a network.

The currents of the irreversible model can be written in terms of the rate constants by using equations (2.33) and the extreme currents:

$$\mathbf{j}_A = \left( \frac{(f-1)}{2}, \frac{(1+f)}{2}, 1, 0, 1 \right)$$

$$\mathbf{j}_C = (f, 0, 1, \frac{1+f}{2}, 1)$$

which are valid in the region  $f > 1$ . The following relations are then obtained:

$$k_1 = K_1 A = 1/Y_O \left\{ \frac{(f-1)}{2} j_A + f j_C \right\}$$

$$k_2 = K_2 = 1/X_O Y_O \left\{ \frac{(1+f)}{2} j_A \right\}$$

$$k_3 = K_3 B = 1/X_O \left\{ j_A + j_C \right\}$$

$$k_4 = K_4 = 1/X_O^2 \left\{ \frac{(1+f)}{2} j_C \right\}$$

$$k_5 = K_5 = 1/Z_O \left\{ j_A + j_C \right\}$$



Using the second and fourth relations above, the instability condition (3.1) becomes

$$j_A/j_C = K_2 Y_O / K_4 X_O > 5.4$$

at  $f = 1.1$ . Since the steady state concentrations are functions of the rate constants also, the relations

$$Z_O = K_3 B X_O / K_5$$

$$Y_O = f K_3 B X_O / (K_1 A + K_2 X_O) \quad (3.2)$$

$$-2K_2 K_4 X_O^2 + X_O ((1-f) K_2 K_3 B - 2K_1 K_4 A) + (1+f) K_1 K_3 A B = 0,$$

which are obtained from the solution of the kinetic equations at steady state, can be used to eliminate the concentration parameter from the instability conditions.

At  $f = 1$  the instability condition  $x > 2z$  in Table 3.1c can be written as

$$K_3 B X_O / K_5 > 2X_O \quad (3.3)$$

where the equation for  $Z_O$  in (3.2) has been used in addition to the definitions  $x = 1/X_O$ ,  $y = 1/Y_O$ . This equation can be used to give the upper limit on  $K_5$  for which instability occurs at  $f = 1$ . In order to compare this value to the one obtained by Field and Noyes,<sup>24</sup> the values  $B = 6 \times 10^{-2}$  M and  $K_3 = 8 \times 10^3$  M<sup>-1</sup> sec<sup>-1</sup> used in their analysis are substituted into equation (3.3). The factor of 2 in front of  $Z$  was absent in step (5) of



their model (compare with (1.6)), and so the factor of 2 in equation (3.3) is also absent. Finally, this yields

$$K_5 < K_3 B = 480 \text{ sec}^{-1}$$

for unstable states in the Oregonator model at  $f = 1$ .

The value obtained by Field and Noyes was  $k_5 = 444 \text{ sec}^{-1}$ .



### 3.3. The Reversible Model

In this section the boundary of the unstable steady states for the reversible model is given in a parallel fashion to the preceding irreversible case. The kinetics used for each step of the reversible model is determined by the following table, where the indicated kinetic order is with respect to each species:<sup>24</sup>

	forward kinetic order	reverse kinetic order
1. $A + Y \rightleftharpoons X + P$	1st	1st
2. $X + Y \rightleftharpoons 2P$	1st	1st
3. $B + X \rightleftharpoons 2X + 2Z$	1st	2nd in X, 1st in Z
4. $2X \rightleftharpoons Q$	2nd	1st
5. $2Z \rightleftharpoons fY$	1st	1st

These reactions yield thirteen extreme currents in each region of  $f$ , which are given in figure 3.6. The extreme currents labelled C,  $C^-$ , D,  $D^-$ , 1, 2, 3, 4 and 5 are valid for all values of the stoichiometric parameter  $f$ . The four remaining extreme currents A,  $A^-$ , B and  $B^-$  differ in the regions  $f < 1$  and  $f > 1$ , but are equivalent at  $f = 1$ . Note  $A = B$  and  $A^- = B^-$  at  $f = 1$ .

In a reversible network, the extreme currents can be divided into two groups: the *equilibrium extreme currents (EEC's)* and the *non-equilibrium extreme currents (NEEC's)*. The EEC's consist of a reaction and its reverse



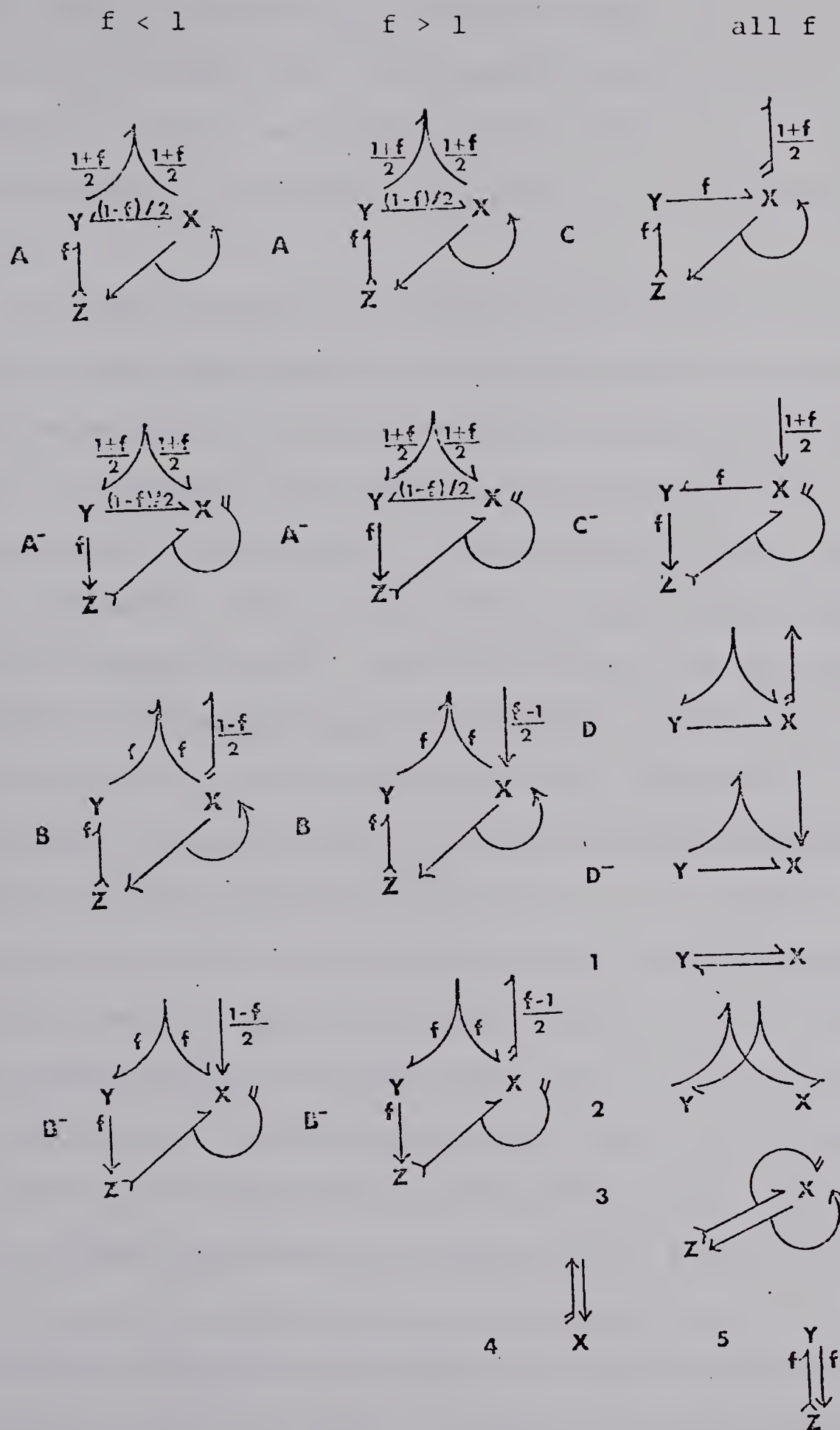


Figure 3.6

The extreme currents of the reversible model.



only, and are identified with the extreme currents labelled 1 to 5 (in figure 3.6).\* The NEEC's contain two or more reactions, and no two reactions in a NEEC are the reverse of each other. The NEEC's in figure 3.6 are labelled A to D.

The EEC's represent the steady state current in a reaction when the forward and reverse rates are equal, or in other words the EEC's satisfy *detailed balance*.

Shear<sup>46</sup> has proved that chemical systems which are decomposable into elementary reactions satisfying mass action kinetics always have stable steady states when detailed balance holds. From this it follows that any positive linear combination of the EEC's which have mass action kinetics must be stable for all values of the parameters. Only the EEC's 1, 2 and 4 have mass action kinetics in the reversible model for  $f \neq 1$ . However, the remaining EEC's 3 and 5 do not have any distinguishing behavior as a result of their non-mass action kinetics, and so need not be discussed separately in this model. The thermodynamic equilibrium steady state will be some positive linear combination of the EEC's in the network. Such a steady state will rule out any net flow of matter

---

\* Because of difficulties which may arise in non-mass action systems, future articles will use a stronger definition of EEC which restricts the reactions that make up an EEC to those having mass action kinetics.



in a closed reaction sequence (NEEC), since the flow in the forward direction is equal to the flow in the reverse direction.

Far from equilibrium, a steady state can exist without the reactions satisfying detailed balance, although a flow of matter through the system is necessary to maintain the steady state (open system). A NEEC represents a possible steady state in which the reverse of the reactions present in the NEEC have zero rate constants, and thus represents a possible steady state far from equilibrium. In the special case where all the reverse rate constants are set equal to zero, the NEEC's which exist are those found in the corresponding irreversible network.

The current polytope  $\Pi_C$  for the reversible model lies in a six dimensional subspace of the seven dimensional space in which  $\tilde{v}^0$  lies, as the application of the theory in section 2.2 shows. Any general steady state of the network is a positive linear combination of the extreme currents and is represented by a point in  $\Pi_C$ . When the steady state is given by an extreme current, the system is represented by an extreme point of  $\Pi_C$ , and the reactions not included in the extreme current have zero velocity. Two extreme points are adjacent in  $\Pi_C$  when they have the maximum number of reactions in common, since this is equivalent to having the maximum number of components of



the corresponding basis vectors (extreme currents) in common. The NEEC's A and B have three out of four possible reactions in common as do the NEEC's B and C, and so these NEEC's lie on a common face of  $\Pi_C$ . Similarly the NEEC's  $A^-$ ,  $B^-$  and  $C^-$  lie on a common face of  $\Pi_C$ . However none of the extreme currents  $A^-$ ,  $B^-$  and  $C^-$  are adjacent to A, B or C. The NEEC D has two out of three possible reactions in common with the extreme currents C and  $A^-$  and so is adjacent to these NEEC's, while the NEEC  $D^-$  is adjacent to  $C^-$  and A when  $f < 1$ . In the region  $f > 1$ , the NEEC D is adjacent to C and  $B^-$ , while  $D^-$  is adjacent to  $C^-$  and B. The EEC's represent five extreme points in a four dimensional subspace of  $\Pi_C$  which is a simplex since each EEC is adjacent to every other EEC. The relationship of the extreme currents to each other in  $\Pi_C$  is shown in figure 3.7.

On the basis of the destabilizing cycles given in the theorems of section 2.5, the network is unstable when the currents in the network are close to the NEEC's A or B (the AB edge of  $\Pi_C$ ). The extreme currents C,  $D^-$ , 1, 2, 3, 4, and 5 are adjacent to either A or B in  $\Pi_C$ , while the remaining extreme currents  $A^-$ ,  $B^-$ ,  $C^-$  and D are not adjacent to either A or B. Therefore, the extreme currents  $A^-$ ,  $B^-$ ,  $C^-$  and D were eliminated from this analysis. The effect of the deleted NEEC's on the network will be discussed in section 3.4. Even with this



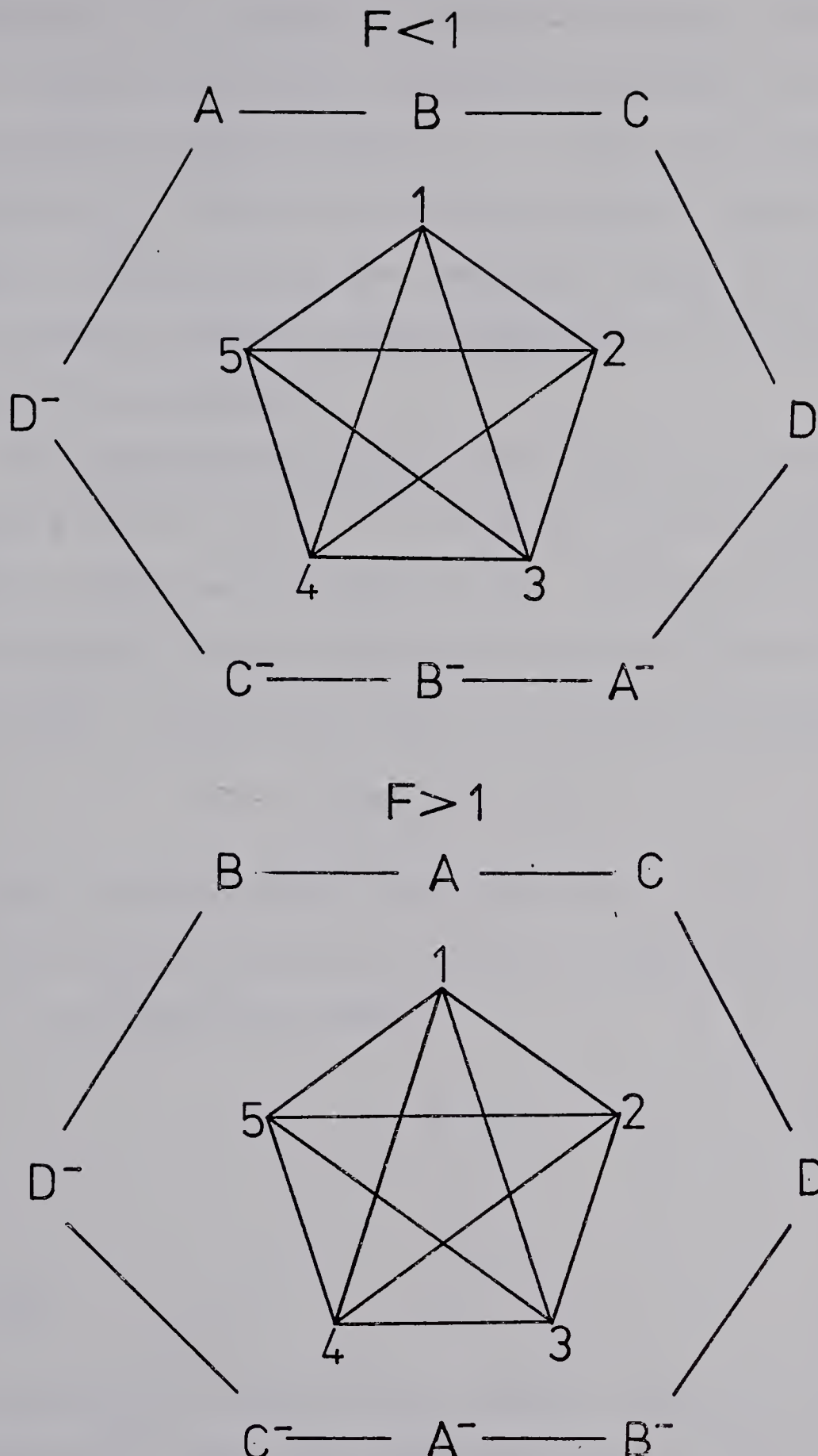


Figure 3.7

The relationship between the extreme currents of the reversible model in the current polytope  $\Pi_c$ .



reduction in the number of extreme currents, the analysis still requires thirteen parameters including the reciprocal steady state concentrations  $x$ ,  $y$ ,  $z$  and the stoichiometric parameter  $f$ . The set of extreme currents chosen form a subset of the complete set, and will serve to illustrate the effect of adding reverse reactions to an unstable irreversible network.

The interaction diagrams corresponding to the extreme currents  $A$ ,  $B$ ,  $C$ ,  $D^-$ ,  $1$ ,  $2$ ,  $3$ ,  $4$  and  $5$  are given in figure 3.8 for both regions of  $f$ . The NEEC  $A$  has been multiplied by two to remove fractions as in the irreversible model. Once again the Lienard-Chipart conditions

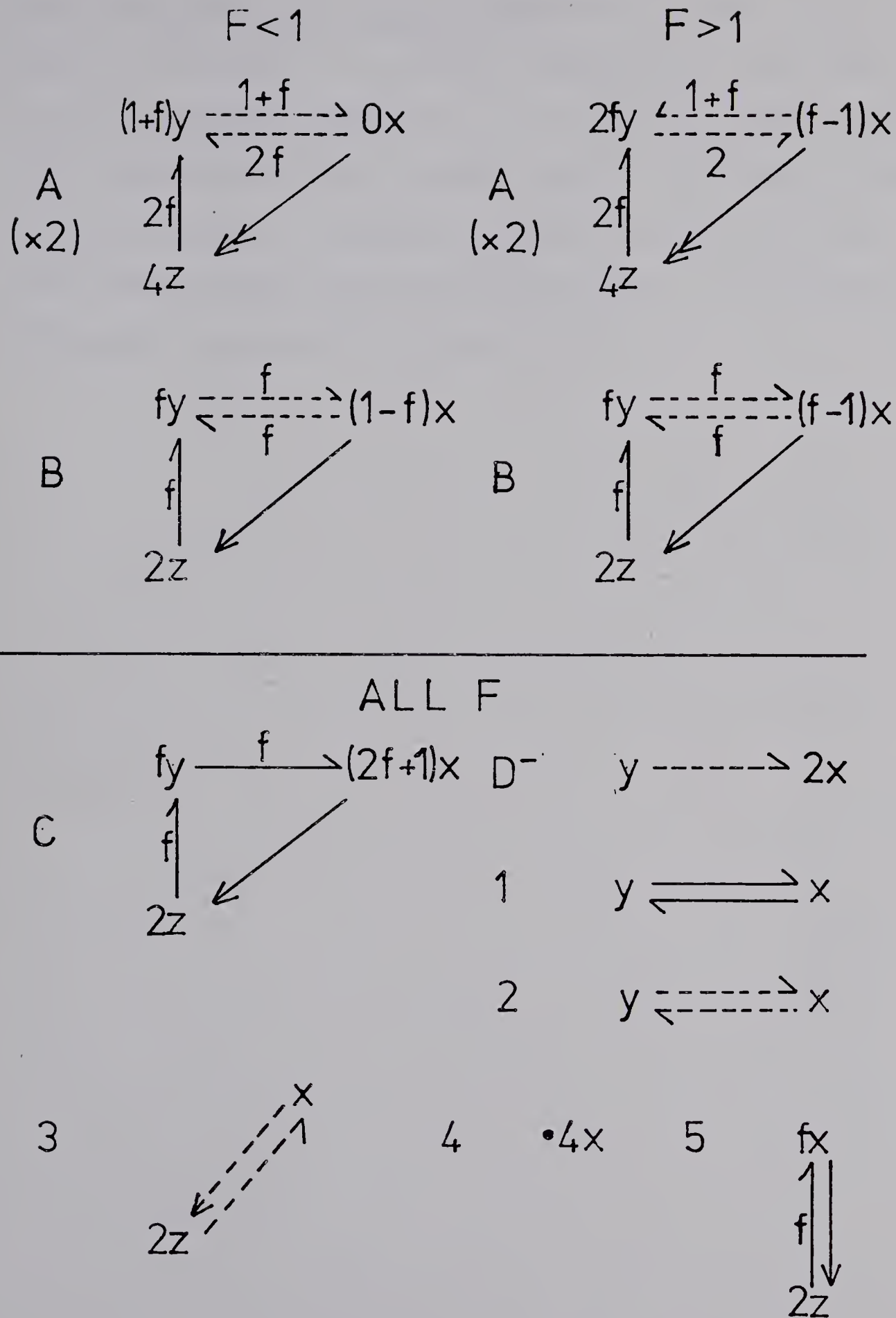
$$\alpha_1 > 0, \alpha_3 > 0, \Delta_2 > 0$$

are used in addition to the inequality  $\alpha_2 > 0$ . At least one negative term occurred in these inequalities according to the following table:

	$f < 1$	$f = 1$	$f > 1$
$\alpha_2$	-	-	-
$\alpha_3$	+	+	-
$\Delta_2$ (NMO)	-	-	+

As discussed in the previous section, only the NMO destabilizing terms are considered in  $\Delta_2$ , since only these terms can cause appreciable extension of the unstable region as defined by the union of the negative



Figure 3.8

The interaction diagrams used in the reversible model analysis.



cones of  $\alpha_2$  and  $\alpha_3$ . A quick comparison to the table given in section 3.2.2 for the irreversible case shows that the negative terms in  $\alpha_3$  ( $f > 1$ ) and  $\Delta_2$  ( $f < 1$ ) are new. The destabilizing terms found in each region above will now be given, together with the instability conditions derived from the edge approximation. A summary of the results appears in section 3.3.4.



### 3.3.1. The Cone of Negative $\alpha_2$

The possibly destabilizing terms in  $\alpha_2$  can be selected from the interaction diagrams in figure 3.8 by summing the inhibitory positive feedback (PFI) 2-cycles and stabilizer diagrams as was done for the irreversible model shown in section 3.2.1. However, the large number of current parameters in the reversible model necessitated the use of computer programs, developed for finding the vertices and edges of exponent polytopes in higher dimensional spaces,<sup>45</sup> before the instability conditions were determined. In addition, programs which calculate the terms in the stability inequalities were used to expand the determinant in the characteristic equation for  $\underline{M}$ .<sup>42</sup>

Four destabilizing terms exist in  $\alpha_2$ , two of which are pure terms derived from the NEEC's A and B. The remaining two are mixed terms involving either current A or B. The destabilizing cycle in each term is the PFI 2-cycle which occurs in both NEEC A and B. Table 3.4 tabulates the coefficients and the unstable range of  $f$  for each destabilizing term in  $\alpha_2$ , where the corresponding exponent vectors are defined by

$$\pi = (\log j_A, \log j_B, \log j_C, \log j_{D^-}, \log j_1, \log j_2, \log j_3, \log j_4, \log j_5, \log x, \log y, \log z).$$

The fifth exponent vector in Table 3.4 is a vertex of the exponent polytope  $\Pi_{\alpha_2}$  only at  $f = 0.5$  and  $1 + \sqrt{2}$ ,



Table 3.4

The negative vertices of  $\Pi_{\alpha_2}$  for the reversible model.

$\pi = (\log j_A, \log j_B, \log j_C, \log j_D, \log j_1, \log j_2,$   
 $\log j_3, \log j_4, \log j_5, \log x, \log y, \log z)$

Vertex	Coefficient							
	$f < 1$	$f = 1$	$f > 1$	$f^2 - 2f - 1$	$f^2 - 2f - 1$	$f^2 - 2f - 1$	$f^2 - 2f - 1$	$f^2 - 2f - 1$
1. (2000000000110)	$-2f(1+f)*$	$-4*$						
2. (0200000000110)	$f(1-2f)$	$-1$						
3. (1000010000110)	$-2f*$	$-2*$						
4. (0100010000110)	$1-2f$	$-1$						
5. (1100000000110)	$1-f-4f^2 (f=0.5)$							
	$f < 0.5$	$f=0.5$	$0.5 < f < 1$	$f=1$	$1 < f < 2$	$f=2$	$2 < f < 1+\sqrt{2}$	$f=1+\sqrt{2}$
1. (2000000000110)	-	-	-	-	-	-	0	+
2. (0200000000110)	+	0	-	-	-	-	-	-
3. (1000010000110)	-	-	-	-	0	+	+	-
4. (0100010000110)	+	0	-	-	-	-	-	-
5. (1100000000110)	-							

\* At  $f = 1$ ,  $j_A = 2j_B$ .



and is a midpoint of the  $j_A^2 - j_B^2$  edge for other values of  $f$ . At  $f = 0.5$  the pure destabilization  $j_B^2 xy$  vanishes, while at  $f = 1 + \sqrt{2}$  the pure destabilizing term  $j_A^2 xy$  vanishes, truncating the polytope  $\Pi_{\alpha_2}$  and allowing the midpoint corresponding to the term  $j_A^2 j_B^2 xy$  to become a vertex of  $\Pi_{\alpha_2}$ . Note from Table 3.4 that the destabilizing terms in  $\alpha_2$  change sign at either  $f = 0.5, 2$  or  $1 + \sqrt{2}$ .

The  $\alpha_2$  destabilizing terms all contain the PFI 2-cycle which passes through  $x$  and  $y$  in the interaction diagrams of figure 3.8. The sum of this 2-cycle and the stabilizer diagram for the EEC 2 has a coefficient of zero, and so the EEC 2 cannot form a pure destabilizing term in  $\alpha_2$ . As a result, the mixed destabilizing terms  $j_A j_2^2 xy$  and  $j_B j_2^2 xy$ , which would have corresponded to midpoints of the  $j_A^2 - j_2^2$  and  $j_B^2 - j_2^2$  edges of  $\Pi_{\alpha_2}$  respectively, correspond to vertices of  $\Pi_{\alpha_2}$  instead.

The cone of negative  $\alpha_2$ ,  $C_{\alpha_2}$ , for any value of  $f$  is the union of the cones  $C_{\alpha_2}^i$  resulting from each negative vertex in  $\Pi_{\alpha_2}$ . Each of the cones  $C_{\alpha_2}^i$  gives the region of dominance of the corresponding negative vertex  $i$  in  $\Pi_{\alpha_2}$ . Since the coefficients of the terms in  $\alpha_2$  are, in general, quadratic functions of  $f$ , the bounding hyperplanes of the cones  $C_{\alpha_2}^i$  will shift as  $f$  varies. At the values of  $f$  where a coefficient vanishes, the exponent polytope becomes truncated and new conditions for instability appear, corresponding to new edges of  $\Pi_{\alpha_2}$ .



In figures 3.9a and 3.9b the adjacent vertices of the pure NEEC negative vertices corresponding to the terms  $j_A^2 xy$  and  $j_B^2 xy$  are shown in each region of  $f$ . The minimum number of edges occurs in the region  $f > 1$ , where the exponent polytope is maximal. The adjacent vertices in the region  $f > 1$  are indicated by the first column in figures 3.9a and 3.9b. When a vertex vanishes, the polytope  $\Pi_{\alpha_2}$  becomes truncated and the appearance of new vertices occurs in a regular way. The adjacent vertices in figures 3.9a and b which vanish at either  $f \leq 1$  or  $f = 1$  are indicated by a star and a double star respectively. The new vertices which then appear adjacent to the pure negative vertices are indicated by the remaining columns of figures 3.9a and b. The interesting feature in these figures is that the new vertices which appear are all derived from one of the starred vertices by substituting one of the current components of the starred vertex by the current component of each of the other extreme currents in the network. An exception occurs when the EEC 5 is involved in two vertices which both vanish.

In the region  $f > 1$ , no NEEC has a critical 1-cycle and the exponent polytope  $\Pi_{\alpha_2}$  is maximal unless  $f = 2$ ,  $1 + \sqrt{2}$ . The truncation of the polytope which occurs at  $f = 2$  and  $f = 1 + \sqrt{2}$  is minimal because only the coefficient of a destabilizing term vanishes. This can be compared to the situation in the irreversible model at  $f = 1 + \sqrt{2}$ .



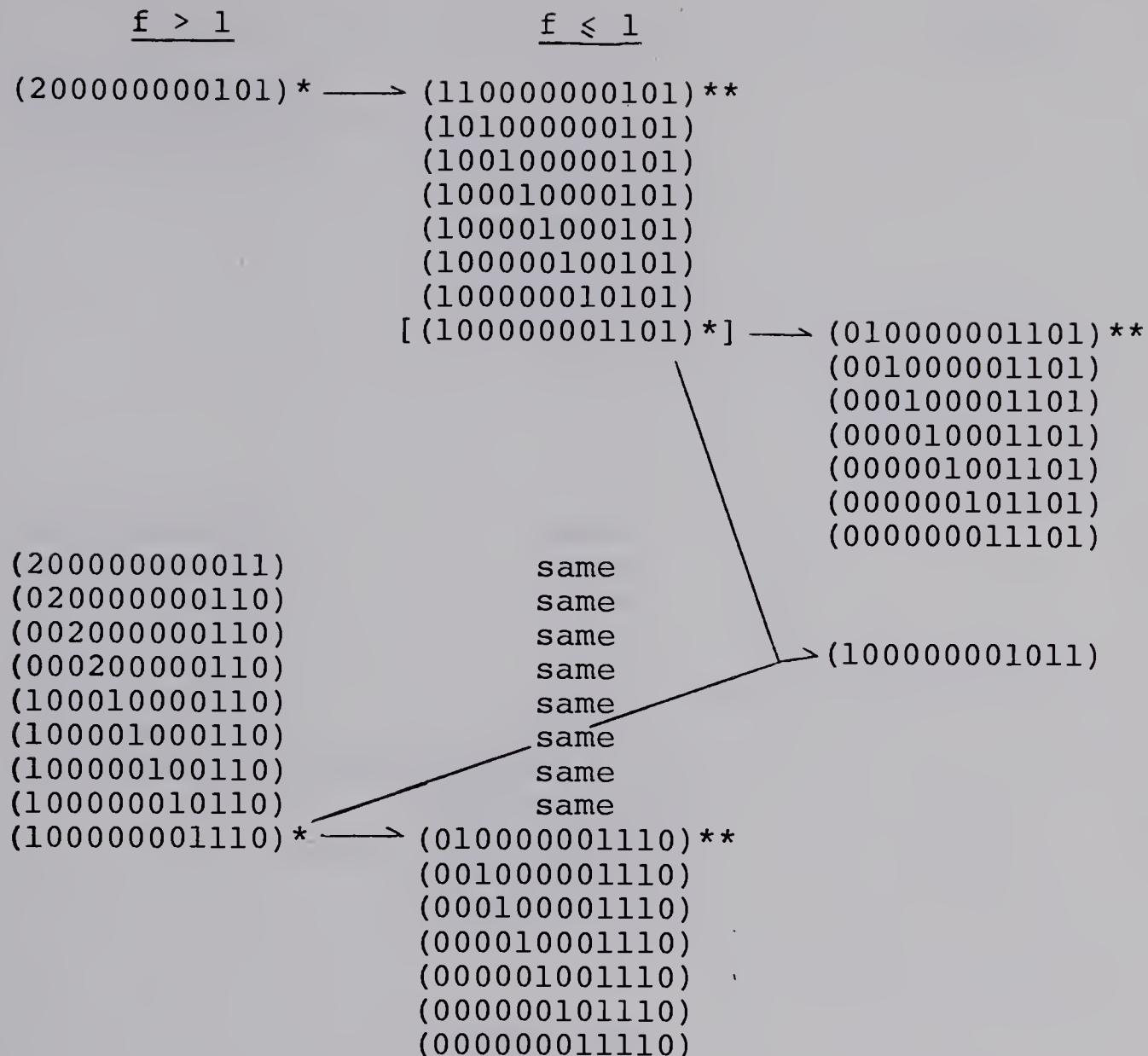


Figure 3.9a

The appearance of new adjacent vertices as  $f$  varies for the pure destabilizing term  $j_A^2 xy$ , which corresponds to the vertex (20000000110) in  $\Pi_{\alpha_2}$ .

\* Terms vanish when  $f \leq 1$ .    \*\* Terms vanish at  $f = 1$  only.



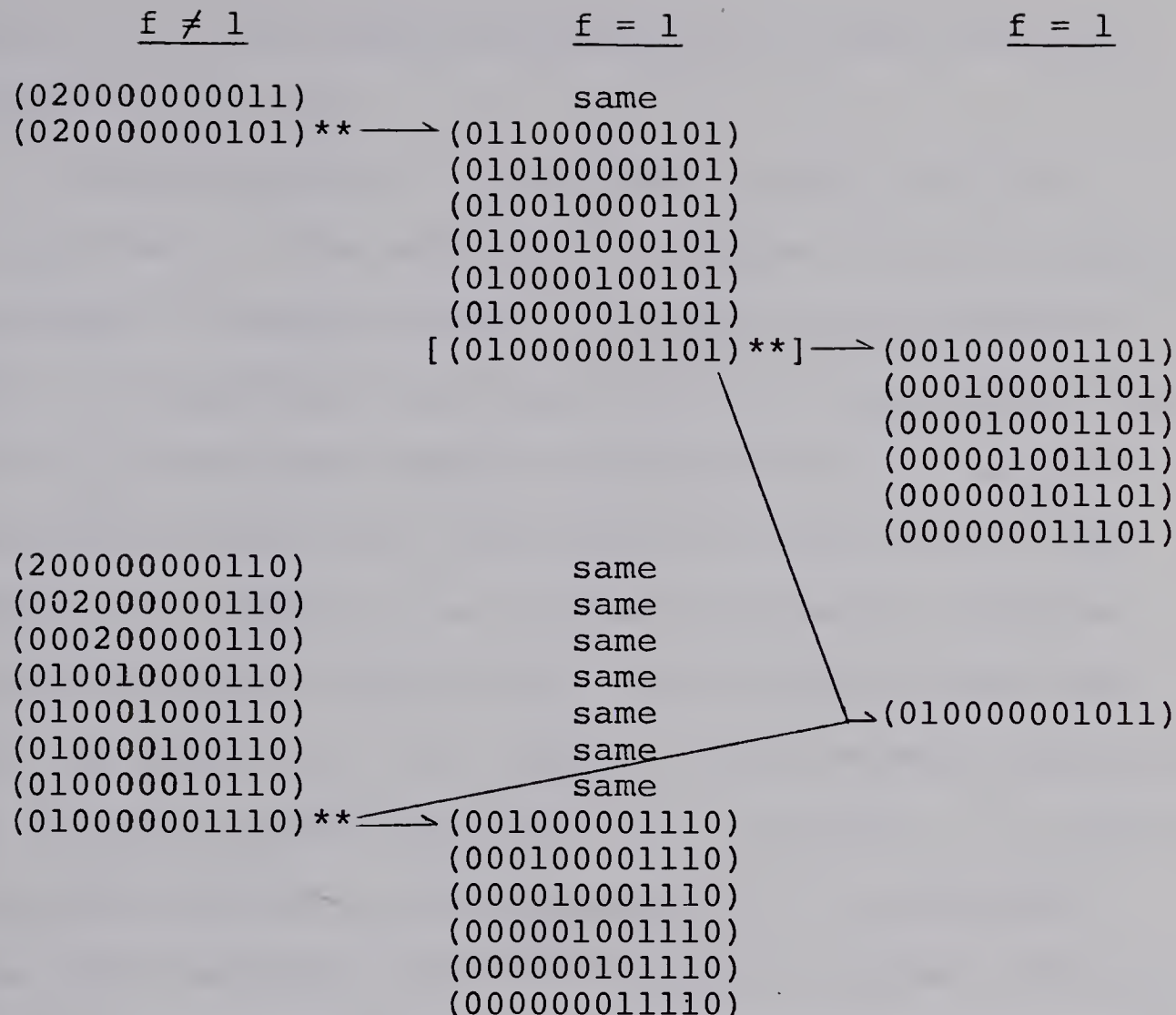


Figure 3.9b

The appearance of new adjacent vertices of the pure destabilizing term  $j_B^2 xy$  corresponding to the vertex  $(020000000110)$  in  $\Pi_{\alpha_2}$ . The ten vertices in the first column are adjacent to  $(020000000110)$  for  $f < 1$  and  $f > 1$  (except special cases).

\*\* Terms vanish at  $f = 1$  only due to a critical 1-cycle at  $n$  in the NEEC B.



When  $f > 1$ , the negative vertices in  $\Pi_{\alpha_2}$  have only ten adjacent vertices.

In the region  $f < 1$ , the NEEC A has a critical 1-cycle at  $x$ . The resulting truncation of the exponent polytope is severe because no 2-cycle exists between  $x$  and  $z$  in the NEEC A, and the vertex corresponding to the term  $j_A^2xz$  vanishes causing possibly eight new adjacent vertices to form with the vertex corresponding to the term  $j_A^2xy$ . However, one of the new adjacent vertices involves the EEC 5 which does not have an  $x$ -stabilizer for any value of  $f$ . As a result, this vertex, represented by a square bracket in figure 3.9a, vanishes. In addition, one other adjacent vertex present at  $f > 1$  involving the EEC 5 vanishes for  $f < 1$ . Hence a further truncation of  $\Pi_{\alpha_2}$  occurs and fifteen new edges appear as shown in figure 3.9a.

When  $f = 1$ , the NEEC B also has a critical 1-cycle at  $x$ . As a result, three of the adjacent vertices present at  $f < 1$  vanish in figure 3.9a, but no new adjacent vertices form. This may be attributed to the severe truncation of  $\Pi_{\alpha_2}$  already present at  $f < 1$  about the vertex corresponding to the pure destabilizing term  $j_A^2xy$ . A further truncation of the polytope at  $f = 1$  involves vertices with current components from the NEEC B. The vertex corresponding to the pure destabilizing term  $j_B^2xy$  has nineteen new edges which replace two vanishing edges



of  $\Pi_{\alpha_2}$  at  $f = 1$  as shown in figure 3.9b. Actually the truncation of  $\Pi_{\alpha_2}$  at  $f = 1$  is artificial since the NEEC's A and B are equal at  $f = 1$ . However, the truncation of  $\Pi_{\alpha_2}$  and the subsequent appearance of new positive vertices pictured in figures 3.9a and b explains the changes in the instability conditions which occur for the pure A and B destabilizing terms in each region of  $f$ .

The instability conditions for each destabilizing term in  $\alpha_2$  are given in tabular form for each region of  $f$  in which they apply. Table 3.5 summarizes which of the sets of instability conditions given in Tables 3.6 to 3.10 are applicable in each region of  $f$ .

An examination of the instability conditions for  $\alpha_2$  in each region of  $f$  yields several important results. First, in the region  $f > 1$  the only difference in the adjacent positive vertices of the pure A and B negative vertices is that current A replaces current B. Similarly the mixed current negative vertices have adjacent vertices which differ only by the current components A and B. This is to be expected since the interaction diagrams for the NEEC's A and B in the region  $f > 1$  differ only by the coefficient of the PFI 2-cycle.

In the region  $f < 1$  a similar parallel amongst the pure and mixed negative vertices is observed, except for the additional instability conditions which appear for the pure A vertex.



Table 3.5

A guide to the use of the tables of instability conditions for  $\alpha_2$  in the reversible model: the region of  $f$  in which the instability conditions given in Tables 3.6-3.10 apply.

	<u><math>f &lt; 1</math></u>	<u><math>f = 1</math></u>	<u><math>f &gt; 1</math></u>
1. (200000000110)	3.6a	3.6a	3.6b ( $f < 1 + \sqrt{2}$ )
2. (020000000110)	3.7a ( $f > 0.5$ )	3.7b	3.7c
3. (100001000110)	3.8a	3.8a,b	3.8b ( $f < 2$ )
4. (010001000110)	3.9a ( $f > 0.5$ )	3.9a,b	3.9b
5. (110000000110)	3.10a ( $f = 0.5$ )	-	3.10b ( $f - 1 + \sqrt{2}$ )



Table 3.6a  $0 \leq f \leq 1$   $-2f(f+1) = (200000000110)$ 

Adjacent Vertex	Instability Condition
1. (200000000011)	$fx > 2z$
2. (100010000110)	$f(f+1)j_A > (2f+1)j_1$
3. (100001000110)	$(f+1)j_A > j_2$
4. (100000100110)	$2fj_A > 2j_3$
5. (100000010110)	$fj_A > 2j_4$
6. (100000001011)	$fj_A x > j_5 z$
7. (020000000110)	$2f(f+1)(j_A/j_B)^2 > (4f^2 + f = 1)j_A/j_B + f(2f-1)$
8. (002000000110)	$2f(f+1)(j_A/j_C)^2 > (4f^2 + 3f + 1)(j_A/j_C)^2 + f(2f+1)$
9. (000200000110)	$f(f+1)(j_A/j_D)^2 > j_A/j_D - 1$
10. (010000001110)	$2(f+1)j_A^2 > (1-f)j_B j_5$
11. (001000001110)	$2(f+1)j_A^2 > (1+2f)j_C j_5$
12. (000100001110)	$(f+1)j_A^2 > j_D - j_5$
13. (000010001110)	$2(f+1)j_A^2 > j_1 j_5$
14. (000001001110)	$2(f+1)j_A^2 > j_2 j_5$
15. (000000101110)	$2(f+1)j_A^2 > j_3 j_5$
16. (000000011110)	$(f+1)j_A^2 > 2j_4 j_5$
17. (110000000101)	$f(f+1)j_A y > 2(1-f)j_B z$
18. (101000000101)	$f(f+1)j_A y > 2(2f+1)j_C z$
19. (100100000101)	$f(f+1)j_A y > 4j_D - z$
20. (100010000101)	$f(f+1)j_A y > 2j_1 z$
21. (100001000101)	$f(f+1)j_A y > 2j_2 z$
22. (100000100101)	$f(f+1)j_A y > 4j_3 z$
23. (100000010101)	$f(f+1)j_A y > 8j_4 z$
24. (010000001101)	$f(f+1)j_A^2 y > (1-f)j_B j_5 z$



Table 3.6a (continued)

25. (001000001101)	$f(f+1)j_A^2y > (1+2f)j_Cj_5z$
26. (000100001101)	$f(f+1)j_A^2 > 2j_D - j_5z$
27. (000010001101)	$f(f+1)j_A^2 > j_1j_5z$
28. (000001001101)	$f(f+1)j_A^2y > j_2j_5z$
29. (000000101101)	$f(f+1)j_A^2y > j_3j_5z$
30. (000000011101)	$f(f+1)j_A^2y > 4j_4j_5z$

---



Table 3.6b  $f > 1$   $2(f^2 - 2f - 1)$  (200000000110)

Adjacent Vertex	Instability Condition
1. (200000000101)	$ f^2 - 2f - 1 y > 2(f-1)z$
2. (200000000011)	$ f^2 - 2f - 1 x > 4fz$
3. (020000000110)	$2 f^2 - 2f - 1 (j_A/j_B)^2 > 2f(f-3)(j_A/j_B) + f$
4. (002000000110)	$ f^2 - 2f - 1 (j_A/j_C)^2 > 2f(1+3f)(j_A/j_C) + f(1+2f)$
5. (000200000110)	$ f^2 - 2f - 1 (j_A/j_D^-) > 2(2f-1)(j_A/j_D^-) + 1$
6. (100010000110)	$ f^2 - 2f - 1 j_A > (1+2f)j_1$
7. (100001000110)	$ f^2 - 2f - 1 j_A > (2-f)j_2$
8. (100000100110)	$ f^2 - 2f - 1 j_A > f j_3$
9. (100000010110)	$ f^2 - 2f - 1 j_A > 4f j_4$
10. (100000001110)	$2 f^2 - 2f - 1 j_A > f(f-1)j_5$

Table 3.7a  $0.5 < f < 1$   $f(1-2f)$  (020000000110)

Adjacent Vertex	Instability Condition
1. (020000000011)	$(2f-1)x > 2z$
2. (020000000101)	$f(2f-1)y > 2(1-f)z$
3. (200000000110)	$f(2f-1)(j_B/j_A)^2 > (4f^2 + f - 1)(j_B/j_A) + 2f(f+1)$
4. (002000000110)	$(2f-1)(j_B/j_C)^2 > 2(1+f)(j_B/j_C) + (1+2f)$
5. (000200000110)	$f(2f-1)(j_B/j_D^-)^2 > j_B/j_D^- + 2$
6. (010010000110)	$f(2f-1)j_B > (2f+1)j_1$
7. (010001000110)	$fj_B > j_2$
8. (010000100110)	$(2f-1)j_B > j_3$
9. (010000010110)	$(2f-1)j_B > 4j_4$
10. (010000001110)	$(2f-1)j_B > (1-f)j_5$



Table 3.7b	$f = 1$	$f(1-2f) \quad (020000000110)$
	Adjacent Vertex	Instability Condition
1. (020000000011)		$(2f-1)x > 2z$
2. (010010000110)		$f(2f-1)j_B > (2f+1)j_1$
3. (010001000110)		$f(2f-1)j_B > (2f-1)j_2$
4. (010000100110)		$(2f-1)j_B > j_3$
5. (010000010110)		$(2f-1)j_B > 4j_4$
6. (010000001011)		$(2f-1)j_B x > 2j_5 z$
7. (200000000110)		$f(2f-1) (j_B/j_A)^2 > (4f^2+f-1) (j_B/j_A) + 2f(f+1)$
8. (002000000110)		$(2f-1) (j_B/j_C)^2 > 2(1+f) (j_B/j_C) + (1+2f)$
9. (000200000110)		$f(2f-1) (j_B/j_D)^2 > j_B/j_D - 2$
10. (001000001110)		$(2f-1)j_B^2 > (1+2f)j_C j_5$
11. (000100001110)		$(2f-1)j_B^2 > 2j_D - j_5$
12. (000010001110)		$(2f-1)j_B^2 > j_1 j_5$
13. (000001001110)		$(2f-1)j_B^2 > j_2 j_5$
14. (000000101110)		$(2f-1)j_B^2 > j_3 j_5$
15. (000000011110)		$(2f-1)j_B^2 > 4j_4 j_5$
16. (011000000101)		$f(2f-1)j_B y > 2(f+2)j_C z$
17. (010100000101)		$f(2f-1)j_B y > 4j_D - z$
18. (010010000101)		$f(2f-1)j_B y > 2j_1 z$
19. (010001000101)		$f(2f-1)j_B y > 2j_2 z$
20. (010000100101)		$f(2f-1)j_B y > 2(3-f)j_B z$
21. (010000010101)		$f(2f-1)j_B y > 8j_4 z$
22. (001000001101)		$f(2f-1)j_B^2 y > 2(1+2f)j_C j_5 z$
23. (000100001101)		$f(2f-1)j_B^2 y > 4j_D - j_5 z$
24. (000010001101)		$f(2f-1)j_B^2 y > 2j_1 j_5 z$



Table 3.7b (continued)

25. (000001001101)	$f(2f-1)j_B^2 y > 2j_2 j_5 z$
26. (000000101101)	$f(2f-1)j_B^2 y > 2j_3 j_5 z$
27. (000000011101)	$f(2f-1)j_B^2 y > 8j_4 j_5 z$

Table 3.7c  $f > 1$        $-f$       (020000000110)

Adjacent Vertex	Instability Condition
1. (020000000011)	$x > 2z$
2. (020000000101)	$fy > 2(f-1)z$
3. (200000000110)	$f(j_B/j_A)^2 > 2f(f-3)j_B/j_A + 2(1+2f-f^2)$
4. (002000000110)	$(j_B/j_C)^2 > 4f(j_B/j_C) + (1+2f)$
5. (000200000110)	$f(j_B/j_D)^2 > (2f-1)j_B/j_D - 2$
6. (010010000110)	$fj_B > (4f-1)j_1$
7. (010001000110)	$fj_B > j_2$
8. (010000100110)	$j_B > j_3$
9. (010000010110)	$j_B > 4j_4$
10. (010000001110)	$j_B > (f-1)j_5$



<u>Table 3.8a</u> $0 \leq f \leq 1$		$-2f \quad (100001000110)$
Adjacent Vertex	Instability Condition	
1. (100001000011)	$fx > 2z$	
2. (100001000101)	$fy > 2z$	
3. (010001000110)	$2fj_A > \pm (1-2f) j_B \quad \begin{cases} +f < 0.5 \\ -f > 0.5 \end{cases}$	
4. (001001000110)	$2fj_A > (1+4f) j_C$	
5. (000101000110)	$fj_A > j_D -$	
6. (000011000110)	$fj_A > 2j_1$	
7. (200000000110)	$j_2 > (f+1) j_A$	
8. (000001100110)	$2fj_A > j_3$	
9. (000001010110)	$fj_A > 2j_4$	
10. (000001001110)	$2j_A > j_5$	

<u>Table 3.8b</u> $1 \leq f \leq 2$		$2(f-2) \quad (100001000110)$
Adjacent Vertex	Instability Condition	
1. (100001000011)	$(2-f)x > 2z$	
2. (100001000101)	$(2-f)y > 2z$	
3. (010001000110)	$2(2-f)j_A > j_B$	
4. (001001000110)	$2(2-f)j_A > (1+4f)j_C$	
5. (000101000110)	$(2-f)j_A > j_D -$	
6. (000011000110)	$(2-f)j_A > 2j_1$	
7. (200000000110)	$(2-f)j_2 > (1+2f-f^2)j_A$	
8. (000001100110)	$2(2-f)j_A > j_3$	
9. (000001010110)	$(2-f)j_A > 2j_4$	
10. (000001001110)	$2(2-f)j_A > f j_5$	



Table 3.9a  $0.5 < f \leq 1$   $(1-2f)$   $(010001000110)$ 

Adjacent Vertex	Instability Condition
1. $(010001000011)$	$(2f-1)x > 2z$
2. $(010001000101)$	$(2f-1)y > 2z$
3. $(100001000110)$	$(2f-1)j_B > 2fj_A$
4. $(001001000110)$	$(2f-1)j_B > (1+4f)j_C$
5. $(000101000110)$	$(2f-1)j_B > 2j_D -$
6. $(000011000110)$	$(2f-1)j_B > 4j_1$
7. $(020000000110)$	$j_2 > f j_B$
8. $(000001100110)$	$(2f-1)j_B > j_3$
9. $(000001010110)$	$(2f-1)j_B > 4j_4$
10. $(000001001110)$	$(2f-1)j_B > f j_5$

Table 3.9b  $f \geq 1$   $-1$   $(010001000110)$ 

Adjacent Vertex	Instability Condition
1. $(010001000011)$	$x > 2z$
2. $(010001000101)$	$y > 2z$
3. $(100001000110)$	$j_B > 2(2-f)j_A$
4. $(001001000110)$	$j_B > (1+4f)j_C$
5. $(000101000110)$	$j_B > 2j_D -$
6. $(000011000110)$	$j_B > 4j_1$
7. $(020000000110)$	$j_2 > f j_B$
8. $(000001100110)$	$j_B > j_3$
9. $(000001010110)$	$j_B > 4j_4$
10. $(000001001110)$	$j_B > f j_5$



Table 3.10 a  $f = 0.5$       Vertex (110000000110)  $(1-f-4f^2)$

Adjacent Vertex	Instability Condition
1. (200000000110)	$ 1-f-4f^2 j_B > 2f(f+1)j_A$
2. (020000000101)	$ 1-f-4f^2 j_Ay > 2(1-f)j_Bz$
3. (020000000011)	$ 1-f-4f^2 j_Ax > 2fj_Bz$
4. (100001000110)	$ 1-f-4f^2 j_B > 2fj_2$
5. (011000000110)	$ 1-f-4f^2 j_A > 2f(f+1)j_C$
6. (010100000110)	$ 1-f-4f^2 j_A > j_D -$
7. (010010000110)	$ 1-f-4f^2 j_A > j_1$
8. (010000100110)	$ 1-f-4f^2 j_A > f j_3$
9. (010000010110)	$ 1-f-4f^2 j_A > 4f j_4$
10. (010000001110)	$ 1-f-4f^2 j_A > f(1-f)j_5$

Table 3.10b  $f = 1 + \sqrt{2}$       Vertex (110000000110)  $2f(f-3)$

Adjacent Vertex	Instability Condition
1. -(020000000110)	$2(f-3)j_A > j_B$
2. (200000000101)	$f(3-f)j_By > 2(f-1)j_Az$
3. (200000000011)	$(3-f)j_Bx > 4j_Az$
4. (101000000110)	$(3-f)j_B > (3f+1)j_C$
5. (100100000110)	$f(3-f)j_B > (f-1)j_D -$
6. (100010000110)	$f(3-f)j_B > (1+2f)j_1$
7. +(100001000110)	$f(3-f)j_B > (f-2)j_2$
8. (100000100110)	$(3-f)j_B > j_3$
9. (100000010110)	$(3-f)j_B > 4j_4$
10. (100000001110)	$2(3-f)j_B > (f-1)j_5$



Secondly, a parallel exists between each of the mixed destabilizing terms and the corresponding pure destabilizing term from which it was derived. In the region  $f > 1$ , for example, if one replaces one of the  $j_A$ 's in an adjacent positive vertex of the pure negative vertex by  $j_2$ , then an adjacent positive vertex of the mixed negative vertex is obtained. The same situation holds for the pure B destabilizing term and the mixed destabilizing term derived from it when  $f > 1$ . In the region  $f > 1$ , the instability conditions for each pure destabilizing term are identical, in all cases but one, to those of the corresponding mixed destabilizing terms, except that the coefficient  $|c^+/c^-|$  is modified. The exception occurs in the instability condition which involves the currents of the mixed destabilizing terms, (i.e.,  $j_A$  and  $j_2$  or  $j_B$  and  $j_2$ ). In this case, the inequality involving those currents in the pure destabilizing terms is reversed in the corresponding mixed destabilizing term inequality. For example, the NEEC B pure term  $j_B^2 xy$  has the instability condition  $fj_B > j_2$  in the region  $f > 1$ , and the corresponding mixed term  $j_B j_2 xy$  has the instability condition  $j_2 > fj_B$ . This instability condition implies that the cones of negative  $\alpha_2$  due to each of these destabilizing terms have a common hyperplane and that if  $fj_B > j_2$  then the cone due to the pure destabilizing term applies. Since both the adjacent



vertices are negative for this hyperplane, it does not form part of the boundary of stability. Furthermore, any hyperplane corresponding to the remaining instability conditions for the pure term  $j_B^2 xy$  lies parallel to the corresponding hyperplane in the mixed term  $j_B j_2 xy$ , and the most destabilizing hyperplane is determined by the coefficient  $|c^-/c^+|$ . This coefficient is always smaller for the pure destabilizing term instability conditions and so the hyperplanes for this term destabilize a greater volume of parameter space, since they are less restrictive. Similarly the pure destabilizing term  $j_A^2 xy$  has instability conditions which destabilize a greater volume of parameter space than the mixed term  $j_A j_2 xy$ . In conclusion, in the region  $f > 1$  where  $\Pi_{\alpha_2}$  is maximal, the instability conditions due to a pure destabilizing term in  $\alpha_2$  determines a cone of negative  $\alpha_2$  which *contains* the corresponding cone due to the mixed destabilizing term. It follows that when the current in the EEC 2 is large ( $j_2 \gg j_A$  or  $j_B$ ) then the cone of negative  $\alpha_2$  defined by the corresponding pure destabilizing term is replaced by the cone defined by the mixed destabilizing term, and so the unstable region in parameter space shrinks.

In the region  $f < 1$ , the situation is the same for the pure and mixed destabilizing terms involving the NEEC B. However, the pure destabilizing term  $j_A^2 xy$  lies



in a truncated region of  $\Pi_{\alpha_2}$  when  $f < 1$ . The truncation of  $\Pi_{\alpha_2}$  due to the critical 1-cycle at  $x$  eliminates the positive vertices (200000000101) and (1000000001110) which are adjacent to the vertex corresponding to the pure A destabilizing term for  $f > 1$ . As discussed before, this occurs because neither the NEEC A nor the EEC 5 have an  $x$ -stabilizer, and no 2-cycle can be formed between the parameters of the terms  $j_A^2xz$  and  $j_Aj_5xy$ . The net result is that the instability conditions  $2j_A > j_5$  and  $fy > 2z$  present in Table 3.8a for the mixed destabilization term  $j_Aj_2xy$  cannot be formed in the pure A destabilizing term. It follows that many new instability conditions appear for the pure destabilizing term in Table 3.6a. However, if the missing inequalities given above are multiplied by the remaining instability conditions of Table 3.8a, then the Table 3.6a is obtained, apart from the correct coefficients. The coefficients  $|c^+/c^-|$  of the instability conditions due to the pure destabilizing term are smaller than the coefficients of the corresponding mixed destabilizing term, and hence destabilize a greater portion of parameter space. It follows once again that the cone of negative  $\alpha_2$  due to the mixed destabilizing term is contained in the cone due to the pure destabilizing term. This result holds for  $f < 1$ , in the case of the NEEC A. When  $f = 1$  the NEEC B also has a critical 1-cycle of  $x$ , although since the NEEC A equals the NEEC B at  $f = 1$ ,



this reduces to the case described above for the pure A destabilizing term in the region  $f < 1$ .

In summary, the cones of negative  $\alpha_2$  due to the mixed destabilizing terms are contained in the cones defined by the corresponding pure destabilizing terms. When the current in the EEC 2 is large, the cones due to the mixed destabilizing terms apply, and stabilize the unstable region in  $\alpha_2$  as defined by the pure destabilizing terms. The cone of negative  $\alpha_2$  can be given as a first approximation by the union of the cones defined by the pure destabilizing terms. In this case the instability condition defined between the currents of the mixed destabilizing term is dropped from the complete set given for the corresponding pure destabilizing term. This approximation would overestimate the unstable region in  $\alpha_2$  when the current in the EEC 2 is large, but can be used to give an upper bound on the unstable volume of parameter space resulting from the  $\alpha_2$  instability.



### 3.3.2. The Cone of Negative $\alpha_3$

When  $f \leq 1$ , all of the terms in  $\alpha_3$  are positive. In the region  $f > 1$ , two mixed destabilizing terms occur as follows:

- 1)  $j_B^2 j_3 xyz - 2f(f-1)$
- 2)  $j_B j_2 j_3 xyz - 2(f-1)$

The diagrams which sum to form these terms are given in figure 3.10, along with the coefficients in each region of  $f$ , as found from the interaction diagrams in figure 3.8. These  $\alpha_3$  terms have the positive coefficients  $6f(1-f)$  and  $6(1-f)$  in the region  $f < 1$ , for the first and second terms above, respectively.

The change in sign of these terms varies in a regular way with the parameter  $f$ . The stabilizers are dominated by the inhibitory positive feedback (PFI) 2-cycle between  $x$  and  $y$ , and the inhibitory positive feedback (PFI) 3-cycle when  $f > 1$ . At  $f = 1$ , these diagrams have coefficients which cancel each other. When  $f < 1$ , the stabilizers are greater than the destabilizing 2 and 3-cycles.

If the PFI 3-cycle was absent these  $\alpha_3$  terms would be positive for all  $f$  showing that it is the addition of this 3-cycle to the PFI 2-cycle which causes the instability in  $\alpha_3$ . The NEEC A also forms these cycles with the EEC's 2 and 3, but has a positive coefficient for all  $f$ . Only the NEEC B in the region  $f > 1$  forms a PFI



Vertex 1 (020000100111)  $(j_B^2 j_3 xyz)$

$$\alpha_3 = \begin{array}{c} \bullet \bullet + \bullet \bullet - \begin{array}{c} \searrow \swarrow \\ \bullet \end{array} - \begin{array}{c} \searrow \swarrow \\ \uparrow \downarrow \end{array} - \begin{array}{c} \nearrow \nwarrow \\ \bullet \end{array} \end{array}$$

$$f > 1 \quad 2f(f-1) + 2f - 2f^2 - 2f^2 + 2f = -2f(f-1)$$

$$f < 1 \quad 2f(1-f) + 2f - 2f^2 - 2f^2 + 2f = 6f(1-f)$$

Vertex 2 (010001100111)  $(j_B j_2 j_3 xyz)$

$$\alpha_3 = \begin{array}{c} \bullet \bullet + \bullet \bullet + \bullet \bullet - \begin{array}{c} \searrow \swarrow \\ \bullet \end{array} - \begin{array}{c} \searrow \swarrow \\ \bullet \end{array} - \begin{array}{c} \searrow \swarrow \\ \uparrow \downarrow \end{array} - \begin{array}{c} \nearrow \nwarrow \\ \bullet \end{array} \end{array}$$

$$f > 1 \quad 2f + 2(f-1) + 2 - 2f - 2f - 2f - 2f + 2 = -2(f-1)$$

$$f < 1 \quad 2f + 2(1-f) + 2 - 2f - 2f - 2f - 2f + 2 = 6(1-f)$$

Figure 3.10

The diagrams contributing to the  $\Pi_{\alpha_3}$  negative vertices in the region  $f > 1$  for the reversible model. The coefficients of these terms are positive when  $f < 1$ .



2-cycle and PFI 3-cycle which are large enough to dominate the positive diagrams. From figure 3.10 it can be seen that these destabilizing cycles increase a power of  $f$  faster than the positive diagrams only when  $f > 1$ . It is interesting to note that extreme current  $B$  is the only NEEC with the reverse of reaction (4) (except  $B^-$ ,  $C^-$ ,  $D^-$  which were eliminated from the analysis). This reaction in the forward direction increases the value of the  $x$ -stabilizer with second order kinetics.

One of the most significant points about the  $\alpha_3$  destabilizing terms is that the presence of the EEC 3 is necessary before the PFI 3-cycle can be formed with the NEEC  $B$ . In particular, the corresponding pure NEEC term  $j_B^3 xyz$  is positive. This is quite different from the  $\alpha_2$  case discussed previously, in which the mixed destabilizing terms did not occur without a corresponding pure destabilizing term.

The instability conditions which define the cone of negative  $\alpha_3$  for  $f > 1$  are given in Table 3.11. Several of the instability conditions in Table 3.11 occur in the  $\alpha_2$  instability conditions for the destabilizing terms involving the NEEC  $B$ , only the coefficients are modified. The remaining instability conditions are new. Therefore the cone of negative  $\alpha_3$  partly overlaps the cone of negative  $\alpha_2$ . It follows that both the unstable regions defined by  $\alpha_2$  and  $\alpha_3$  are necessary to describe the boundary of the unstable steady states in the reversible model.



**Table 3.11** The instability conditions for  $\alpha_3$ .

$(f > 1)$	$-2f(f-1)$	$(020000100111)$
Adjacent Vertex	Instability Condition	
1. $(200000100111)$	$f(f-1)j_B^2 > 2(f^2-1)j_A^2 + 4f(f+1)j_Aj_B$	
2. $(100000101111)$	$f(f-1)j_B^2 > (f^2-1)j_Aj_5$	
3. $(030000000111)$	$j_3 > j_B$	
4. $(020000001111)$	$j_3 > j_5$	
5. $(010010100111)$	$f(f-1)j_B > (1+5f)j_1$	
6. $(010001100111)$	$fj_B > j_2$	
7. $(010000110111)$	$(f-1)j_B > 4j_4$	
8. $(002000100111)$	$(f-1)(j_B/j_C)^2 > 4(1+f)j_B/j_C + 3(1+f)$	
9. $(001000101111)$	$(f-1)j_B^2 > 3(1+f)j_Cj_5$	
10. $(000200100111)$	$f(f-1)(j_B/j_D^-)^2 > f(j_B/j_D^-) + 2$	
11. $(000100101111)$	$f(f-1)j_B > (1+f)j_D^- - j_5$	
12. $(000010101111)$	$f(f-1)j_B^2 > 2(1+f)j_1j_5$	
13. $(000000111111)$	$(f-1)j_B^2 > 4j_4j_5$	

$(f > 1)$	$-2(f-1)$	$(010001100111)$
1. $(200001000111)$	$j_Bj_3 > 8j_A^2$	
2. $(200000100111)$	$(f-1)j_Bj_2 > 2(f^2-1)j_A^2$	
3. $(100001001111)$	$j_Bj_3 > 4j_Aj_5$	
4. $(100000101111)$	$(f-1)j_Bj_2 > (f^2-1)j_Aj_5$	
5. $(020001000111)$	$j_3 > j_B$	
6. $(020000100111)$	$j_2 > f j_B$	
7. $(010001001111)$	$j_3 > j_5$	
8. $(001001100111)$	$(f-1)j_B > 3(1+f)j_C$	
9. $(001000101111)$	$(f-1)j_Bj_2 > 3f(1+f)j_Cj_5$	



10. (000101100111)  $(f-1)j_B > 2j_D$
11. (000100101111)  $(f-1)j_B j_2 > (1+f)j_D - j_5$
12. (000011100111)  $(f-1)j_B > 4j_1$
13. (000010101111)  $(f-1)j_B j_2 > 2(1+f)j_1 j_5$
14. (000001110111)  $(f-1)j_B > 4j_4$
15. (000001111111)  $(f-1)j_B j_2 > 4fj_4 j_5$



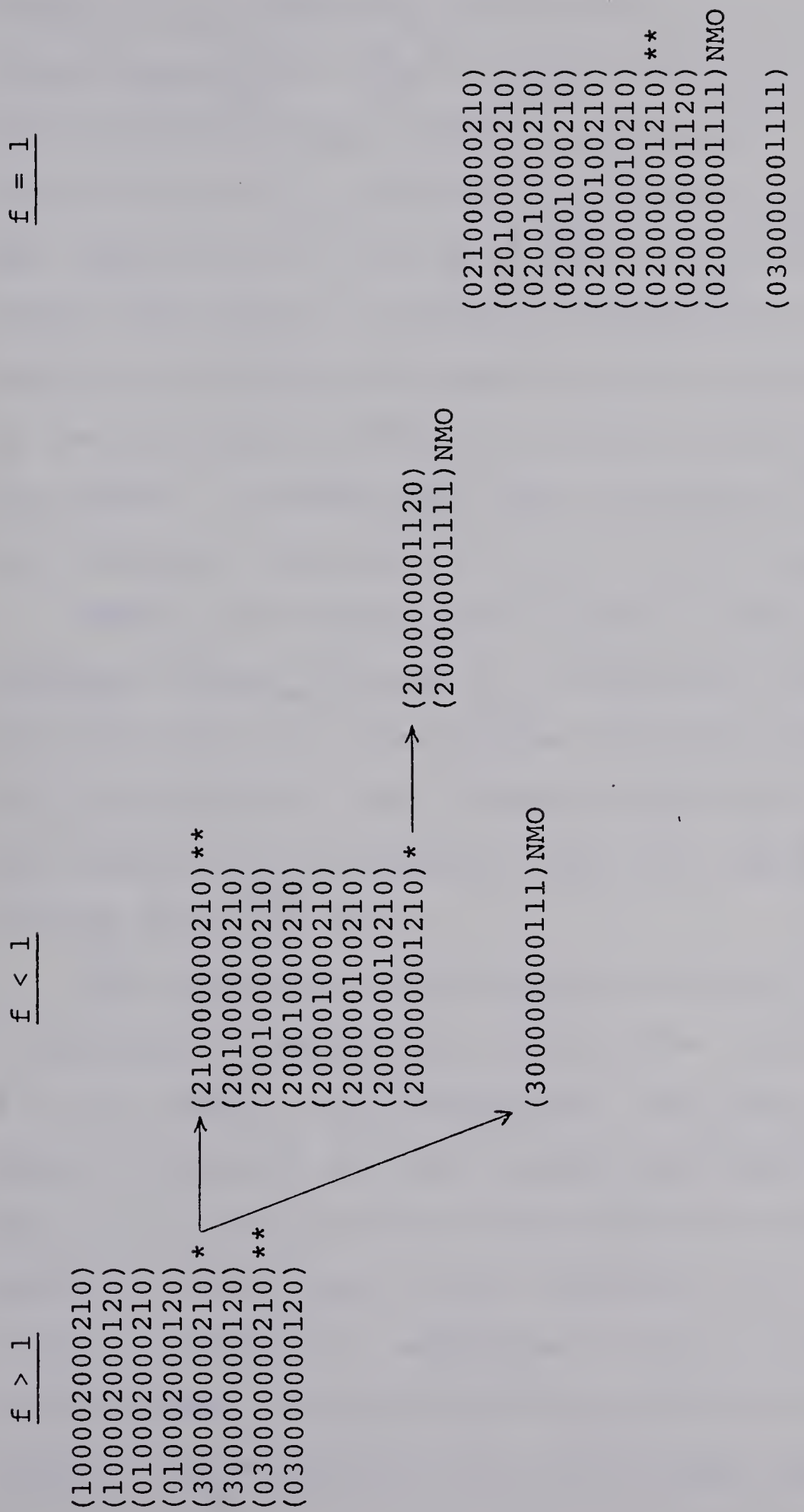
### 3.3.3. The Cone of Negative $\alpha_2$

The destabilizing terms in  $\alpha_2$  generate many negative vertices in  $\Pi_{\Delta_2}$  through the product  $\alpha_1 \alpha_2$ . However, as discussed in section 3.2.2, it is the NMO negative vertices which have a negative feedback (NF) 3-cycle passing through a critical 1-cycle that may extend the unstable region in the network by an appreciable amount.

In the region  $f > 1$  there are eight negative vertices in  $\Pi_{\Delta_2}$ , and none of these are NMO vertices. The exponent polytope  $\Pi_{\Delta_2}$  has maximum configuration in this region of  $f$ , except at  $f = 2$  and  $1 + \sqrt{2}$ . At  $f = 1 + \sqrt{2}$  the destabilizing terms  $j_A^3 x^2 y$ ,  $j_A^3 x y^2$ ,  $j_A j_2^2 x^2 y$  and  $j_A j_2^2 x y^2$  vanish in  $\Delta_2$  because the coefficient of the  $\alpha_2$  term  $j_A^2 x y$  is zero. The polytope  $\Pi_{\Delta_2}$  is truncated and two new negative vertices appear, corresponding to the terms  $j_A^2 j_B x^2 y$  and  $j_A^2 j_B x y^2$ , which are on an edge of the maximum polytope. These terms have MOD's and do not destabilize the network beyond the cone of negative  $\alpha_2$ . At  $f = 2$ , no new negative vertices appear, in parallel with  $\alpha_2$  results. The negative vertices in  $\Pi_{\Delta_2}$  are listed in figure 3.11 for  $f > 1$ .

In the region  $f < 1$ , there are seventeen negative vertices in  $\Pi_{\Delta_2}$ . This large increase in the number of negative vertices occurs because the critical 1-cycle in the NEEC A causes many of the MO vertices in  $\Pi_{\Delta_2}$  to vanish. At the special case of  $f = 0.5$ , the coefficient



Figure 3.11

The appearance of new negative vertices in  $\Pi_{\Delta_2}$  with  $f$ . \* Term vanishes  $f < 1$ .  
 \*\* Term vanishes  $f = 1$  only.



of the  $\alpha_2$  term  $j_B^2 xy$  vanishes and the polytope  $\Pi_{\Delta_2}$  is further truncated because the MO vertices corresponding to the terms  $j_B^3 x^2 y$ ,  $j_B^3 xy^2$ ,  $j_B j_2^2 x^2 y$  and  $j_B j_2^2 xy^2$  vanish. No new destabilization occurs in the network, however, because the new  $\Pi_{\Delta_2}$  vertices  $j_A j_B x^2 y$  and  $j_A j_B xy^2$  which are negative lie on the  $j_A^3 - j_B^3$  edge in  $\Pi_{\Delta_2}$  which lies inside the region of instability determined by  $\alpha_2$ . The other new vertices which appear are all positive as the  $\alpha_1$  term  $j_B x$  still exists (i.e., the x-stabilizer does not vanish). The NMO term  $j_B^3 xyz$  is positive and corresponds to a midpoint of an edge of  $\Pi_{\Delta_2}$  at  $f = 0.5$ , as expected.

When  $f = 1$ , the critical 1-cycle in the NEEC B vanishes and the polytope  $\Pi_{\Delta_2}$  is truncated further still. For this value of  $f$ , 24 negative vertices exist. However, this is artificial since current A equals current B and the polytope  $\Pi_{\Delta_2}$  is symmetric about the hyperplane through the  $j_A^3 - j_B^3$  edge.

The appearance of new negative vertices in  $\Pi_{\Delta_2}$  with  $f$  is shown in figure 3.11, although the special cases  $f = 0.5$ , 2 and  $1 + \sqrt{2}$  are omitted. Only when the polytope is truncated from its maximum configuration at  $f > 1$  due to a critical 1-cycle, do NMO negative vertices appear. Although the polytope is also truncated for  $f = 0.5$ , 2 and  $1 + \sqrt{2}$  when the coefficient of an  $\alpha_2$  destabilizing term vanishes, no additional NMO negative vertices are formed. The truncation of  $\Pi_{\Delta_2}$  that occurs for these



values of  $f$  is not destabilizing since the stabilizers present before the truncation all exist and contribute to the diagrams which define the positive adjacent vertices to the negative vertices. The new negative vertices that did appear were midpoints on a destabilizing edge before truncation occurred. Hence they cannot define hyperplanes which lie outside the unstable region of the maximal polytope.

The negative vertices which occur in  $\Pi_{\Delta_2}$  are listed in Table 3.12. The coefficients in this table were calculated by summing all the possible diagrams which can be formed in the product  $\alpha_1 \alpha_2 - \alpha_3$ . The possible diagrams contributing to this product are given in the interaction diagrams in figure 3.8. Only the product  $\alpha_1 \alpha_2$  is needed to calculate the MO vertices, while the NMO vertices have  $\alpha_3$  diagrams that must be subtracted from the diagonal product  $\alpha_1 \alpha_2$ . Only when the negative feedback 3-cycle in  $\alpha_3$  survived total cancellation did negative NMO vertices result.

Two negative NMO vertices occur in  $\Pi_{\Delta_2}$  throughout the region  $f < 1$ , and they correspond to the following destabilizing terms:

$j_A^3 xyz$	$-8f(1+f)$	(Vertex 3, table 3.12)
$j_A^3 j_5 xyz$	$-4f(1+f)$	(Vertex 23, table 3.12)

Both of these terms are due to a negative feedback (NF)



Table 3.12  $\Delta_2$  Negative Vertices

term	coefficient $f < 1$	$f > 1$
1. (300000000210)	0	$2f^3 - 6f^2 + 2f + 2$
2. (300000000120)	$-2(1+f)^2 f$	$4f(f^2 - 2f - 1)$
3. (300000000111)	$-8f(1+f)$	$16f(f-2)$
4. (210000000210)	$-2f(1+f)(1-f)$	$2(2f^2 - 7f^2 + 4f + 1)$
5. (030000000210)	$f(2f^2 - 3f + 1)$	$f(1-f)$
6. (030000000120)	$f^2(1-2f)$	$-f^2$
7. (030000000111)	$-2f(3f-2)$	$-2f(2-f)$
8. (201000000210)	$-2f(2f+1)(f+1)$	$9f^3 - 9f^2 - 9f - 3$
9. (200100000210)	$-4f(1+f)$	$2(4f^2 - 7f - 1)$
10. (200010000210)	$-2f(f+1)$	$2(3f^2 - 3f - 2)$
11. (200001000210)	$-2f(f+1)$	$2(2f^2 - 5f + 1)$
12. (021000000210)	$-3f(2f^2 - 1)$	$f(4f^2 - 6f - 1)$
13. (020100000210)	$-4f^2 + f + 1$	$2f^2 - 5f + 1$
14. (020010000210)	$-4f^2 + 2f + 1$	$4f^2 - 2f + 1$
15. (020001000210)	$1-2f$	$1-2f$
16. (100002000210)	$-2f$	$2(f-2)$
17. (100002000120)	$-2f$	$-4$
18. (010002000210)	$(1-2f)$	$-1$
19. (010002000120)	$(1-2f)$	$-1$
20. (20000100210)	$-2f(f+1)$	$5f^2 - 8f - 1$
21. (200000010210)	$-8f(f+1)$	$8(2f^2 - 3f - 1)$
22. (200000001120)	$-2f^2(f+1)$	$2f(2f^2 - 3f - 1)$
23. (200000001111)	$-4f(f+1)$	$8f(2f-3)$
24. (020000100210)	$f(2-3f)$	$f(f-2)$
25. (020000010210)	$4f(2-3f)$	$4f(f-2)$
26. (020000001120)	$f^2(2-3f)$	$f^2(f-2)$
27. (020000001111)	$-2f(5f-4)$	$-2f(4-3f)$



Table 3.12 (continued) Sign in the Region of Dominance.

	$f=0$	$0 < f < 0.5$	$f=0.5$	$0.5 < f < 1$	$f=1$	$2 > f > 1$	$f > 2$	$2.414 < f$
1.	0	0	0	0	0	-	-	+
2.	0	-	-	-	-	-	-	+
3.	0	-	-	-	-	-	-	-
4.	0	-	-	-	0	-	-	-
5.	0	+	- <sup>(1)</sup>	-	0	-	-	-
6.	0	+	- <sup>(2)</sup>	-	-	-	-	-
7.	0					-		
8.	0	-	-	-	-	-		
9.	0	-	-	-	-	-		
10.	0	-	-	-	-	-		
11.	0	-	-	-	-	-		
12.	0					-		
13.	+1					-		
14.	+1					-		
15.	+1					-		
16.	0	-	-	-	-	-	+	+
17.	0	-	-	-	-	-	-	-
18.	+1	0		-	-	-	-	-
19.	+1	0		-	-	-	-	-
20.	0	-	-	-	-	-		
21.	0	-	-	-	-	-		
22.	+4	-	-	-	-	-		
23.	0	-	-	-	-	-		
24.	+1					-		
25.	0					-		
26.	0					-		
27.	0					-		

(1) At  $f = 0.5$  vertex 5 is replaced by (120000000210)

(2) At  $f = 0.5$  vertex 6 is replaced by (120000000120)



3-cycle which passes through a critical 1-cycle. The diagrammatic simplification for these terms is shown in figure 3.12. The critical 1-cycle at  $x$  in the NEEC A ( $f < 1$ ) prevents the cancellation of the NF 3-cycle, which originates in  $\alpha_3$ , by the product  $\alpha_1 \alpha_2$ . In the mixed current vertex, the NEEC A ( $f < 1$ ) overlaps with the EEC 5 which is the only other extreme current without an  $x$ -stabilizer. Again, this prevents the formation of a stabilizer diagram in the product  $\alpha_1 \alpha_2$ .

The instability conditions which define the cone of negative  $\Delta_2$  for the NMO negative vertices above are given in Table 3.13. The hyperplanes defined by the adjacent positive vertices are identical to hyperplanes found in the instability conditions for the  $\alpha_2$  term  $j_A^2 xy$  when  $f < 1$  (Table 3.6a). The remaining instability conditions in Table 3.13 are due to adjacent negative vertices with MOD's and do not form part of the boundary of stability. As in the  $\alpha_2$  case, the instability conditions for the  $\Delta_2$  NMO terms can be multiplied to give the additional inequalities which appear in Table 3.6a. The cones of negative  $\Delta_2$  defined by the NMO vertices 3 and 23 do not extend the cone of negative  $\alpha_2$  defined by the destabilizing term  $j_A^2 xy$ . When the current in the EEC 2 is large and the boundary of stability in  $\alpha_2$  is described by the mixed destabilizing term  $j_A j_2 xy$ , the network cannot be further destabilized by  $\Delta_2$  either, since the cones of



Vertex 3 (300000000111)  $j_A^3 xyz$

$$\Delta_2 = \alpha_1 \alpha_2 - \alpha_3$$

$$\Delta_2 = - \begin{array}{c} \overrightarrow{\text{---}} \\ \cdot \end{array} - \left\{ - \begin{array}{c} \overrightarrow{\text{---}} \\ \cdot \end{array} - \begin{array}{c} \overrightarrow{\text{---}} \\ \diagup \diagdown \end{array} \right\}$$

$$= + \begin{array}{c} \overrightarrow{\text{---}} \\ \diagup \diagdown \end{array} = -8f(1+f), f \neq 1$$

Vertex 23 (200000001111)  $j_A^2 j_5 xyz$

$$\Delta_2 = + \begin{array}{c} \overrightarrow{\text{---}} \\ \diagup \diagdown \end{array} = -4f(1+f), f \neq 1$$

Vertex 7 (030000000111)  $j_B^3 xyz$

$$\Delta_2 = 2 \begin{array}{c} \cdot \cdot \\ \cdot \cdot \end{array} + \begin{array}{c} \overrightarrow{\text{---}} \\ \diagup \diagdown \end{array} = -2f(3f-2), f=1$$

Vertex 27 (020000001111)  $j_B^2 j_5 xyz$

$$\Delta_2 = 2 \begin{array}{c} \cdot \cdot \\ \cdot \cdot \end{array} + 2 \begin{array}{c} \cdot \cdot \\ \cdot \cdot \end{array} + \begin{array}{c} \overrightarrow{\text{---}} \\ \diagup \diagdown \end{array} = -2f(5f-4), f=1$$

Figure 3.12

The diagrams contributing to the  $\Pi_{\Delta_2}$  NMO negative vertices in the region  $f < 1$  for the reversible model.



Table 3.13 The instability conditions for the NMO  $\Delta_2$  vertices in the reversible model.

$\Delta_2$	NMO Vertex 3	$(300000000111) - 8f(f + 1)$	$f < 1$
Adjacent Vertex	Coefficient	Instability condition	
1. (30000000012)	$16(1+f)$	$fz > 2z$	
2. (300000000120)	$-2(1+f)^2 f$	$4z > (1+f)y$	
3. (210000000210)	$-2f(1+f)(1-f)$	$4zj_A > (1-f)xj_B$	
4. (201000000210)	$-2f(2f+1)(1+f)$	$4zj_A > (2f+1)xj_C$	
5. (200100000210)	$-4f(1+f)$	$2zj_A > xj_D$	
6. (200010000210)	$-2f(1+f)$	$4zj_A > xj_1$	
7. (200001000210)	$-2f(1+f)$	$4zj_A > xj_2$	
8. (200000100210)	$-2f(1+f)$	$4zj_A > xj_3$	
9. (200000010210)	$-8f(1+f)$	$zj_A > xj_4$	
10. (210000000120)	$16(1-f)$	$f(f+1)yj_A > 2(1-f)zj_B$	
11. (201000000102)	$16(2f+1)$	$f(f+1)yj_A > 2(2f+1)zj_C$	
12. (200100000102)	32	$f(f+1)yj_A > 4zj_D$	
13. (200010000102)	16	$f(f+1)yj_A > 2zj_1$	
14. (200001000102)	16	$f(f+1)yj_A > 2zj_2$	
15. (200000100102)	32	$f(f+1)yj_A > 4zj_3$	
16. (200000010102)	64	$f(f+1)yj_A > 8zj_4$	
17. (200000001111)	$-4f(1+f)$	$2j_A > j_5$	



Table 3.13 (continued)

$\Delta_2$	NMO Vertex 23	(200000001111) - 4f(f+1)	
1.	(300000000111)	-8f(l+f)	$j_5 > 2j_A$
2.	(210000000210)	-2f(l+f)(l-f)	$2zj_5 > (l-f)xj_B$
3.	(201000000210)	-2f(2f+1)(l+f)	$2zj_5 > (2f+1)xj_C$
4.	(200100000210)	-4f(l+f)	$zj_5 > xj_D -$
5.	(200010000210)	-2f(l+f)	$2zj_5 > xj_1$
6.	(200001000210)	-2f(l+f)	$2zj_5 > xj_2$
7.	(200000100210)	-2f(l+f)	$2zj_5 > xj_3$
8.	(200000010210)	-8f(l+f)	$zj_5 > xj_4$
9.	(200000001120)	$-2f^2(l+f)$	$2z > fy$
10.	(100000002012)	4(l+f)	$fxj_A > zj_5$
11.	(010000002102)	4(l-f)	$f(l+f)yj_A^2 > (l-f)zj_Bj_5$
12.	(001000002102)	4(l+2f)	$f(l+f)yj_A^2 > (l+2f)zj_Cj_5$
13.	(000100002102)	8	$f(l+f)yj_A^2 > 2zj_D - j_5$
14.	(000010002102)	4	$f(l+f)yj_A^2 > zj_1j_5$
15.	(000001002102)	4	$f(l+f)yj_A^2 > zj_2j_5$
16.	(000000102102)	4	$f(l+f)yj_A^2 > zj_3j_5$
17.	(000000012102)	16	$f(l+f)yj_A^2 > 4zj_4j_5$



negative  $\Delta_2$  defined in Table 3.13 lie inside the  $\alpha_2$  cone due to the pure destabilizing term  $j_A^2 xy$ .

When  $f = 1$  a critical 1-cycle in the NEEC B appears, allowing the NF 3-cycle present in this extreme current to dominate in  $\Delta_2$ . Two new negative NMO vertices appear corresponding to the following destabilizing terms:

$j_B^3 xyz$	-2	(Vertex 7, table 3.12)
$j_B^2 j_5 xyz$	-2	(Vertex 27, table 3.12)

The diagrams corresponding to these NMO terms are also given in figure 3.12. Note that the NMO term  $j_B^3 xyz$  is the same NMO destabilizing term which occurred at  $f = 1$  in the irreversible model. For  $f < 1$  the stabilizer diagrams from  $\alpha_1 \alpha_2$  are only partially cancelled, and the terms become positive for  $f < 2/3$  and  $f < 4/5$ . However, these terms are no longer vertices of  $\Pi_{\Delta_2}$  when  $f < 1$ . Since the extreme currents A and B are equal at  $f = 1$ , these NMO vertices need not be considered since they are equivalent to the negative NMO vertices involving current A previously described.



### 3.3.4. Summary

The region of instability in the reversible model is a union of the cones of negative  $\alpha_2$  and  $\alpha_3$  for  $f > 1$ , and is given by a union of the cones of negative  $\alpha_2$  and  $\Delta_2$  for  $f < 1$ . The dominant cycles of the destabilizing terms are summarized in Table 3.14, along with the range of  $f$  in which these cycles destabilize the network and the extreme currents involved. The unstable range of  $f$  is  $f > 0$  in the reversible model.

In the reversible model, there are two pure destabilizing terms in  $\alpha_2$  which arise from the NEEC's A and B. In addition there are two mixed destabilizing terms resulting from the overlap of current A or B with the EEC 2. The cone of negative  $\alpha_2$  due to either of the pure destabilizing terms contains the cone due to the corresponding mixed destabilizing term. It follows that when the current in the EEC 2 is larger than that in the NEEC's A and B by a certain amount, the unstable region in  $\alpha_2$  is determined by the mixed destabilizing terms. This reduces the unstable volume of parameter space that would be found if the pure destabilizing terms were used as an approximation to the unstable region of  $\alpha_2$  alone. The two NMO destabilizing terms in  $\Delta_2$  present at  $f < 1$  do not extend the boundary of the unstable steady states as defined by  $\alpha_2$ , and so are not necessary to describe the unstable region in the network.



Table 3.14

The destabilizing cycles found in the reversible model analysis.

Destabilizing cycles	Extreme currents involved	Range of $f$ (unstable)
$\alpha_2:$ 	pure A	$f < 1 + \sqrt{2}$
	pure B	$f > 0.5$
	mixed A, 2	$f < 2$
	mixed B, 2	$f > 0.5$
$\alpha_3:$ 	mixed B, 3	$f > 1$
	mixed B, 3, 2	$f > 1$
$\Delta_2$ (NMO) 	pure A	$f \leq 1$
	pure B	$f = 1$
	mixed A, 5	$f \leq 1$
	mixed B, 5	$f = 1$

\* A critical 1-cycle at x was necessary in addition.



In the region  $f > 1$ , two mixed destabilizing terms appear in  $\alpha_3$ . The inhibitory positive feedback 3-cycle, which is necessary for the  $\alpha_3$  destabilization, requires the presence of the EEC's to be formed. It follows that the  $\alpha_3$  destabilizing terms cannot be formed without the reverse reactions and that this destabilization will be absent in the irreversible model, as the results of section 3.2.3 confirm.  $C_{\alpha_3}$  extends the boundary defined by  $C_{\alpha_2}$  only for certain hyperplanes and values of  $f (>1)$ . This extension depends on the value of the coefficients of the destabilizing terms in  $\alpha_2$  and  $\alpha_3$ . For example, take the instability condition on the currents  $j_B$  and  $j_4$ . The inequalities are:

$$\alpha_2: j_B > 4j_4 \quad (\text{table 3.7c})$$

$$\alpha_3: (f-1)j_B > 4j_4 \quad (\text{table 3.11})$$

In the region  $1 \leq f < 2$ ,  $C_{\alpha_2}$  determines the boundary; for  $f > 2$   $C_{\alpha_3}$  determines the boundary. At  $f = 2$ ,  $C_{\alpha_2} = C_{\alpha_3}$  on this hyperplane, i.e., in summary

$$\begin{array}{ll} 1 < f < 2 & C_{\alpha_3} \subset C_{\alpha_2} \\ f = 2 & C_{\alpha_3} = C_{\alpha_2} \\ f > 2 & C_{\alpha_3} \supset C_{\alpha_2} \end{array}$$

The  $\alpha_2$  instability condition is less restrictive close to  $f = 1$  and therefore destabilizes a greater portion of parameter space in this region of  $f$ .



The destabilizing cycles found in this analysis support previous findings, are:

$\alpha_2$ : inhibitory positive feedback 2-cycle  
(competition interaction<sup>28</sup>)

$\alpha_3$ : inhibitory positive feedback 2-cycle  
inhibitory positive feedback 3-cycle<sup>28</sup>

$\Delta_2$  (NMO): negative feedback 3-cycle<sup>28</sup>

Field and Noyes<sup>24</sup> found the same unstable range of  $f$  in the irreversible model:  $0.5 < f < 1 + \sqrt{2}$ . The extension of unstable  $f$  in the reversible model was later calculated by Field<sup>28</sup> to be  $0 \leq f \leq 1.51$  for the rate constants of step (5) in the model (1.6) given by the arbitrarily chosen values  $k_5 = 1 \text{ sec}^{-1}$  and  $k_{-5} = 10^{-5} \text{ sec}^{-1}$ .



### 3.4. Re-evaluation of the omitted extreme currents

The extreme currents  $A^-$ ,  $B^-$ ,  $C^-$  and  $D$  were eliminated from the preceding analysis of the reversible model, to reduce the number of parameters and because the unstable region was thought to lie close to the AB edge of the current polytope  $\Pi_C$ . However, on the basis of the destabilization found in  $\alpha_3$ , it is possible that mixed destabilizing terms involving the EEC's could be formed with the omitted NEEC's above. In  $\alpha_2$ , the mixed destabilizing terms cannot form unless a corresponding pure destabilizing term is present. Only in  $\alpha_3$  is a mixed destabilizing term without a corresponding pure destabilizing term possible.

The interaction diagrams for the extreme currents  $A^-$ ,  $B^-$ ,  $C^-$  and  $D$  are given in figure 3.13 for each region of  $f$ . The only destabilizing cycle present is the PFI 2-cycle between  $x$  and  $z$ . As expected, the  $\alpha_2$  pure terms are positive in the region  $f > 1$  and positive or zero in the region  $f < 1$ . Similarly the  $\alpha_3$  pure terms are positive or zero. The absence of a critical 1-cycle prevents the destabilization of  $\Delta_2$  by an NMO terms involving the negative feedback 3-cycle found in the NEEC's  $C^-$  and  $A^-$  ( $f > 1$ ). In conclusion no pure destabilizing terms can be formed in the NEEC's  $A^-$ ,  $B^-$ ,  $C^-$  and  $D$ .

The results of the reversible model analysis suggest that the only possible source of destabilization involving



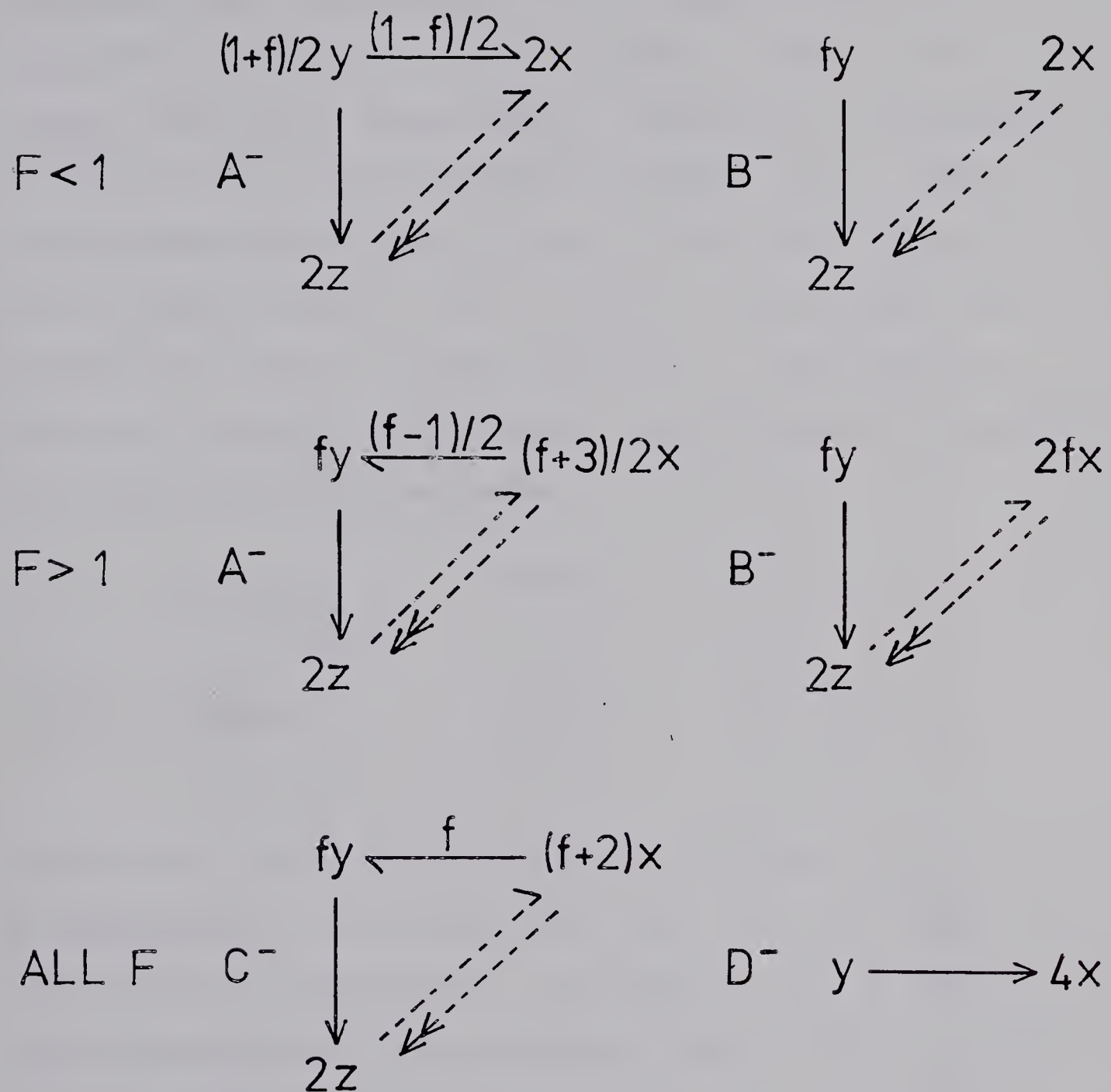


Figure 3.13

The interaction diagrams of the extreme currents  $A^-$ ,  $B^-$ ,  $C^-$  and  $D$  in the reversible model.



NEEC's  $A^-$ ,  $B^-$  and  $C^-$  is the formation of mixed inhibitory positive feedback (PFI) 3-cycles in  $\alpha_3$ . The EEC 2 has a inhibitory positive feedback (PFI) 2-cycle which can contribute an inhibitor (dashed arrow) to form a PFI 3-cycle with any of these NEEC's. The EEC 3 is necessary in addition for another mixed PFI 3-cycle in  $\alpha_3$ . When the diagrams contributing to each of the terms  $j_i^2 j_2 xyz$  and  $j_i j_2 j_3 xyz$ , where  $i = A^-$ ,  $B^-$  or  $C^-$ , were summed, only the NEEC's  $B^-$  and  $C^-$  in the region  $f < 1$ , were found to result in a negative coefficient. The diagrams corresponding to the destabilizing terms

$j_B^2 - j_2 xyz$	$2(f-1)$	$f < 1$
$j_B - j_2 j_3 xyz$	$2(f-1)$	$f < 1$
$j_C^2 - j_2 xyz$	$2(3f-1)$	$f < 1/3$
$j_C - j_2 j_3 xyz$	$2(3f-1)$	$f < 1/3$

found in the region  $f < 1$  are given in figure 3.14. It is interesting to note that both NEEC's  $B^-$  and  $C^-$  have the reverse of reaction (4). The NEEC  $B$  ( $f > 1$ ) which was responsible for the  $\alpha_3$  destabilizing terms in section 3.3.2 also has the reverse of reaction (4). It can be seen that reaction (4) increases the value of the x-stabilizer, and so has a stabilizing effect, when present in an NEEC. Both NEEC's  $B^-$  and  $C^-$  in the region  $f < 1$  form destabilizing mixed terms in which positive feedback (PFI) 2 and 3-cycles are independent of  $f$ , while the



Destabilizing term  $j_B^2 - j_2 xyz$

$$\alpha_3 = \begin{array}{c} \bullet \quad \bullet \\ \bullet \quad \bullet \\ \bullet \quad \bullet \end{array} + \begin{array}{c} \bullet \quad \bullet \\ \bullet \quad \bullet \\ \bullet \quad \bullet \end{array} - \begin{array}{c} \bullet \quad \nearrow \\ \bullet \quad \bullet \\ \bullet \quad \bullet \end{array} - \begin{array}{c} \bullet \quad \nearrow \\ \bullet \quad \bullet \\ \bullet \quad \bullet \end{array}$$

$$f < 1 = 4 + 2f - 4 - 2 = 2(f-1)$$

$$f > 1 = 4f + 2f - 4 - 2 = 6(f-1)$$

Destabilizing term  $j_B - j_2 j_3 xyz$

$$\alpha_3 = \begin{array}{c} \bullet \quad \bullet \\ \bullet \quad \bullet \\ \bullet \quad \bullet \end{array} + \begin{array}{c} \bullet \quad \bullet \\ \bullet \quad \bullet \\ \bullet \quad \bullet \end{array} + \begin{array}{c} \bullet \quad \bullet \\ \bullet \quad \bullet \\ \bullet \quad \bullet \end{array} - \begin{array}{c} \bullet \quad \nearrow \\ \bullet \quad \bullet \\ \bullet \quad \bullet \end{array} - \begin{array}{c} \bullet \quad \nearrow \\ \bullet \quad \bullet \\ \bullet \quad \bullet \end{array} - \begin{array}{c} \bullet \quad \nearrow \\ \bullet \quad \bullet \\ \bullet \quad \bullet \end{array}$$

$$f < 1 = 2 + 2f + 4 - 4 - 2 - 2 = 2(f-1)$$

$$f > 1 = 2 + 2f + 4f - 4 - 2 - 2 = 6(f-1)$$

Destabilizing term  $j_C^2 - j_2 xyz$

$$\alpha_3 = \begin{array}{c} \bullet \quad \bullet \\ \bullet \quad \bullet \\ \bullet \quad \bullet \end{array} + \begin{array}{c} \bullet \quad \bullet \\ \bullet \quad \bullet \\ \bullet \quad \bullet \end{array} - \begin{array}{c} \bullet \quad \nearrow \\ \bullet \quad \bullet \\ \bullet \quad \bullet \end{array} - \begin{array}{c} \bullet \quad \nearrow \\ \bullet \quad \bullet \\ \bullet \quad \bullet \end{array} - \begin{array}{c} \bullet \quad \nearrow \\ \bullet \quad \bullet \\ \bullet \quad \bullet \end{array}$$

$$= 2(f+2) + 2f - 4 + 2f - 2 = 2(3f-1) \quad -, f < 1/3$$

Destabilizing term  $j_C - j_2 j_3 xyz$

$$\alpha_3 = \begin{array}{c} \bullet \quad \bullet \\ \bullet \quad \bullet \\ \bullet \quad \bullet \end{array} + \begin{array}{c} \bullet \quad \bullet \\ \bullet \quad \bullet \\ \bullet \quad \bullet \end{array} + \begin{array}{c} \bullet \quad \bullet \\ \bullet \quad \bullet \\ \bullet \quad \bullet \end{array} - \begin{array}{c} \bullet \quad \nearrow \\ \bullet \quad \bullet \\ \bullet \quad \bullet \end{array} - \begin{array}{c} \bullet \quad \nearrow \\ \bullet \quad \bullet \\ \bullet \quad \bullet \end{array} - \begin{array}{c} \bullet \quad \nearrow \\ \bullet \quad \bullet \\ \bullet \quad \bullet \end{array} - \begin{array}{c} \bullet \quad \nearrow \\ \bullet \quad \bullet \\ \bullet \quad \bullet \end{array}$$

$$= 2 + 2(f+2) + 2f + 2f - 2 - 4 - 2 = 2(3f-1), \quad -, f < 1/3$$

Figure 3.14

The diagrams contributing to the mixed destabilizing terms in  $\alpha_3$  for  $f < 1$ , in the reversible model, corresponding to the omitted NEEC's,  $B^-$ ,  $C^-$ .



positive diagrams have  $f$  dependence. This allows the PFI 2 and 3-cycles to dominate when  $f < 1$ . Note also the direction of the PF 3-cycles in the terms involving  $B^-$  and  $C^-$  are reversed in direction with respect to the 3-cycle in the  $B$  ( $f > 1$ ) term.

The method of destabilization found in  $\alpha_3$  in the region  $f < 1$  is the same as the previously found case in the region  $f > 1$ . There is one difference, however, and that is the lack of  $\alpha_2$  destabilization by the NEEC's  $C^-$ ,  $B^-$ . In fact, the NEEC's  $C^-$  and  $B^-$  do not form any pure destabilizing terms in  $\alpha_2$ ,  $\alpha_3$  or  $\Delta_2$ . This means that in the current polytope  $\Pi_C$  for the reversible model, an unstable region appears on the edge joining the NEEC  $B^-$  ( $f < 1$ ) and the EEC 2 or the NEEC  $C^-$  ( $f < 1$ ) and the EEC 2, although all the extreme points of  $\Pi_C$  corresponding to these extreme currents are stable steady states. When the EEC 3 is included, an isolated volume of unstable steady states occurs in  $\Pi_C$ , which does not extend to any of the extreme points.

It is significant that the EEC's are necessary for this instability, and that there is no relationship between the  $\alpha_3$  destabilization in the region  $f < 1$  and the irreversible model. In fact, if all the reactions in the irreversible model are simply reversed, the Oregonator is stable for all  $f$  values.



The cones of negative  $\alpha_3$  due to the  $\alpha_3$  destabilizing terms in the region  $f < 1$  can be estimated by inspection of the instability conditions found previously for the  $\alpha_3$  instability in the region  $f > 1$  (Table 3.11). The resulting sets of instability conditions are shown in Tables 3.15 a to d. The actual cones of negative  $\alpha_3$  will always lie inside the cones defined by the instability conditions of Tables 3.15 a to d, because if an adjacent positive vertex of  $\Pi_{\alpha_3}$  has been omitted the actual cone of negative  $\alpha_3$  is smaller.



<u>Table 3.15a</u> (020001000111) 2(f-1) 0 < f < 1	
Adjacent Vertex	Instability Condition
1. (002001000111)	$(1-f)j_B^2 > (1-3f)j_C^2$
2. (000201000111)	$(1-f)j_B^2 > 3j_D^2$
3. (021000000111)	$(1-f)j_2 > f(f+3)j_C$
4. (020100000111)	$(1-f)j_2 > 4fj_D$
5. (020010000111)	$(1-f)j_2 > (1+f)j_1$
6. (020000010111)	$(1-f)j_2 > 4fj_4$
7. (010011000111)	$(1-f)j_B > 4j_1$
8. (010001100111)	$j_B > j_3$
9. (010001010111)	$(1-f)j_B > 4j_4$
10. (010001001111)	$j_B > j_5$
11. (110001000111)	$j_B > j_A$

<u>Table 3.15b</u> (010001100111) 2(f-1) 0 < f < 1	
Adjacent Vertex	Instability Condition
1. (020001000111)	$j_3 > j_B$
2. (020000100111)	$j_2 >$
3. (001001100111)	$(1-f)j_B > (3f-1)j_C$
4. (000101100111)	$(1-f)j_B > 6j_D$
5. (000011100111)	$(1-f)j_B > 4j_1$
6. (000001110111)	$(1-f)j_B > 4j_4$
7. (100000101111)	$2j_B j_2 > (f+2)j_A j_5$
8. (100001001111)	$j_B j_3 > 2j_A j_5$
9. (010001001111)	$j_3 > j_5$
10. (001000101111)	$(1-f)j_B j_2 > f(1+f)j_C j_5$
11. (000100101111)	$(1-f)j_B j_2 > (1+5f)j_D j_5$
12. (000010101111)	$(1-f)j_B j_2 > 4(1+f)j_1 j_5$
13. (000000111111)	$(1-f)j_B j_2 > 4fj_4 j_5$



Table 3.15c (002001000111) 2(3f-1) 0 < f < 1/3

Adjacent Vertex	Instability Condition
1. (020001000111)	$(1-3f) j_C^2 > (1-f) j_B^2$
2. (101001000111)	$j_C > j_A$
3. (000201000111)	$(1-3f) j_C^2 > 3j_D^2$
4. (003000000111)	$(1-3f) j_2 > f(1+f) j_C$
5. (001011000111)	$(1-3f) j_C > 4j_1$
6. (001001100111)	$j_C > j_3$
7. (001001010111)	$(1-3f) j_C > 4j_4$
8. (001001001111)	$(1-3f) j_C > (1+f) j_5$
9. (201000000111)	$(1-3f) j_C j_2 > f j_A^2$

Table 3.15d (001001100111) 2(3f-1) 0 < f < 1/3

Adjacent Vertex	Instability Condition
1. (002001000111)	$j_3 > j_C$
2. (002000100111)	$(1-3f) j_2 > f(1+f) j_C$
3. (010001100111)	$(1-3f) j_C > (1-f) j_B$
4. (000101100111)	$(1-3f) j_C > 6j_D$
5. (000011100111)	$(1-3f) j_C > 4j_1$
6. (000001110111)	$(1-3f) j_C > 4j_4$
7. (100000101111)	$2(1-3f) j_C j_2 > (1-f)(f+2) j_A j_5$
8. (100001001111)	$(1-3f) j_C j_3 > 2(1-f) j_A j_5$
9. (001001001111)	$(1-3f) j_3 > (1+f) j_5$
10. (001000101111)	$(1-3f) j_2 > f(1+f) j_5$



### 3.5. Comparison of the reversible and irreversible model results.

The effect of reversibility in a network is demonstrated by the change in the complete set of extreme currents when the reverse reactions are added to the irreversible network. All the extreme currents present in an irreversible network are of the NEEC type and appear in the corresponding reversible network. As a result, an instability if present in an irreversible network always appears in the reversible case as well. If new instability is to occur in the reversible network, it must involve the extreme currents of the reversible network which cannot be formed in the irreversible case. Any such extreme current will contain at least one reversed reaction. The new extreme currents in the reversible Oregonator model consist of the EEC's and the new NEEC's which were formed by:

- i) Reversing all the reactions in one of the NEEC's of the irreversible model, for example:  $A^-$  ( $f > 1$ ),  $B^-$  ( $f < 1$ ) and  $C^-$ .
- ii) Mixing different forward and reverse reactions to form new NEEC's, for example:  $D$ ,  $D^-$ ,  $A$  ( $f < 1$ ) and  $B$  ( $f > 1$ ).

Note that a reaction and its reverse can only appear together in an EEC, and every reaction step in a network forms an EEC of the network.



The results of the analysis performed on the Oregonator model are most easily compared at  $f = 1$ , since in this case the extreme currents A and B are equal. The instability in the irreversible model at  $f = 1$  is due to one pure destabilizing term in  $\alpha_2$  which is derived from the NEEC B (=A). In the reversible model the same pure destabilizing term occurs in  $\alpha_2$  at  $f = 1$ , while the new NEEC's  $B^-$ ,  $C^-$ ,  $D$ ,  $D^-$  and the EEC's 1 to 5 cause no additional pure destabilizing terms. As discussed previously the pure NMO destabilizing term in  $\Delta_2$  does not extend the unstable region in either model beyond the boundary defined by  $\alpha_2$ . The new mixed destabilizing terms in  $\alpha_2$  and  $\Delta_2$  of the reversible model also define cones of instability which do not extend the unstable region defined by the pure destabilizing term in  $\alpha_2$ .

At  $f = 1$  the reversible model instability conditions for the pure and mixed destabilizing terms in  $\alpha_2$  contain the irreversible model instability conditions. Therefore, the  $\alpha_2$  destabilizing terms in the reversible model at  $f = 1$  cannot extend the unstable region defined by the irreversible model hyperplanes. The instability conditions for the reversible model will define hyperplanes between the new current parameters in addition to the hyperplanes found in the irreversible model instability conditions. The new hyperplanes of the reversible model cause further bounds on the unstable region of parameter



space. For example, in the reduced set of extreme currents used in the reversible model analysis, the rate of the reverse reactions (3) and (5) are given by  $j_3$  and  $j_5$  respectively. Hence the new instability conditions involving these currents such as  $j_B > j_3$  (Table 3.7b,  $f = 1$ ) are equivalent to conditions on the rates of the reverse reactions necessary for instability.

When  $f$  differs from one the situation changes, although the destabilizing terms in both cases (reversible vs. irreversible) still contain the NEEC's A or B. The destabilizing extreme currents in the irreversible model are the NEEC's A ( $f > 1$ ) and B ( $f < 1$ ). If the reactions are allowed to reverse, then NEEC B can be extended into the region  $f > 1$ , and NEEC A can be extended into the region  $f < 1$ , by reversing reactions (4) and (1) respectively. This extension of the NEEC's A and B in the reversible model is diagrammed in figure 3.15. These new NEEC's cannot be combined with the corresponding irreversible model NEEC's since a reaction when reversed, alters the interaction diagram. Compare, for example, the NEEC's A ( $f < 1$ ) and A ( $f > 1$ ) in figure 3.15 with their interaction diagrams in figure 3.8. In general, when an arrow has a coefficient which is a function of a varying parameter, such as  $f$ , so that the arrow changes sign at some value, the extreme current has to be considered separately in each region.



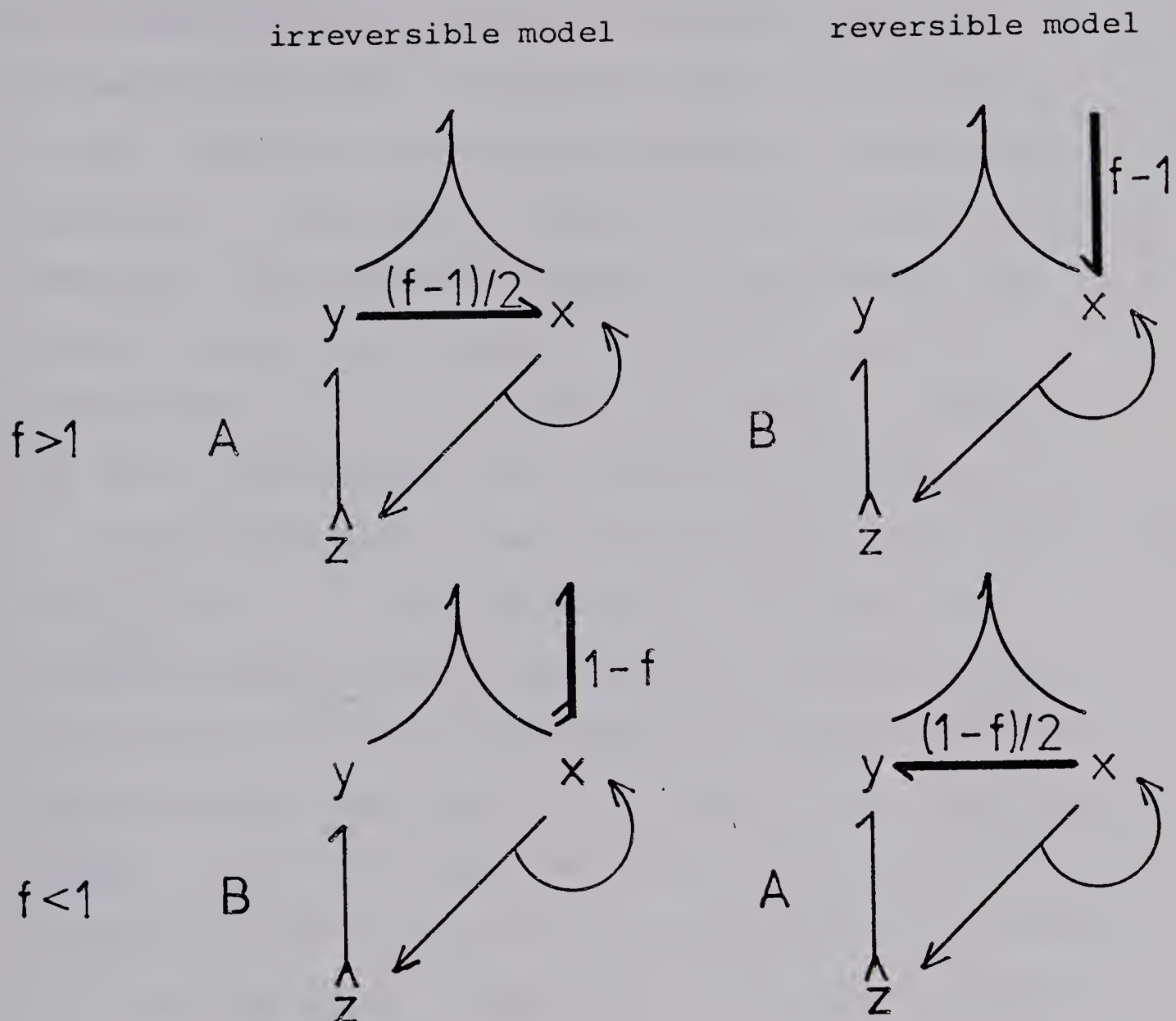


Figure 3.15

The extension of the NEEC's A and B in the reversible model.

The heavy line indicates the reaction which is reversed in the irreversible model extreme current, when the new destabilizing extreme current is formed in the reversible model.



The new NEEC's A ( $f < 1$ ) and B ( $f > 1$ ) each define a pure destabilizing term in  $\alpha_2$  of the reversible model. As a result of these terms, the unstable range of  $f$  in the reversible model is extended below 0.5 and above  $1 + \sqrt{2}$ , the limits for unstable behavior in the irreversible model. The question now arises as to whether these terms can also extend the bounding hyperplanes of the unstable region for  $f$  within the unstable range of the irreversible model. To answer this question, consider the three irreversible model instability conditions in  $\alpha_2$  corresponding to the pure destabilizing terms  $j_A^2 xy (f > 1)$  and  $j_B^2 xy (f < 1)$ . These instability conditions are present in the reversible model also, however the coefficients for the same hyperplanes are modified for the destabilizing terms  $j_A^2 xy (f < 1)$ ,  $j_B^2 xy (f > 1)$ ,  $j_A j_2 xy$  and  $j_B j_2 xy$ . Table 3.16 lists the three irreversible model instability conditions and the coefficient as a function of  $f$ , as they appear in the four destabilizing terms in  $\alpha_2$  of the reversible model.

When a plot of  $|C^+/C^-|$  versus  $f$  is made as in figure 3.16, the term in  $\alpha_2$  which determines the most destabilizing hyperplane can be found. The coefficient of each destabilizing term corresponding to one of the hyperplanes labelled (1), (2) and (3) in Table 3.16 is plotted in figure 3.16a, b and c respectively. The label R means that the curve corresponds to a coefficient which occurs



Table 3.16

Comparison of the irreversible model hyperplanes found in the four  $\alpha_2$  destabilizing terms of the reversible model.

$f < 1$	$ c^+/c^- $
(1) $j_A^2 xy$ (Table 3.6a)	
1. $1/2f(1+f) (j_A/j_C)^2 > 1/2(1+3f+4f^2) j_A/j_C + f(1+2f)$	
2. $-$	
3. $fx > 2z$	$2/f$
(2) $j_A j_2 xy$ (Table 3.8a)	
1. $fj_A > (1+4f) j_C$	$1+4f/f$
2. $fy > 2z$	$2/f$
3. $fx > 2z$	$2/f$
(3) $j_B^2 xy$ (Table 3.7a) (irreversible)	
1. $(2f-1) (j_B/j_C)^2 > (1+2f) + 2(1+f) j_B/j_C$	
2. $f(2f-1)y > 2(1-f)z$	$2(1-f)/f(2f-1)$
3. $(2f-1)x > 2z$	$2/(2f-1)$
(4) $j_B j_2 xy$ (Table 3.9a)	
1. $(2f-1)j_B > (1+4f) j_C$	$1+4f/(2f-1)$
2. $(2f-1)y > 2z$	$2/(2f-1)$
3. $(2f-1)x > 2z$	$2/(2f-1)$

(continued on next page)



Table 3.16 (continued)

$f > 1$	$ C^+/C^- $
(1) $j_A^2 xy$ (Table 3.6b) (irreversible)	
1. $1/2  f^2 - 2f - 1  (j_A/j_C)^2 > f(1+2f) + f(1+ef) j_A/j_C$	
2. $ f^2 - 2f - 1  y > 2(f-1)z$	$\frac{2(f-1)}{ f^2 - 2f - 1 }$
3. $ f^2 - 2f - 1  x > 4fz$	$\frac{4f}{ f^2 - 2f - 1 }$
(2) $j_A j_2^{xy}$ (Table 3.8b)	
1. $(2-f) j_A > (1+4f) j_C$	$\frac{(1+4f)}{(2-f)}$
2. $(2-f) y > 2z$	$2/2-f$
3. $(2-f) x > 2z$	$2/2-f$
(3) $j_B^2 xy$ (Table 3.7c)	
1. $(j_B/j_C)^2 > 4f(j_B/j_C) + (1+2f)$	
2. $f y > 2(f-1)z$	$2(f-1)/f$
3. $x > 2z$	2
(4) $j_B j_2^{xy}$ (Table 3.9b)	
1. $j_B > (1+4f) j_C$	$1+4f$
2. $y > 2z$	2
3. $x > 2z$	2



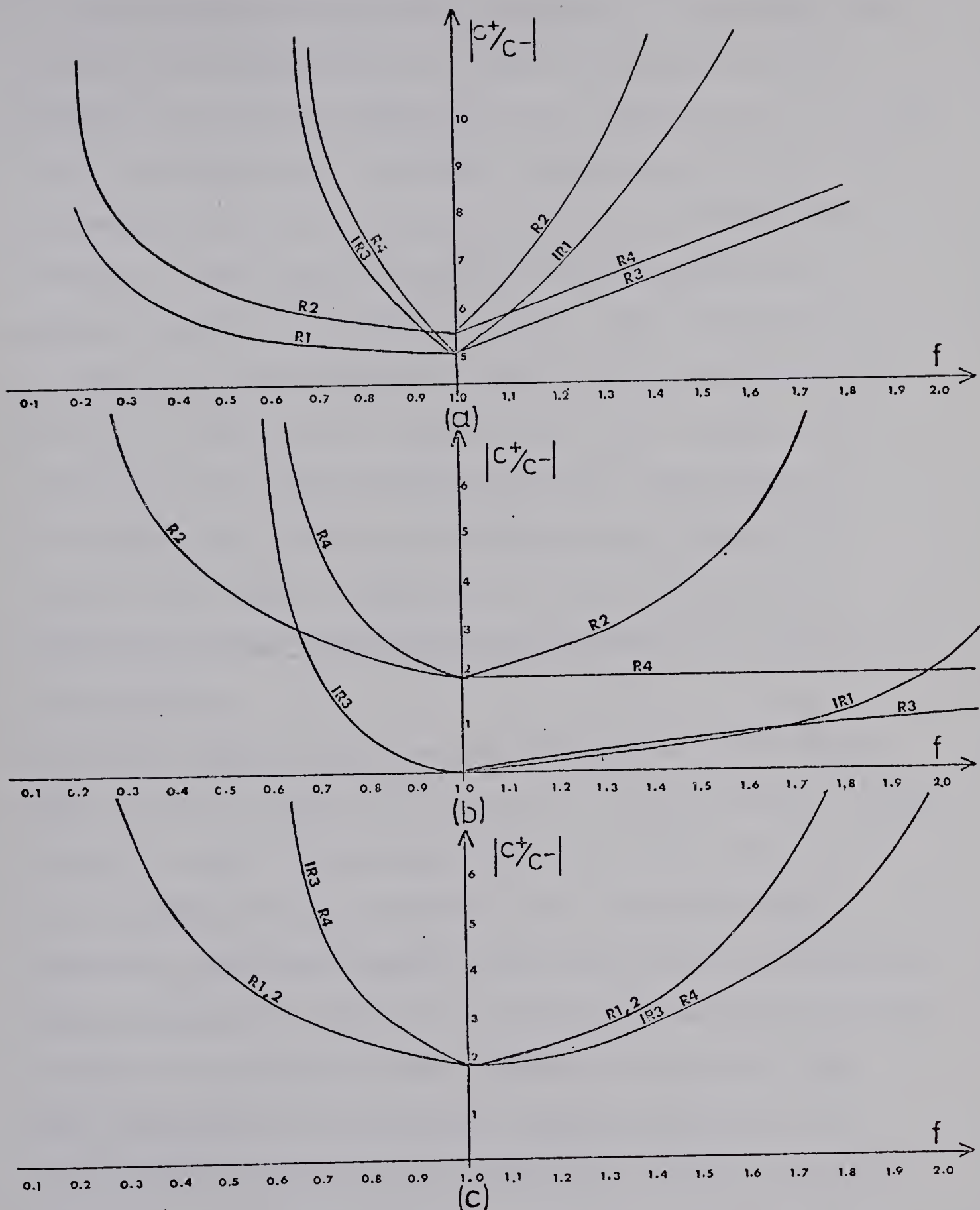


Figure 3.16

Plot of the coefficients in Table 3.16 versus  $f$ , where (a), (b), (c) correspond to the first, second and third hyperplanes in Table 3.16, respectively.



in the reversible model only, while an IR means that the coefficient is the same as in the irreversible model hyperplane. If the coefficient of a hyperplane is smaller than the coefficient of another hyperplane with the same parameters, then the hyperplane with the smaller coefficient is less restrictive and hence destabilizes a greater portion of parameter space. The parameters  $x$ ,  $y$ , and  $z$  are the reciprocal steady state concentrations  $x_o$ ,  $y_o$ ,  $z_o$  and so if  $x > y$  then  $y_o > x_o$ . However, the relative relationship between parallel hyperplanes is the same, since all the inequalities are inverted in  $(x_o, y_o, z_o)$  space. Therefore, it is sufficient to determine the most destabilizing hyperplane in the  $x$ ,  $y$ ,  $z$  parameters.

The first thing to note is that the NEEC's A and B are equal at  $f = 1$ , and so no extension of the unstable region defined by the irreversible model can occur due to the pure  $\alpha_2$  destabilizing terms of the reversible model. Secondly, the mixed destabilizing terms in the reversible model always lie either on or inside the boundary defined by their corresponding pure destabilizing term. The only extension of the unstable region defined by the irreversible model that can take place in the reversible model due to  $\alpha_2$ , is related to the pure terms involving the new NEEC's  $A(f < 1)$  and  $B(f > 1)$ . It follows that the mixed destabilizing terms present at  $f = 1$  cannot



destabilize the reversible model and so no extension occurs at  $f = 1$  for any hyperplane, as stated in the beginning of this section.

If the instability conditions in Table 3.16 which are independent of the current parameters are considered, several comparisons can be made. In the region  $f < 1$ , the unstable range of  $f$  is extended below 0.5 in the reversible model. The second instability conditions for the destabilizing term  $j_A^2 xy$  ( $f < 1$ ) in Table 3.16 ( $f < 1$ ) is missing, but other inequalities in Table 3.6a yield restrictions on the ratio of  $y/z$ , which will either be the same or less restrictive than the corresponding mixed destabilizing term instability condition. It can be seen from the coefficient of the hyperplane (R2) in figure 3.16b that this hyperplane is more destabilizing than the corresponding irreversible model hyperplane (R3) for  $f < 0.67$ . In other words, close to  $f = 1$  the instability condition found in the irreversible model determines the most destabilizing hyperplane. The third instability condition in Table 3.16 for  $f < 1$  due to the NEEC A ( $f < 1$ ) defines a hyperplane (R1) in figure 3.16c, which is less restrictive than the corresponding hyperplane (IR3) in the irreversible model, for all  $f < 1$ . Therefore, the unstable region of parameter space is extended by this hyperplane in the reversible model, within the unstable range of  $f$  for the irreversible model, as



well as below it. However, as  $f \rightarrow 0$ , the stabilizing effect of the positive dominant terms which occur in the remaining reversible instability conditions increases rapidly, because the EEC's define terms which are independent of  $f$ , while the NEEC A ( $f < 1$ ) has  $f^2$  dependence (EEC 5 has  $f$  dependence only.) From figure 3.16c it can be seen that the hyperplane (R1) is very restrictive for  $f < 0.5$ , since the coefficient increases rapidly as  $f \rightarrow 0$ . Hence, the unstable volume of parameter space shrinks as  $f \rightarrow 0$ .

In the region  $f > 1$ , the new NEEC B( $f > 1$ ) causes the unstable range of  $f$  present in the irreversible model to be extended into the region  $f > 1 + \sqrt{2}$ . Two of the instability conditions in Table 3.16 are independent of the current parameters. The instability condition (3) defines a hyperplane (R3) in figure 3.16c, involving the NEEC B( $f > 1$ ), which has a smaller coefficient and so is less restrictive than the corresponding hyperplanes defined by any of the other destabilizing terms. In this case the new hyperplane in the reversible model destabilizes a greater portion of parameter space for  $f > 1$ , and the bounding hyperplane of the unstable region in the irreversible model is extended. The second instability condition due to NEEC B( $f > 1$ ) defines the hyperplane (R3) in figure 3.6b which extends the unstable region beyond the corresponding irreversible model hyperplane (IR1) only for  $f > 1.6$ . Therefore, there is no



extension of the unstable region defined by this hyperplane in the irreversible model for  $f$  close to one.

When the first instability condition of each destabilizing term in Table 3.16 are compared, the trend found for the concentration parameters is continued. By referring to figure 3.16a, it can be seen that the hyperplane defined by the pure destabilizing terms destabilize a greater portion of parameter space than the corresponding mixed destabilizing terms and that the hyperplanes defined by the terms involving the new NEEC current parameters,  $A(f < 1)$  and  $B(f > 1)$ , determine the most destabilizing hyperplane in the regions  $f < 1$  and  $f > 1$ , respectively. It is also evident that the coefficients of the most destabilizing terms increase rapidly as  $f \rightarrow 0$  and  $f \rightarrow \infty$ , shrinking the unstable volume of parameter space.

In summary, the new NEEC's  $A(f < 1)$  and  $B(f > 1)$  have introduced instability into  $\alpha_2$ , not present in the irreversible model. In addition to extending certain of the bounding hyperplanes defined by the irreversible model in parameter space, the range of unstable  $f$  itself was increased from  $0.5 < f < 1 + \sqrt{2}$  to  $f > 0$ . However, the region of instability in parameter space rapidly diminishes as  $f$  drops below  $f = 0.5$  due to the NEEC  $A(f < 1)$  destabilizing term increasing as  $f^2$ . Also, as  $f$  increases above  $f = 1 + \sqrt{2}$ , stabilization of the destabilizing NEEC  $B(f > 1)$  term again occurs, since the adjacent



NEEC A( $f > 1$ ) dominant term is positive for  $f > 1 + \sqrt{2}$  and increases as  $f^2$ . In addition the NEEC C increases as  $f^2$  so that the destabilization hyperplane (R3) in figure 3.16a becomes highly restrictive, and only for a very large current in the NEEC B( $f > 1$ ), will the network be unstable.

As discussed in section 3.3.4, the  $\alpha_3$  mixed destabilizing terms in the reversible model are also necessary for describing the unstable region of the network. The  $\alpha_3$  instability requires the presence of EEC's, and so does not occur in the irreversible model for any value of  $f$ . The  $\alpha_3$  instability conditions involve only the current parameters and the only inequality that can be compared with the ones in Table 3.16 is

$$(f-1)j_B/j_C)^2 > 4(1+f)(j_B/j_C) + 3(1+f) \quad (\text{Table 3.11})$$

which involves the new NEEC B( $f > 1$ ). The corresponding hyperplane for this instability condition does not destabilize the  $\alpha_2$  hyperplane (R3) in figure 3.16a until  $f > 1 + \sqrt{2}$ . For example, at  $f = 2.5$ ,  $j_B/j_C > 10.03$  while the coefficient at  $f = 1.1$  is 84.73. The large  $f$  values required for the  $\alpha_3$  instability to be important follow from the factor  $(1-f)$  contained in the coefficient of this destabilizing term. Note that the equivalent factor  $(f-1)$  appears in the NEEC B( $f < 1$ )  $\alpha_3$  destabilizing terms discussed in section 3.4. Since the experimentally



determined range of  $f$  is  $0 < f < 2$ ,<sup>25</sup> the  $\alpha_3$  instability present in the region  $f > 1$  is uninteresting experimentally. In addition, the NEEC's involved in the  $\alpha_3$  instability all contain the reverse of reaction (4), which has a very small rate constant ( $1.6 \times 10^{-10} \text{ M}^{-2} \text{ sec}^{-1}$ .<sup>28</sup>)

So far, the discussion in this section has dealt with the shift in the hyperplanes of the irreversible model when the reverse reactions are included in the network. However, this change in the boundary of the unstable steady states is small in comparison to the possible effect of new hyperplanes defined by the remaining reversible model instability conditions, when  $f$  is within the unstable range of the irreversible model. These new hyperplanes involve the new extreme currents which have a stabilizing effect on the network since they place additional requirements on the unstable NEEC current parameters that must be fulfilled for a steady state to be unstable. These requirements are missing in the irreversible network, and so the validity of the irreversible model when  $0.5 < f < 1 + \sqrt{2}$ , as an approximation to the reversible model rests on the restrictiveness of the new hyperplanes. There are new hyperplanes involving the currents of each of the EEC's for every destabilizing term in the reversible model. If the current in either of the EEC's 1, 3, 4 or 5 ( $f > 1$ ) is large (large  $K_{eq.}$ ) then many of the unstable steady states



accessible in the irreversible model would be unattainable in the reversible network, since the current in the unstable NEEC's A and B would have to be very large in order to destabilize the network. This condition need not be satisfied by the EEC 2. As discussed in section 3.3.1, if the current in the EEC 2 is large then the reversible network is destabilized by the cones of negative  $\alpha_2$  due to the mixed destabilizing terms in  $\alpha_2$ , and although these cones lie inside the cones defined by the corresponding pure destabilizing  $\alpha_2$  terms, the boundary of the unstable region is not severely restricted.

Similarly, for  $f < 1$  a large current in the EEC 5 will still allow the destabilization of the network by the mixed destabilizing term in  $\Delta_2$  involving the EEC 5. In conclusion the irreversible model is a good approximation of the reversible model when the currents in the EEC's which are not involved in any mixed destabilizing terms in the network are small, and  $f$  is within  $0.5 < f < 1 + \sqrt{2}$ .

A summary of the destabilizing extreme currents in the reversible and irreversible models is given in Table 3.17, together with the corresponding range of  $f$ .



Table 3.17

Summary of the destabilizing extreme currents in the irreversible and reversible models.

	Extreme Current	Irreversible	Reversible	Destabilizing Cycle
$\alpha_2$	$A(f > 1)$	$1 \leq f < 1 + \sqrt{2}$	$1 \leq f < 1 + \sqrt{2}$	PFI 2-cycle
	$B(f < 1)$	$0.5 < f \leq 1$	$0.5 < f \leq 1$	
	$A(f < 1)$		$0 < f \leq 1$	
	$B(f > 1)$		$f \geq 1$	
	$A(f > 1), 2$		$1 \leq f < 2$	no extra instability
	$B(f > 1), 2$		$f \geq 1$	
	$A(f < 1), 2$		$0 < f \leq 1$	
	$B(f < 1), 2$		$0.5 < f \leq 1$	
$\alpha_3$	$B(f > 1), 3$		$f > 1$	PFI 2-cycle
	$B(f > 1), 2, 3$		$f > 1$	PFI 3-cycle
	$B^-(f < 1), 2$		$0 < f < 1$	
	$B^-(f < 1), 2, 3$		$0 < f < 1$	
	$C^-(f < 1), 2$		$0 \leq f < 1/3$	
	$C^-(f < 1), 2, 3$		$0 \leq f < 1/3$	
$\Delta_2$	$A=B$	$f=1$	$f=1$	NF 3-cycle with a critical 1-cycle no extra instability
	$A(f < 1)$		$0 < f \leq 1$	
	$A(f < 1), 5$		$0 < f \leq 1$	



### 3.6. General Conclusions

In any chemical system there are only so many ways of taking a linearly independent sum of the reactions with positive coefficients, which preserves the steady state concentrations of the internal species. Each of these ways corresponds to an extreme current of the system, and any general steady state of the system is a positive linear combination of the extreme currents. Two broad classes of extreme currents can be identified in a reversible network: the equilibrium extreme currents (EEC's) and the non-equilibrium extreme currents (NEEC's). In the preceding analysis, the specific relationships between instability and the extreme currents were discussed for the reversible Oregonator model. The more general consequences of the analysis are now summarized by considering the destabilizing cycles that were necessary for a cone of instability in the network.

The pure destabilizing terms which occur in a reversible network are derived from the NEEC's and the destabilizing cycles are the same as those given in section 2.5 as a result of previous work on irreversible networks. The fact that the unstable range of the stoichiometric parameter  $f$  was extended in the reversible model analysis by new NEEC's, points out that an irreversible network can be completely stable and yet the network



is unstable when the reactions are allowed to reverse. The discussion of the previous section pointed out that the unstable volume of parameter space is small in such cases, and that the current in the responsible unstable NEEC must be large for an unstable steady state to form.

The mixed destabilizing terms which appear in a reversible network all have a current component from a NEEC, which may or may not form a pure destabilizing term alone. The mixed destabilizing terms in  $\alpha_2$  do not occur without a corresponding pure destabilizing term derivable from the same NEEC. The rule for the formation of such a mixed destabilizing term is as follows:

A network which is destabilized by an inhibitory positive feedback (PFI) 2-cycle in  $\alpha_2$  will form a new mixed destabilizing term whose dominant cycle is a mixed current PFI 2-cycle, when an EEC with an overlapping PFI 2-cycle is present in the network.

Such a mixed destabilizing term stabilizes the cone of instability defined by the corresponding pure destabilizing term when the current in the EEC is larger than the current in the NEEC by a value determined by the ratio of the coefficients of the pure and mixed destabilizing terms. If the irreversible model of a network has an instability in  $\alpha_2$  due to a PFI 2-cycle, then the cone of instability produced by the same PFI 2-cycle in the



reversible network will be comparable as long as the currents in the EEC's which do not have the same PFI 2-cycle are small.

The situation differs in  $\alpha_k$ ,  $k > 2$ , where a mixed destabilizing term may exist without a corresponding pure destabilizing term being possible. The characteristic mixed destabilizing cycle in such terms is a mixed PFI  $k$ -cycle,  $k > 2$ , which occurs in addition to a PFI 2-cycle. This combination of destabilizing cycles can be dominant in  $\alpha_k$ ,  $k > 2$ . The required EEC's for a mixed destabilizing term in  $\alpha_k$  are those which can contribute an inhibitor to the PFI  $k$ -cycle. This form of destabilization can be summarized as follows:

Given a reversible model which contains a NEEC with a PFI 2-cycle, which may or may not destabilize the network in pure form, then the formation of mixed destabilizing terms in  $\alpha_k$ ,  $k > 2$ , is possible, if the only  $k$ -cycle which forms is a mixed PFI  $k$ -cycle with one or more inhibitors contributed by the EEC's.

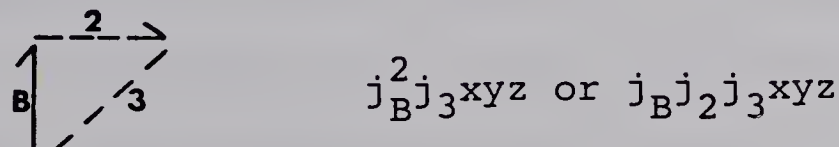
This form of destabilization occurs only in reversible networks. If the NEEC involved has a pure stabilizing term in  $\alpha_k$ , because it can form a negative feedback (NF)  $k$ -cycle, then the cone of instability due to the mixed current PFI  $k$ -cycle will be important only if the currents in the EEC's involved in the PFI  $k$ -cycle are



large. For example, in the reversible Oregonator model, the  $\alpha_3$  mixed destabilizing terms for  $f > 1$  are  $j_B^2 j_3 xyz$  and  $j_B j_2 j_3 xyz$ . The NEEC B( $f > 1$ ) has a NF 3-cycle which stabilizes the pure B term in  $\alpha_3$  for  $f > 1$ :



When the current in the EEC 3 is large enough, the mixed PFI 3-cycle



will dominate and the steady state becomes unstable. The inhibitor in the EEC 3 which causes the PFI 3-cycle above is a result of the reverse of reaction (3). The corresponding instability conditions found in  $\alpha_3$  are:

$$j_3 > j_B$$

for the destabilizing term  $j_B^2 j_3 xyz$  and

$$j_2 > j_B$$

$$j_3 > j_B$$

in the case of  $j_B j_2 j_3 xyz$ .

As a final case, the formation of mixed destabilizing terms in  $\Delta_2$  will be discussed. This rule is actually an extension of the theorem given in section 2.5, which



gave the conditions under which a pure destabilizing term can be formed in  $\Delta_2$ . The formation of mixed destabilizing terms in  $\Delta_2$  does not occur without a corresponding pure destabilizing term as in the  $\alpha_2$  case, and can be summarized as follows:

If a network is destabilized in  $\Delta_2$  by a NF 3-cycle which passes through a critical 1-cycle,<sup>11</sup> then an EEC, which has a vanishing stabilizer at the same parameter as the critical 1-cycle, produces a new mixed destabilizing term which has a mixed NF 3-cycle which differs only by the substitution of one arrow from the original pure destabilizing cycle.

This rule will also hold in the case that NF  $k$ -cycles in  $\Delta_{k-1}$  destabilize a network. The cone of instability determined by the mixed destabilizing term in  $\Delta_2$  will be important in the reversible model when the current in the EEC involved is large.



## REFERENCES

1. A. T. Winfree, Rotating Reactions, *Scientific American*, June 1974.
2. I. Prigogine and R. Lefever, Stability and Thermo-dynamic Properties of Dissipative Structures in Biological Systems, *Stability and Origin of Biological Information*, Editor I. R. Miller (Wiley, New York, 1975) p. 26.
3. G. Nicolis, *Advances in Chem. Phys.*, 19, 209 (1971).
4. G. Nicolis and J. Portnow, *Chem. Rev.*, 73, 365 (1973).
5. S. Chandrasekhar, *Hydrodynamics and Hydromagnetic Stability* (Oxford, Clarendon Press, 1961).
6. K. Maltman and W. G. Laidlaw, *J. Chem. Phys.*, 64, 2335 (1976).
7. T. C. Koopmans, *Activity Analysis of Production and Allocation*, Cowles Commission Monograph, New York, Wiley (1957) (Cowles Foundation for Research in Economics at Yale University).
8. R. M. May, *J. Theoret. Biol.*, 51, 511 (1975).
9. J. Quirk and R. Ruppert, *Rev. Econ. Studies*, 32, 311 (1965).
10. C. Jeffries, *Ecology*, 55, 1415 (1974).
11. B. L. Clarke, *J. Chem. Phys.*, 62, 773 (1975).
12. D. B. Shear, *J. Chem. Phys.*, 48, 4144 (1968).
13. F. Horn, *Proc. Roy. Soc. London*, A334, 299 (1973).



14. P. Glandsdorff and I. Prigogine, *Thermodynamic Theory of Structure, Stability and Fluctuations* (Wiley, London, 1971).
15. I. Prigogine, *Thermodynamics of Irreversible Processes* (Interscience Publ. 1967).
16. G. F. Oster, *The Structure of Reaction Networks*, see (2) above.
17. B. L. Clarke, *J. Chem. Phys.*, 58, 5606 (1973).
18. B. L. Clarke, *J. Chem. Phys.*, 62, 3726 (1975).
19. B. L. Clarke, *J. Chem. Phys.*, 60, 1481 (1974).
20. N. Minorsky, *Nonlinear Oscillations*, (D. Van Nostrand Co. 1962).
21. S. R. de Groot and P. Mazur, *Non-equilibrium Thermodynamics*, (North-Holland, 1962).
22. R. Lefever, *Dissipative Structures and Onset Mechanism; Fluctuations, Instabilities and Phase Transitions*. Editor, T. Riste (Plenum Press, 1975).
23. D. Edelson, R. J. Field and R. M. Noyes, *Intern. J. of Chem. Kinet.*, VII, 417 (1975).
24. R. J. Field and R. M. Noyes, *J. Chem. Phys.*, 60, 1877 (1974).
25. J. J. Jwo and R. M. Noyes, *J. Am. Chem. Soc.*, 97, 5422 and 5431 (1975).
26. R. J. Field and R. M. Noyes, *Faraday Symposium, Phys. Chem. of Oscillating Phenonema*, 21 (1974).
27. R. J. Gelinas, *J. Comput. Phys.*, 9, 222 (1972).



28. R. J. Field, *J. Chem. Phys.*, 63, 2289 (1975).
29. S. P. Hastings and J. P. Murray, *SIAM. J. Applied Math.*, 28, 678 (1975).
30. J. S. Turner, *Phys. Letters*, 56A, 155 (1976).
31. B. L. Clarke, *J. Chem. Phys.*, 64, 4165 (1976).
32. B. L. Clarke, *J. Chem. Phys.*, 64, 4179 (1976).
33. J. K. Hale, *Oscillations in Nonlinear Systems* (McGraw-Hill Co. Inc., 1963).
34. I. Herstein, *Topics in Algebra* (John Wiley and Sons Inc., 1975).
35. E. A. Coddington and N. Levinson, *Theory of Ordinary Differential Equations* (McGraw-Hill, New York).
36. J. L. Goldberg and A. J. Schwartz, *Systems of Ordinary Differential Equations, an introduction* (New York, Harper and Row, 1972).
37. F. R. Gantmakher, *Applications of the Theory of Matrices*, New York, Interscience Publ. (1959).
38. B. L. Clarke, *SIAM. J. Appl. Math.* (to appear).
39. M. M. Vainberg and V.A. Trenogin, *Theory of Branching of Solutions of Non-linear Equations* (Noordhoff Int. Publ., 1974).
40. M. Gerstenhaber, *Theory of Convex Polyhedral Cones*, Chapter (XVII) (see reference 7).
41. G. Hadley, *Linear Programming* (Addison-Wesley, 1962).
42. B. L. Clarke, unpublished.
43. R. M. Noyes, *J. Chem. Phys.*, 65, 848 (1976).



44. G. Hadley, Linear Algebra (Addison-Wesley, 1973).
45. B. Von Hohenbalken, Math. Programming, 13, 49 (1977).
46. D. Shear, J. Theoret. Biol., 16, 212 (1967).









B30200